Endosomal organizers of *post*-Golgi apical trafficking in polarized epithelial cells

Dissertation
zur
Erlangung des Doktorgrades
der Naturwissenschaften
(Dr. rer. nat.)

dem Fachbereich Biologie
der Philipps-Universität Marburg
vorgelegt von

Dipl.-Bioch. Ksenia Astanina
Murmansk
Russland

Marburg 2010

Die Untersuchungen der vorliegenden Arbeit wurden in der Zeit von August 2006 bis Juli 2010 am Institut für Klinische Zytobiologie und Zytopathologie in Marburg, unter der Leitung von Prof. Dr. Ralf Jacob angefertigt.

Vom Fachbereich Biologie der Philipps-Universität Marburg als Dissertation
angenommen am: 12. Juli 2010

Erstgutachter: Prof. Dr. Uwe Maier

Zweitgutachter: Prof. Dr. Ralf Jacob

Tag der mündlichen Prüfung: 25. Oktober 2010

To my beloved family

Abstract

Polarized traffic in epithelial cells depends on well organized pathways that direct newly synthesized proteins to the apical or basolateral membrane. In MDCK cells, apical trafficking can further be divided into a lipid raft-dependent and raft-independent route, which separate biosynthetic cargo in a *post*-Golgi endosomal compartment.

The current study was focused on the trafficking machinery in apical transport. As model proteins, raft-associated sucrase-isomaltase and non-raft-associated neurotrophin receptor p75 and lactase-phlorizin hydrolase have been used. In biochemical and fluorescence studies two novel proteins – KIF5C and annexin XIIIb – were shown to play a general role in *post*-Golgi apical trafficking early after TGN-release, before the two apical pathways are segregated into distinct vesicle populations.

Key words: annexin, apical trafficking, endosomes, epithelial cells, KIF5, kinesin, MDCK

Contents

1. Introduction

1.1. Cell polarity. Epithelial cells.

The establishment and maintenance of polarized traffic of proteins, membranes and organelles, as well as the formation of polarized cytoarchitecture is prerequisite for fundamental functions of many cells, from bacteria to vertebrates (Drubin, 1991; Lombardi et al., 1985; Rodriguez-Boulan and Nelson, 1989). For example, bacterium *Caulobacter crescentus* develops asymmetric protein distribution to generate two types of daughter cells: a flagellated swarmer cell and a nonmotile stalked cell (Gober et al., 1991). In budding yeast, newly synthesized proteins are selectively transported to the site of budding (Field and Schekman, 1980).

In higher organisms, cell polarity is also an important factor during the development (Fleming and Johnson, 2003) and for the functioning of highly polarized tissues such as epithelia and neurons (Dotti and Simons, 1990). A similar polarity was shown in the presumptive myocardium (Peng et al., 1990). Motile cells, such as macrophages, T-cells and fibroblasts, react to some external stimuli (for example, chemoattractant) with directed movement and polarized re-organization of the organelles (Bergmann et al., 1983). Therefore, polarity can be described as a general pattern common to many cell types. One of the best studied examples of polarized cell organization are epithelial cells.

An epithelium is the cellular covering of internal and external surfaces of the body, including the lining of vessels and other small cavities. It consists of cells joined by small amounts of cementing substances. Establishment and maintenance of an intact epithelium is critical for tissue integrity. Therefore, the plasma membrane of epithelial cells is divided into two distinct domains: apical, facing the outer lumen, and basolateral, contacting with basement membrane (basal lamina). Apical and basolateral membrane domains are separated by tight junctional complexes: an intracellular junctional structure that mediates adhesion between epithelial cells and prevents free diffusion across the epithelial cell sheet. Tight junctions consist of transmembrane and peripheral membrane proteins, which interact with each other to form a complex network. The transmembrane proteins occludin, claudin and JAM link to the actin cytoskeleton through interactions with scaffolding proteins such as ZO (Fig. 1.1). Other tight junctional proteins (ZONAB, Rab13, cingulin) play a role in signal transduction and control cell proliferation by participating directly in signalling cascades or by regulating gene expression in the nucleus (Shin et al., 2006).

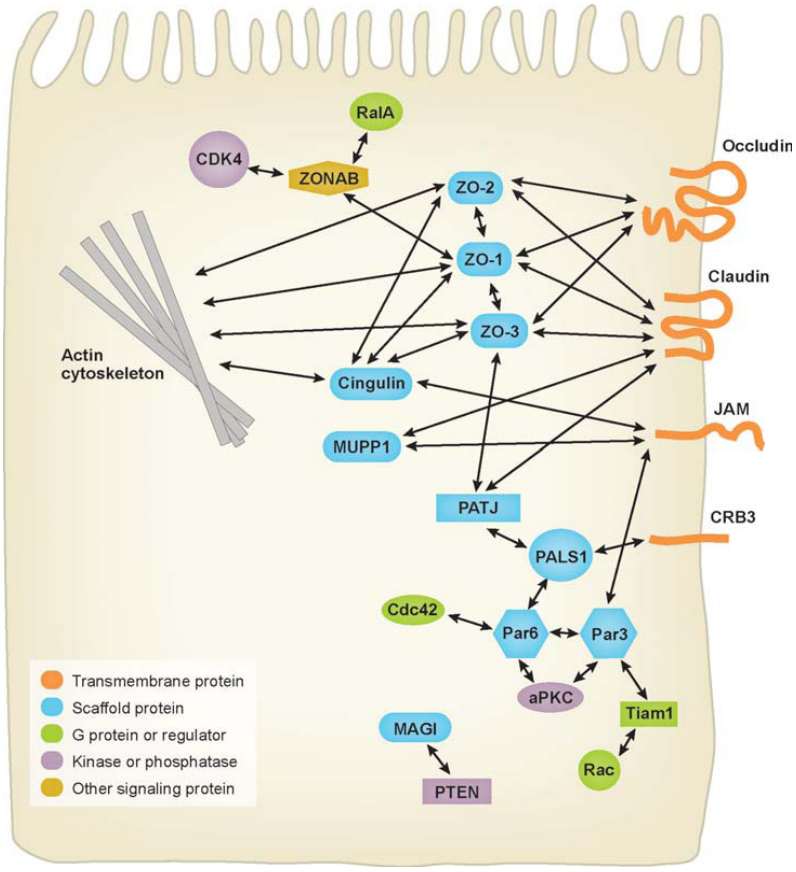

Figure 1.1. Complexity of protein-protein interactions at the tight junction

Some of these interactions, such as those between claudins and ZO proteins, are necessary for the structural integrity of the tight junction. Others regulate signalling pathways (for example, ZO proteins and the transcription factor ZONAB). aPKC, atypical protein kinase C; CDK4, cell division kinase 4; CRB3, Crumbs 3; JAMs, junctional adhesion molecules; MAGI, membrane-associated guanylate kinase with inverted domain structure; MUPP1, multi-PDZ domain protein 1; PALS1, protein associated with Lin seven 1; Par, partitioning defective; PATJ, PALS1-associated tight junction protein; RalA, Ras-like GTPase; Tiam1, T-lymphoma invasion and metastasis; ZO, zonula occludens; ZONAB, ZO-1-associated nucleic acid–binding protein.
(Modified from (Shin et al., 2006))

Membrane domains are also distinct in their protein and lipid composition (Caplan, 1997; Rodriguez-Boulan and Powell, 1992). Thus, for example, the apical plasma membrane of intestinal cells is enriched in intestinal hydrolases, and the basolateral membrane is characterized by the presence of, for example, E-cadherin. Cholesterol and sphingolipids localize to the apical membrane domain, whereas the basolateral domain is enriched in phosphatidylcholine. Tight junctional complexes stabilize the integrity of the two membrane domains and prevent diffusion of proteins and lipids from one domain to another (van Meer and Simons, 1988). The polarity is also maintained by an intracellular machinery that directs newly synthesized material to the correct target membrane (Delacour and Jacob, 2006). The epithelial trafficking machinery ensures that newly synthesized plasma membrane proteins move along the secretory pathway to the *trans*-Golgi network (TGN), where they are sorted into apical or basolateral carriers (Griffiths and Simons, 1986).

1.2. Intracellular protein transport

Protein biosynthesis occurs on the ribosomes. Proteins, which are synthesized on the rough endoplasmic reticulum (ER) are co-translationally translocated in the ER lumen. After the translation is completed, the proteins are moved from the ER to the Golgi, where they are processed before being sorted to their final destination (Mellman and Warren, 2000). Processing steps include proteolytic cleavage and carbohydrate modifications (e.g. glycosylation). Early- and late-acting processing enzymes are concentrated in distinct parts of the Golgi apparatus (Dunphy and Rothman, 1985). The Golgi apparatus is composed of membrane stacks known as cisternae. Between four to eight cisternae are usually present per cell, but the number can also be higher, as up to sixty in some protists. It consists of four functional regions: the *cis*-Golgi, *medial*-Golgi, *trans*-Golgi and *trans*-Golgi network (TGN). The newly synthesized secreted or membrane proteins travel sequentially from the *cis*-region of the Golgi, to the *medial*- and *trans*-Golgi and then to the TGN, where they are exported in vesicular carriers to their final destination (Griffiths and Simons, 1986). Further sorting delivers the proteins either to the plasma membrane or to lysosomes.

The *trans*-Golgi network (TGN) has classically been viewed as a main compartment of sorting and segregation of secreted or membrane proteins. Although cargo sorting can occur in earlier secretory compartments and also continue beyond the TGN (Jacob and Naim, 2001; Ang et al., 2004), it reaches a very high level of complexity and sophistication at the TGN. Here, the cargo is segregated to various final destinations: apical and basolateral plasma membranes, early and late endosomes, recycling endosomes, the Golgi stack, secretory granules and other specialized compartments. Moreover, in the TGN a lot of proteins receive their final *post*-translational modifications and lipids undergo transfer, insertion and then completion of their synthesis (Naim et al., 1991; Naim and Lentze, 1992; Baeuerle and Huttner, 1987; 'Angelo et al., 2007).

1.2.1. Protein sorting at the TGN

Cargo sorting at the TGN can be described by several main principles. One of them is based on sorting motifs of proteins, which are recognized by adaptor and/or coat proteins. Thus, sorting motifs have been identified in the endosomal- and basolateral-directed proteins. Typical basolateral motifs are tyrosin-based (NPXY, YXXØ) and two leucin residues ([DE]XXXL[LI], DXXLL) (Rodriguez-Boulan et al., 2005). These sorting signals are generally located at the cytosolic domain of a transmembrane protein. It is proposed, that basolateral sorting signals comprise a multitude of secondary structures like α-helices or β-sheets, and can also be localized in distal parts of the cytoplasmic domain (Beau et al., 2004). Basolateral sorting signals can overlap with endocytosis determinants and are recognized by

adaptor proteins of the clathrin complex (Lin et al., 1997). Proteins containing Tyr motifs bind to the γ1-subunit (Ohno et al., 1995; Bonifacino and Dell'Angelica, 1999), and Leu-Leu motifs interact specifically with the β-subunit of the AP-1 adaptor complex (Rapoport et al., 1998). It was also shown that another adaptor complex, AP-1B, is specifically expressed in epithelial cells and is involved in basolateral protein delivery (Folsch et al., 1999).

In general, signals for apical sorting are more heterogeneous and less well understood (Rodriguez-Boulan et al., 2005). In contrast to basolateral sorting, signals for apical membrane trafficking can be situated in any part of the protein and can depend on glycosylation of the protein. Some apical proteins have sorting signals in the cytosolic domain, as basolateral proteins do. The best understood example of these sorting signals is rhodopsin, whose signal motif can redirect heterologous protein to the apical surface (Chuang and Sung, 1998). Apical protein sorting can also depend on a membrane-spanning polypeptide segment of a transmembrane protein (Lin et al., 1998). This segment can associate with specific membrane microdomains (called “rafts”) which can serve as a platform for the apical trafficking (Schuck and Simons, 2004). Apical non-transmembrane proteins can also be sorted via anchoring to the outer leaflet of the membrane by a glycosyl phosphatidyl inositol (GPI) lipid modification, which may lead to raft association (Hannan et al., 1993; Paladino et al., 2006). This modification, together with clustering of the protein, may result in apical sorting. Nevertheless, although GPI-anchoring provides raft association, this is not a general mechanism for protein targeting to the apical membrane. For example, the addition of a GPI-anchoring motif on rat growth hormone (rGH), a soluble protein that is secreted in a non-polarized manner, is not sufficient for apical targeting (Benting et al., 1999).

Additionally, N- and O-linked carbohydrates coupled with the extracellular portion of apical plasma membrane proteins have been proposed to act as apical sorting signals (Rodriguez-Boulan and Gonzalez, 1999; Potter et al., 2004).

First indications for the role of N-glycosylation in apical sorting came from respective inhibitor studies. Thus, treatment of MDCK cells with tunicamicyn, which inhibits the first step of glycosylation, resulted in missorting of the apical protein clusterin (gp80) to both membrane domains (Urban et al., 1987). Glycosylation-deficient cell lines showed mistargeting of the apical glycoprotein gp114 (Le Bivic et al., 1993). On the other hand, introducing N-glycosylation sites to proteins which normally show no preferential targeting in epithelial cells, can result in apical sorting of modified protein. For example, non-glycosylated (wild type) rat growth hormone (rGH) is normally secreted with a slight preference into the basolateral medium. But addition of one glycosylation site reversed the polarity of protein secretion, and the addition of the second glycosylation site leads to a preferential apical sorting of rGH (Scheiffele et al., 1995).

Nevertheless, there are a lot of examples of N-glycosylation-independent apical protein sorting. Thus, neurotrophin receptor p75, an N- and O-glycosylated apical protein, does not require this modification for its apical sorting (Yeaman et al., 1997). Moreover, some basolateral proteins are N-glycosylated, but nevertheless not transported to the apical surface. This can be explained by the additional presence of basolateral targeting signals, which are recognized by adaptor proteins and interfere with apical sorting (Simons and Ikonen, 1997). Indeed, basolateral proteins that lack their cytoplasmic tails are missorted to the apical surface, presumably, as a result of their glycosylation (Scheiffele et al., 1995; Matter and Mellman, 1994).

Another possible mechanism of apical protein sorting is O-glycosylation. The p75 neurotrophin receptor and sucrase-isomaltase (SI), both apical model proteins, are characterized by the presence of heavily O-glycosylated stalk domains. Deletion of these domains leads to the missorting to both membrane domains (Jacob et al., 2000a; Yeaman et al., 1997). Furthermore, attaching the O-glycosylated stalk domain of SI to rGH, which is normally secreted in Caco-2 cells in a non-polarized manner, results in the apical sorting of the protein (Spodsberg et al., 2001). In this case, modified rGH was associated with detergent-resistant microdomains, as observed for SI.

Although all these data prove the role of N- and O-glycosylation in apical protein sorting, the exact mechanism of this process remains unclear. Two models have been proposed to explain the role of glycosylation in apical trafficking (Rodriguez-Boulan and Gonzalez, 1999). The first one postulates that carbohydrates are necessary for the transport-competent conformation of protein, which is required for the forward progress along the biosynthetic pathway. Thus, glycosylation inhibition of some apical proteins results in their retention in TGN (Gut et al., 1998). In contrast, the second model proposes that there are some sorting receptors that recognize carbohydrates or carbohydrate-dependent confirmations. Plausible candidates could be galectins – the protein family of lectins with an affinity for β-galactoside structures (Barondes et al., 1994). It was shown that galectin-3 and galectin-4 can function as glycosylation receptors for raft-independent and raft-dependent apical protein pathways, respectively (Delacour et al., 2005; Delacour et al., 2006).

1.2.2. *Post*-TGN pathways in polarized epithelial cells

Apical *post*-Golgi vesicles are composed of distinct vesicular components and can take various routes to the cell surface (Jacob and Naim, 2001a; Jacob et al., 2003). Some of them depend on membrane lipid rafts, others use separate transport platforms. Typical marker proteins for lipid raft-dependent apical pathways are sucrase-isomaltase (SI) (Danielsen, 1995), influenza virus hemagglutinin (HA) (Fiedler et al., 1993), gp135 (Ojakian and Schwimmer, 1988) and glycosylphosphatidylinositol-anchored proteins (Zurzolo et al., 1994).

For the raft-independent pathway transmembrane proteins as the neurotrophin receptor (p75) (Yeaman et al., 1997), gp114 (Le Bivic et al., 1990; Verkade et al., 2000), endolyn (Ihrke et al., 2001) and lactase-phlorizin hydrolase (LPH) (Jacob et al., 2000a) are commonly studied (see also Table 1.1).

Table 1.1. Apical transmembrane proteins associated or not associated with lipid rafts in epithelial cells

Associated with lipid rafts	Not associated with lipid rafts
Aminopeptidase A and N	Enteropeptidase
Aquaporin 5	gp114
Dipeptidyl peptidase IV	H^+-K^+-ATPase
gp135	Lactase-phlorizin hydrolase (LPH)
Influenza virus hemagglutinin (HA)	Neurotrophin receptor p75 (p75)
Influenza virus neuraminidase	Prominin
MAL proteolipid	
Megalin	
Sucrase-Isomaltase (SI)	

(Modified from (Delacour and Jacob, 2006))

The two vesicle populations (raft-associated and non-raft-associated) are separated from each other first after TGN exit (Jacob and Naim, 2001). It was demonstrated that the large vesicular structures containing both apical proteins (raft-associated SI and raft-independent LPH) in separate subdomains detach from the TGN. Thereafter, the proteins are separated into two distinct vesicle populations. Moreover, it was found that both raft-associated and non-raft-associated apical transport pathways depend on the integrity of microtubules, whereas actin microfilaments are mainly required for cell surface delivery of raft-associated proteins (Jacob et al., 2004; Jacob et al., 2003). The two *post*-TGN vesicle populations differ additionally in the dependence on galectin-3 (for raft-independent pathway) and galectin-4 (for raft-dependent pathway) (Delacour et al., 2009). Another example of a protein that distinguish between raft-associated and raft-independent vesicles is the annexin II-S100A10 complex, which is a component of SI-carrying vesicles, but is absent from LPH-carrying vesicles (Jacob et al., 2004).

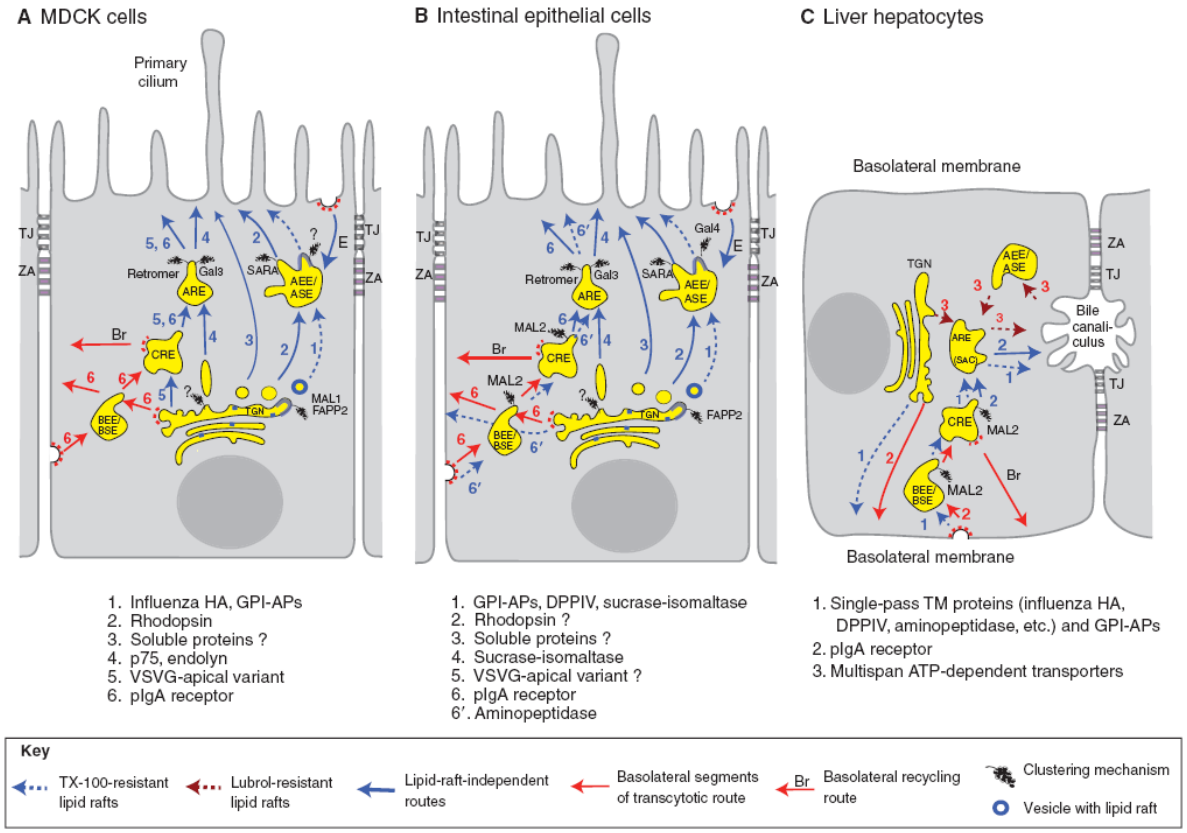

Figure 1.2. Clustering events in apical trafficking routes

Trafficking routes for the indicated cargo proteins are diagrammed. Various candidate molecules or complexes that might contribute to clustering in MDCK (A), intestinal (B) and liver (C) epithelial cells are noted within each cell type. Routes 2 (rhodopsin) and 5 (VSVG-apical variant) are hypothetical in intestinal cells.Br, basolateral recycling route; E, endocytic route; TJ, tight junction; ZA, zonula adherens; AEE/ASE, apical early/sorting endosome; ARE, apical recycling endosome; CRE, common recycling endosome; BEE/BSE, basal early/sorting endosome.
(Modified from (Weisz and Rodriguez-Boulan, 2009))

In spite of these differences, both vesicle populations follow the same transendosomal route on the way from TGN to the apical membrane (Cramm-Behrens et al., 2008). Analysis of the *post*-TGN transport in polarized as well as non-polarized cells revealed a sequential passage of LPH and SI through Rab4-, Rab8- and Rab11-containing compartments. This finding also supports the idea that endosomes function as organizing centers in apical trafficking. It is already known that a significant fraction of basolateral cargo is directed to the common recycling endosome (CRE) after TGN exit. For example, basolateral VSVG traverses a few minutes after TGN exit the transferrin-positive CRE (Leitinger et al., 1995; Ang et al., 2004). The actual model of the role of various endosomal compartments in *post*-TGN polarized trafficking is depicted in Fig. 1.2. Moreover, there is a secretory Golgi bypass route to the apical surface, when cargo is transported from pre-Golgi organelles (Tveit et al., 2009).

1.3. Proteins studied in this thesis

1.3.1. Sucrase-Isomaltase

Sucrase-Isomaltase is one of the classical model proteins for the raft-associated apical transport. For the first time this protein was isolated from the intestinal brush-border membrane (Hauser and Semenza, 1983). It consists of two strongly homologous subunits, sucrase and isomaltase (Fig. 1.3) (Hunziker et al., 1986). These two domains originate from a large polypeptide precursor, pro-SI, by tryptic cleavage occurring in the intestinal lumen (Hauri et al., 1979; Naim et al., 1988). SI is a type II integral membrane protein that is synthesized with an uncleavable signal sequence, which functions also as a membrane anchor (Hunziker et al., 1986). The sucrase-isomaltase complex is a heavily N- and O-glycosylated protein (Naim et al., 1988). The earliest detectable form of pro-SI is a 210 kDa mannose-rich form in the endoplasmic reticulum (ER), that is transported at a relatively slow rate to the Golgi, where it is processed to a complex glycosylated protein (about 245 kDa). O-glycosylation of pro-SI occurs mainly in a Ser/Thr-rich stalk domain located close to the membrane in the Isomaltase subunit (Jacob et al., 2000a).

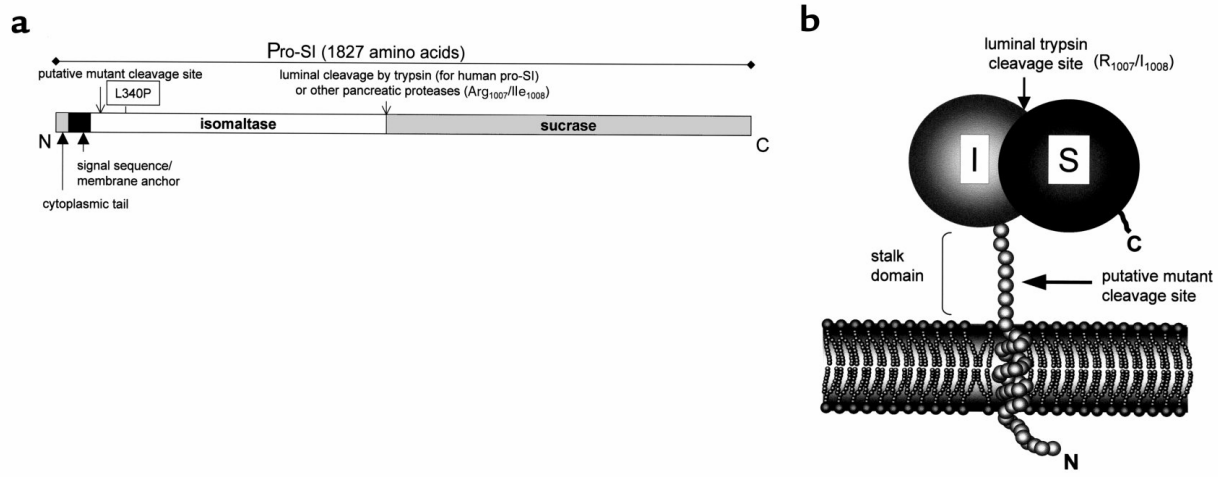

Figure 1.3. Structure and membrane orientation of pro-SI

(**a**) Structural features of pro-SI. The cytoplasmic tail contains 12 amino acid residues and is followed by a membrane anchor of 20 amino acids and a Ser/Thr-rich stalk domain of 28 amino acids that is considered to be part of the isomaltase subunit. Isomaltase ends with amino acid residue Arg_{1007} and sucrase starts immediately thereafter with Ile_{1008}. The location of the putative cleavage site is indicated. The Arg/Ile peptide sequence between isomaltase and sucrase is a trypsin site where the mature large precursor pro-SI is cleaved in the intestinal lumen by pancreatic trypsin (Hauri et al., 1985). (**b**) Schematic drawing of the membrane orientation of pro-SI. The NH_2-terminus on the cytosolic side of the membrane (N), the luminal COOH-terminus (C), the stalk domain, and the putative cleavage region are indicated. I, isomaltase; S, sucrase.
(Modified from (Jacob et al., 2000b))

O-glycosylation of SI, which occurs in the *cis*-Golgi, is crucial for its apical trafficking. O-glycans on the stalk domain of SI lead to its association with lipid rafts (Alfalah et al., 1999). SI-carrying vesicles are transported after TGN exit along microtubules, as well as raft-independent LPH-carrying vesicles (Jacob et al., 2003). But in the cell periphery SI-carrying, but not LPH-carrying, vesicles switch from microtubules to actin filaments. Myosin 1A is a motor protein for this transport which functions, probably, through its interaction with the annexin II-S100A10 complex (Jacob et al., 2004).

1.3.2. Neurotrophin receptor p75

Another, raft-independent, model protein is the neurotrophin receptor p75 (p75NTR, or p75). The p75 receptor is a common receptor for neurotrophins and has important roles in internalization and trafficking of neurotrophins along axons in neuronal cells (Butowt R. & von Bartheld C., 2003). It was first discovered as a nerve growth factor (NGF) receptor (Johnson et al., 1986), but turned out to bind all neurotrophins (Rodriguez-Tebar et al., 1992). For the domain structure of p75 see Fig. 1.4. P75 can contribute to antiapoptotic (pro-survival) signalling as well as pro-apoptotic signalling (Roux and Barker, 2002). Intriguingly, some reports have shown that an astonishing array of diverse proteins, including lectins, pathogens and toxins, bind directly or indirectly to the p75 receptor. These proteins share the ability to be transported efficiently among connected neuronal populations within the nervous system, suggesting that specific binding to p75 may be crucial not only for trafficking of neurotrophins but also for trafficking of other proteins that hijack the existing transport system (Butowt and von Bartheld, 2003). It was also shown that in the Golgi apparatus of neurons p75 may facilitate sorting into a recycling or anterograde transcytosis pathway and avoidance of the degradation pathway (von Bartheld et al., 2001). In polarized transport studies p75 is commonly used as an apical marker protein. It was shown that in MDCK cells transfected with full-length neurotrophin receptor cDNA, p75 is predominantly (80%) expressed in the apical membrane domain (Le Bivic A. et al., 1991).

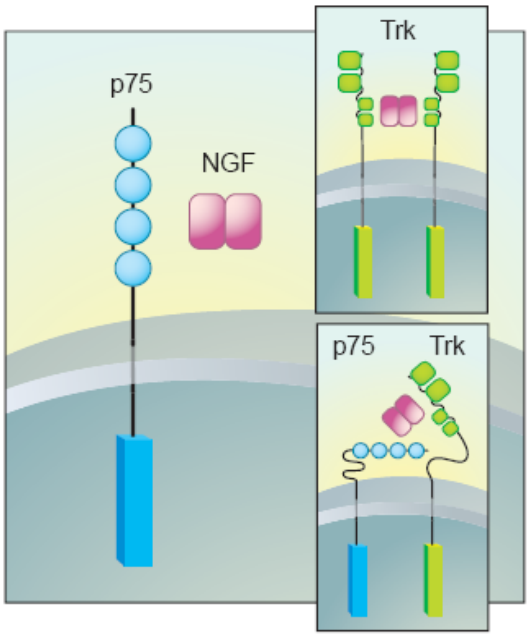

Figure 1.4. Structure and membrane orientation of p75

Nerve growth factor receptor contains an extracellular domain containing four 40-amino acid repeats with 6 cysteine residues at conserved positions followed by a serine/threonine-rich region, a single transmembrane domain, and a 155-amino acid cytoplasmic domain. The cysteine-rich region contains the nerve growth factor binding domain. The NGF dimer binds to a monomeric form of p75, but to a dimeric form of the TrkA receptor. Heterodimers of p75 and Trk are possible, but the receptors would need to be in opposite orientations to accommodate the NGF dimer. NGF, nerve growth factor; Trk, tyrosine kinase
(Modified from (Zampieri and Chao, 2004))

As mentioned above, the structural information for apical sorting of p75 is localized to a juxtamembrane region of the extracellular domain that is rich in O-glycosylated serine/threonine residues (Yeaman et al., 1997). Deletion of this stalk domain results in missorting of p75 to the basolateral membrane. At the same time, the N-glycan present on p75 is not required for apical sorting. After TGN exit in polarized MDCK cells p75 is transported via the raft-independent pathway along microtubules to the apical membrane. Both kinesin and dynamin are required for this transport (Kreitzer et al., 2000). KIF5B, a member of the kinesin-1 group, is involved in raft-independent apical delivery in polarized MDCK cells (Jaulin et al., 2007).

1.3.3. Lactase-phlorizin hydrolase

Lactase-phlorizin hydrolase is a major disaccharidase in the microvillus membrane of small intestinal epithelial cells. The enzyme contains both catalytic sites for lactase, which is responsible for the hydrolysis of lactose, and phlorizin hydrolase. LPH, an integral type I membrane glycoprotein, is 1927 amino acids long containing a membrane anchor of 19 contiguous hydrophobic amino acids and a cytoplasmic domain of 26 amino acids. It is

synthesized as a precursor with apparent molecular masses of 215 and 230 kDa, representing the mannose-rich (pro-LPH_h) and complex (pro-LPH_c) glycosylated forms. Maturation of LPH involves proteolytic cleavage after complex glycosylation of the precursor to yield the brush-border form of 160 kDa (Danielsen et al., 1984; Hauri et al., 1985; Naim et al., 1987; Naim, 1992). Both pro-LPH and the mature-like LPH are predominantly present on the apical membrane of MDCK cells recombinantly expressing LPH (Jacob et al., 1994; Jacob et al., 1997). This indicates that the cleavage process has no influence on the apical sorting of LPH. Studies on deletion mutants followed by expression in MDCK cells point to the existence of an apical sorting signal in the ectodomain (Panzer et al., 1998). This sorting signal is different from that of sucrase-isomaltase as this enzyme is found in the detergent insoluble fraction but the LPH is not (Danielsen, 1995).

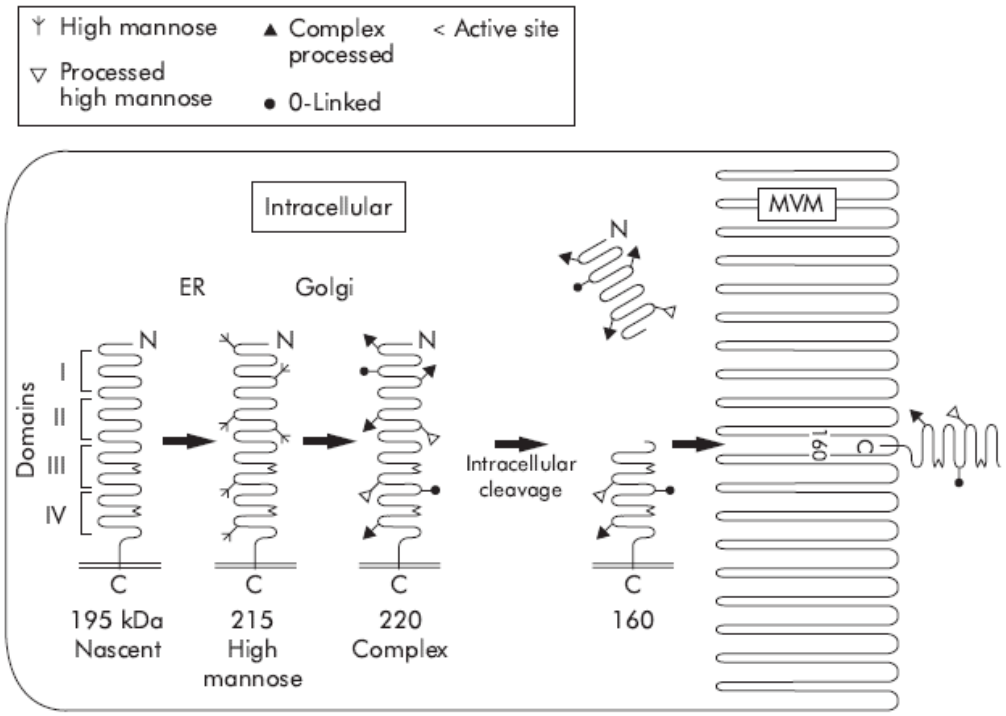

Figure 1.5. Model of the molecular forms of lactase-phlorizin hydrolase during synthesis and processing in the human villus enterocyte

The early changes in apparent molecular size are due to glycosylation, as indicated in the diagram. Note that the two active sites are located in domains III and IV. The subsequently removed domains I and II are important for correct folding of the nascent protein. Although not indicated on this drawing, the enzyme forms a homodimer during processing. The final N terminal cleavage of a small segment is depicted by the elimination of the terminal loop in the microvillus form of the enzyme. The enzyme is synthesized as a single-chain precursor protein and undergoes proteolytic processing during maturation.
(Modified from (Grand et al., 2003))

1.4. Cytoskeleton organization in epithelial cells. The role of motor proteins.

1.4.1. Microtubules and microtubule-associated motors

Subconfluent, non-polarized MDCK cells harbour a classical centrosomal arrangement of microtubules, with dynamic microtubules extending their plus ends towards the cell cortex. In polarized MDCK cells, in contrast, there a large population of stable microtubules is organized vertically in the cells along the apical-basolateral axis of the cell. The plus ends of these microtubules face the basal membrane (Bacallao et al., 1989). The epithelial-specific reorganization of microtubules is controlled by the polarity protein kinase Par1b (Cohen et al., 2004). Recently, it has been shown that polarized MDCK cells have also a small but very dynamic population of microtubules, originating from the MT-organizing center (MTOC), with the plus ends facing apically (Jaulin et al., 2007). It is proposed that the minus ends of dynamic microtubules are captured by the junctional regions of the lateral plasma membrane, originating a population of stable microtubules. This hypothesis comes from the observation that expression of E-cadherin in fibroblasts stabilizes non-centrosomal microtubules (Chausovsky et al., 2000).

The first studies on the role of microtubules in apical and basolateral transport yielded conflicting results (Musch, 2004). In 1987 Rindler et al. showed that disruption of microtubules leads to the loss of apical trafficking of HA, but had no effect on basolateral budding of VSVG (Rindler et al., 1987). Later, it was shown that only kinesin is involved in the transport of VSVG to the basolateral membrane, while both kinesin and dynein are crucial for the apical delivery of HA (Lafont et al., 1994). However, other studies revealed no effect of microtubule disassembly on HA apical trafficking or found only a slight retardation in the HA surface delivery (Salas et al., 1986; van Zeijl and Matlin, 1990). According to the recent finding that the two populations of microtubules exist in polarized MDCK cells (Jaulin et al., 2007), these contradictory results might be explained by the disruption of different microtubules – stable and dynamic – to different extents (Weisz and Rodriguez-Boulan, 2009).

Many studies have been conducted to identify the motor proteins involved in apical transport. Thus, it was demonstrated that the cytosolic tail of rhodopsin interacts with dynein light chain and acts as an apical sorting signal (Chuang and Sung, 1998). On the other hand, minus end-directed kinesin KIFC3 was identified in apical trafficking of raft-associated HA and annexin XIIIb (Noda et al., 2001). Recently, Jaulin et al. showed that p75 is transported by plus end-directed KIF5B in polarized MDCK cells (Jaulin et al., 2007). Interestingly, a different kinesin is required for p75 trafficking in non-polarized MDCK cells (Xue et al., 2010). As mentioned above, the raft-dependent trafficking pathway to the apical surface requires not only microtubules, but also actin filaments (Jacob et al., 2003).

1.4.2. Actin filaments and myosins

Not only microtubules, but also the actin cytoskeleton plays a crucial role in the establishment and maintenance of polarization in epithelial cells. Thus, for example, highly organized microfilaments stabilize microvilli in the apical brush border of epithelial cells (Tilney et al., 1973). These microfilaments are anchored to the meshwork of F-actin filaments and actin binding proteins close to the apical membrane. Disruption of actin cytoskeleton results in abolished apical trafficking of some proteins, for example, SI (Jacob et al., 2003) and polymeric immunoglobulin receptor pIgR (Maples et al., 1997). At the same time, in MDCK cells apical delivery of endogenous gp80 or exogenously expressed LPH is not perturbed by actin-depolarization (Jacob et al., 2003; Parczyk et al., 1989). It is known that actin plays a central role in endocytic trafficking and recycling to the apical pole (Gottlieb et al., 1993), as well as in the basolateral to apical trancytosis (Maples et al., 1997). But also in the protein trafficking from TGN to the apical membrane actin-based transport takes place. Although, only a few motor proteins have been described to be involved in apical trafficking along actin filaments. One candidate is myosin I, which was identified on apical *post*-Golgi vesicles in intestinal and MDCK cells (Jacob et al., 2003; Fath and Burgess, 1993; Montes et al., 1997). Myosin Ia was found on SI-carrying *post*-Golgi vesicles and, moreover, alpha-kinase I (ALPK1), which is associated with the same vesicle population, is capable to phosphorylate myosin I *in vitro* (Jacob et al., 2003; Heine et al., 2005). Moreover, the depletion of ALPK1 results in significant reduction of SI delivery to the apical surface. These data indicate that ALPK1 can play a role in the apical transport of raft-associated vesicle populations.

Another challenging question is which adaptor proteins are required for the *post*-Golgi transport. Annexins are likely candidates for this process. Thus, both annexin II and annexin XIIIb are associated with lipid raft-containing apical vesicles (Fiedler et al., 1995; Lafont et al., 1998; Jacob et al., 2004).

Table 1.2. Sorting mechanisms for constitutive and regulated apical protein delivery

Apical protein	Sorting signal	Presumed sorting mechanism	MT motor
Constitutive apical transport			
Influenza HA	Transmembrane domain	Lipid-raft-association; raft clustering by MAL1, MAL2 and FAPP2	KIFC3
GPI-anchored proteins (e.g. decay-accelerating F factor, folate receptor, GFP-GPI, 5'-nucleotidase, CEA)	GPI	Lipid-raft association and oligomerization; raft clustering by MAL1, MAL2, FAPP2 and galectin-4	?
p75 neurotrophin receptor	O-glycosylated stalk	Clustering by galectin-3; raft-independent	KIF5B
Lactase-Phlorizin Hydrolase	O-glycans	Clustering by galectin-3; raft-independent	?
Sucrase-Isomaltase	Transmembrane domain	Raft association	?
Endolyn	N-glycans	Raft-independent	?
Rhodopsin	Cytoplasmic domain	Dynein light chain; raft-independent	Dynein
pIgR	Apical and basolateral signals	Raft-independent; MAL2	?
Syntaxins 1,2,3	FMDE in cytoplasmic domain	?	?
Megalin	NPXY-like motifs	Clathrin adaptors?	?
Prominins 1,2	Transmembrane domain?	Lubrol-insoluble rafts?	?
Soluble proteins (e.g. growth hormone, erythropoietin, hepatitis virus antigen)	N-glycans, protein motifs	Receptors?	?
Na^+-K^+ ATPase, CD147, MCT1, CAR, apical proteins in renal PCT	Recessive apical signals	Absence of basolateral adaptors	?
Regulated apical transport			?
Vacuolar H^+ ATPase	?	? Regulated by metabolic pH, basal-membrane contacts and hensin	?
Gastric H^+ ATPase	transmembrane domain	? Regulated by gastric content and histamine	?
CFTR, Na-Pi cotransporter, GAT3	PDZ-binding motif	PDZ-domain-containing proteins	?
Aquaporin 2	?	? Regulated by ADH	?
Na, PiIIa	?	? Regulated by ADH	?
Epithelial Na^+ channel	?	? Regulated by aldosterone, vasopressin	?
ATP transporters (BSEP, MDR1, MDR3, ABCG5/8)	Transmembrane domain?	Lubrol-insoluble rafts; regulated by various mechanisms	?
ATP7B (Menkes) copper transporter	?	? Regulated by copper levels	?

ADH, antidiuretic hormone; CAR, coxsackie-adenovirus receptor; CEA, carcinoembryonic antigen; CFTR, cystic fibrosis transmembrane conductance regulator; FAPP, phosphatidylinositol 4-phosphate adaptor protein; GAT, γ-aminobutyric acid transporter; GFP, green fluorescent protein; GPI, glycosylphosphatidylinositol; HA, hemagglutinin; MAL, myelin and lymphocyte protein; MCT, monocarboxylate transporter; PCT, proximal convoluted tubule; PDZ domain, postsynaptic density protein-95/discs large/zonula occludens domain; pIgR, polymeric immunoglobulin receptor; PTH, parathyroid hormone
(Modified from (Weisz and Rodriguez-Boulan, 2009))

1.4.3. The diversity of molecular motors

A motor protein is generally described as a protein that uses energy in the form of ATP to generate directed movement along a filamentous track (Titus and Gilbert, 1999). There are three different classes of motor proteins: myosins, which move along actin filaments, and kinesins and dyneins, which move along microtubules. The dyneins are relatively conserved and there are two main classes of dyneins: axonemal and cytoplasmic (Tanaka et al., 1995;Porter, 1996). In contrast, kinesins and myosins have much more diversity. Thus, there are at least 17 classes of myosin and 14 distinct kinesin classes.

Many molecular motors are dimers with two “heads” connected together at a “stalk” region and a “tail” domain opposite the heads to which the cargo attaches. For both kinesin and myosin family motors, the head domains bind directly to the cytoskeletal substrate, microtubule or actin filament. Kinesins and myosins have a single ATP-binding site per head (Vale and Milligan, 2000), and these motors function as an enzyme to hydrolyze a single ATP molecule per step during movement (Coy et al., 1999;Rief et al., 2000). Some kinesins and myosins are known to be able to take many consecutive steps before detachment *in vitro*, a property known as processivity (Visscher et al., 1999;Rief et al., 2000). When moving *in vitro*, a single kinesin-1 motor protein typically takes about 100 steps with a fixed step size of 8 nm (Visscher et al., 1999;Svoboda and Block, 1994). The kinesin motor can exert a maximum force of about 6 pN and this value is almost independent of ATP concentration. The velocity of kinesin-1 is significantly reduced only at loads more than 3 pN (Visscher et al., 1999). Even under externally applied load, kinesin-1 rarely steps backward (Nishiyama et al., 2002). Amongst the myosins, myosin-V is the primary motor involved in vesicle transport (Vale, 2003). The *in vitro* stall force of myosin-V is about 3 pN and does not depend on ATP concentration (Mehta et al., 1999). Myosin-V does not show any significant back-steps up to loads of about 1 pN. At load of 2 pN, the back-step frequency increases and intermediate steps of half the size of usual step are seen (Rief et al., 2000). Like kinesin-1 and myosin-V, dynein is also a homodimer of two identical heavy chains, which make up the two motor domains. The head domain of dynein is massive (ca. 520 kDa) and much more complex than those of kinesins and myosins. Sequence analysis showed that dynein belongs to the AAA (ATPase associated with diverse cellular activities) class of proteins (King, 2000).

With a molecular weight of about 1.2 MDa, cytoplasmic dynein is a massive multisubunit complex almost ten times bigger than kinesin-1. In contrast to kinesin and myosin, it has multiple ATP-binding sites in each head (Gibbons et al., 1991). Additionally, the help of various accessory proteins, such as the dynactin complex is required for proper function (Burkhardt et al., 1997). The dynein head has seven globular domains, out of which six are AAA domains, arranged in a ring-like conformation around a central cavity (Samso

and Koonce, 2004). An interesting feature of this motor protein is that the dynein head makes contact with the microtubule through an unusual 13 nm long microtubule-binding stalk (Gee et al., 1997). The function of dynein differs significantly from kinesin and myosin. Thus, for example, dynein has a lower stall force: up to 1.1 pN (Mallik et al., 2004). Moreover, its mechanics depends on available ATP: going from micromolar to millimolar ATP concentrations, the stalling force increases by a factor of three, in contrast to the 20% change seen for kinesin-1 (Visscher et al., 1999). Dynein's step size changes significantly as a function of load (Mallik et al., 2004). It shows frequent backward motion and pauses, even when moving under no load (Wang et al., 1995). The mean run lengths for dynein are less than half of that for kinesin-1 (King and Schroer, 2000).

Thus, three classes of motor proteins provide a great diversity and fidelity for the intracellular trafficking machinery.

1.4.4. Kinesins

The kinesin superfamily proteins (also known as KIFs) are important molecular motors that directionally transport various cargos, including membranous organelles, protein complexes and mRNAs. Initially, five major kinesin families were discovered in the mouse brain (Aizawa et al., 1992). It is now thought that there are 45 mammalian KIF genes, but there could be twice as many KIF proteins as multiple isoforms can be generated by alternative mRNA splicing (Miki et al., 2001). All kinesins are divided into 15 families, which are termed kinesin-1 to kinesin-14B according to the results of phylogenetic analyss (Miki et al., 2001; Lawrence et al., 2004). These families can be grouped into three types, depending on the position of the motor domain in the molecule: N-, M- and C-kinesins have the motor domain in the amino-terminal, in the middle or in the carboxy-terminal region, respectively. In general, N- and C-kinesins move to the plus- and minus-ends of microtubules and M-kinesins depolymerize microtubules (Dagenbach and Endow, 2004).

- **Kinesin-1 group**

Kinesin-1, also called KIF5 or conventional kinesin, was the first identified and is the most abundant motor protein (Hirokawa et al., 1989; Vale et al., 1985). Three closely related subtypes: KIF5A, KIF5B and KIF5C compose the kinesin-1 group (Aizawa et al., 1992; Kanai et al., 2000). It is supposed that KIF5B is expressed ubiquitously, whereas KIF5A and KIF5C are neuron-specific (Kanai et al., 2000).

The KIF5 molecule is composed of the globular motor domain, the stalk domain and the tail domain (Hirokawa et al., 1989) (Fig. 1.6). It is a highly processive motor, which is able to take hundreds of 8 nm steps without falling off (Hackney, 1995). There is a general agreement that the two identical motor domains (“heads”) in the kinesin dimer move in a hand-over-hand manner, with the trailing head passing leading head and then attaching to the next available binding site on the microtubule (Yildiz et al., 2004; Asbury et al., 2003).

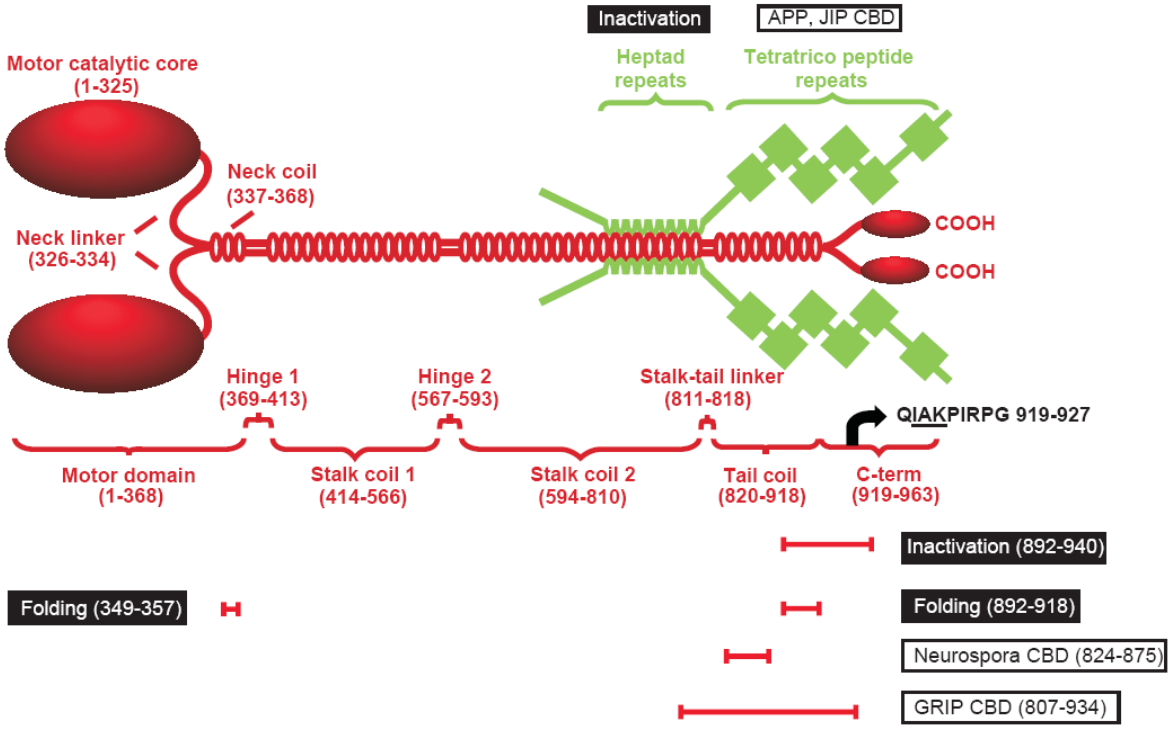

Figure 1.6. Domain organization of kinesin-1 (KIF5)

Heavy and light polypeptide chains are shown in red and green, respectively. Amino-acid residues in parentheses are referenced to the mouse KIF5B. Cargo-binding domains (CBD) are indicated by black on white labels; domains involved in regulation of motor activity are indicated by white on black labels. (Modified from (Schnapp, 2003))

Within a cell, about half of the KIF motor proteins form tetramers with two light chains (KLC) (Gyoeva et al., 2004). KIF5 binds KLCs through light chain-binding domains in the stalk and tail domains (Fig. 1.6) (Diefenbach et al., 1998;Gyoeva et al., 2004). In the tail domains at the C-terminus of the light chain-binding domain a specific cargo-binding region is situated (Seiler et al., 2000; Skoufias et al., 1994). It suggests that KIF5 can transport cargo either by direct binding or indirect through KLCs.

- **Kinesin-1 functions in axonal and dendritic transport**

In the neuronal axons, anterograde transport is powered mainly by N-kinesins, from the microtubule minus ends pointing to the cell body to the microtubule plus ends at the axon terminal. Retrograde transport is powered mainly by cytoplasmic dynein, but also sometimes by C-kinesins. Membrane organelles are transported by so called fast axonal transport at a similar speed to kinesin motors *in vitro* (50-200 mm per day). In contrast, cytoplasmic proteins, such as tubulin and neurofilament proteins, are transported by slow axonal transport (0.1 – 3 mm per day) (Terada, 2003). Although both types of transport are powered by N-kinesins, the mechanism that underlies this speed difference is still unclear. KIF5 motors transport synaptic vesicle precursors that contain synaptotagmin and synaptobrevin,

but also membrane organelles that contain presynaptic plasma membrane proteins, such as syntaxin 1 and SNAP25 (Byrd et al., 2001; Diefenbach et al., 2002; Su et al., 2004). SNAP25 interacts directly with KIF5 motors, whereas syntabulin binds to KIF5 motors and syntaxin 1, acting, probably, as an adaptor protein (Diefenbach et al., 2002; Su et al., 2004).

KIF5 motor proteins also play a role in the axonal transport of mitochondria. Targeted disruption of the kif5b gene in mice resulted in abnormal perinuclear clustering of mitochondria (Tanaka et al., 1998). Interestingly, all KIF5 isoforms – KIF5A, KIF5B, KIF5C – were able to rescue this mutant phenotype (Kanai et al., 2000). The adaptor proteins syntabulin, Ran-binding protein 2 (RanBP2) and the Milton-Miro complex were independently identified as mediators of mitochondrial binding to KIF5 motors (Cai et al., 2005; Glater et al., 2006; Cho et al., 2009).

Kinesin motor proteins are essential in the polarization of neurons. Recent studies suggest that the motor domain of KIF5 predominantly recognizes microtubules in axons and that kinesin-based transport is involved in the specification of a single axon from multiple neurites in neuronal development. Jacobson and colleagues found out that the constitutively active motor protein KIF5C ($KIF5C^{560}$) concentrates in only one or two growth cones at a time in one of the early stages of developing neurons (Jacobson et al., 2006). It is one of the earliest known molecular differences between seemingly equivalent neurits at this stage. But such a polarized distribution of KIF5C in one neurite does not necessarily predict that this neurite will be an axon. Nevertheless, its strong accumulation precedes the fast outgrowth of the axon. The role of KIF5C in this processs is still debatable. According to one hypothesis, polarized membrane flow precedes axon formation (Bradke and Dotti, 1997). Then, the function of KIF5C in neuritis might be an efficient transport of membranes and membrane proteins to the growth cone of the presumptive axon (Ye and Jan, 2006). Alternatively, KIF5C might transport signaling molecules such as GSK3β, Rap1B and CRMP2 to the axonal growth cone, promoting the specification of axons (Ye and Jan, 2006).

KIF5 motors can transport also other cargos in axons. KIF5 motors can bind to their cargo at least through two different regions. The KIF5 stalk domain can bind to KLCs, which in turn associate with certain cargos (Diefenbach et al., 1998), or the specific cargo-binding region of the KIF5 tail domain can bind to cargo directly (Skoufias et al., 1994). The tetratricopeptide repeat (TPR) domain of KLCs binds to cargos such as JUN N-terminal kinase (JNK)-interacting proteins (JIPs) (Verhey et al., 2001). β-Amyloid precursor protein (APP) has also been shown to bind to KLC for transport (Kamal et al., 2000).

Much less is known about the role of kinesin-1 in dendritic transport. It was demonstrated that KIF5 motors can bind directly to and transport large RNase-sensitive granules – messenger ribonucleoprotein (mRNP) complexes, which contain mRNA and at least 40 kinds of proteins (Kanai et al., 2004). Fragile X mental retardation protein (FMRP) has been implicated in the connection of mRNA to the KLC (Dictenberg et al., 2008). Nevertheless, the

detailed mechanism and role of the formation of this complex remains still unknown. The cargo-binding domain of KIF5 binds also to the adaptor glutamate receptor-interacting protein 1 (GRIP1) and this interaction recruits kinesin to the soma and dendrites of neurons (Setou et al., 2002).

- **Kinesin-1 in conventional transport**

Kinesin-1 plays an important role not only in axonal and dendritic transport, but also in transport inside the soma of neurons and in non-neuronal cells. Thus, for example, kinesin-1 transport cargo from the Golgi to the ER and from the *trans*-Golgi network to the plasma membrane. But it should be mentioned that the physiological relevance of KIF5 motors and the 160 kDa isoform of the kinesin-binding protein kinectin in Golgi – ER retrograde transport is debated. Kinectin is localized to the integral ER membrane of non-neuronal cells and it was thought to function in the extension of the ER (Santama et al., 2004). But both kif5b- and kinectin-knockout mice show no abnormalities in ER structure (Tanaka et al., 1998; Plitz and Pfeffer, 2001). A new argument for the role of kinesin-1 in ER-to-Golgi trafficking was the finding that kinesin light chains, KLC1B and KLC1D, bind to rough ER and Golgi vesicles, respectively (Wozniak and Allan, 2006).

Better understood is the role of kinesin-1 in Golgi-to-plasma membrane trafficking. Various marker proteins have been used to study this process. In non-polarized cells, KIF5 have been shown to transport the *post*-Golgi traffic marker, VSVG, to the plasma membrane (Lippincott-Schwartz et al., 1995). In MDCK cells, KIF5B transports the raft-independent apical marker p75 to the plasma membrane, but only after the polarization of the cells (Jaulin et al., 2007). KIF5 motors are also involved in the transport of various endosomal compartments. The dynamic distribution of lysosomes in the cytoplasm was blocked in kif5b-knockout mice and was inhibited by a dominant negative KIF5 mutant (Tanaka et al., 1998; Nakata and Hirokawa, 1995). Also melanosomes are transported by KIF5B, which works together with dynein and KIF3 (Gross et al., 2002). Early endosomes, containing Rab5 and Rab4, are driven by KIF5, as well as by dynein, KIF3 and KIFC2 motors (Bananis et al., 2000; Imamura et al., 2003).

- **Regulation of kinesin-1 interaction with cargo**

Interaction between a motor protein and the cargo should be regulated with high fidelity. Selection and attachment of kinesin to the cargo at the starting point of transport, processive transport itself, detachment from the cargo at the appropriate time and place, inactivation of kinesin – all these processes are important for the effective trafficking in the cells. Phosphorylation is one of the well-studied regulation mechanisms. Kinesins are phosphoproteins and at least two mechanisms for the phosphorylation-dependent regulation

of kinesins were predicted (Hirokawa et al., 2009). First, kinesin phosphorylation can affect the cargo binding, and, second, it may modulate the interaction of kinesins with microtubules. Several examples for the role of phosphorylation in kinesin-1 activity are already known. Thus, protein kinase A-dependent phosphorylation of KIF5-KLC complexes inhibits its association with synaptic vesicles (Sato-Yoshitake et al., 1992). Also glycogen synthase kinase 3 inhibits association of motor protein complex with membrane organelles through KLC phosphorylation (Morfini et al., 2002). JNK can also phosphorylate KIF5 motors, resulting in the weakening of kinesin-microtubule interaction (Morfini et al., 2006; Stagi et al., 2006). Interestingly, genetic experiments revealed that the JNK pathway upregulates, rather than downregulates, KIF5-dependent axonal transport in *C. elegans* and *D. melanogaster* (Horiuchi et al., 2007; Byrd et al., 2001). Also phosphorylation of adaptor proteins might regulate cargo-motor interactions. For example, the adaptor protein UNC76 is required for the axonal transport of synaptotagmin-carrying vesicles in *D. melanogaster* and it is suggested that KIF5 interacts with synaptotagmin through UNC76 (Gindhart et al., 2003). And this interaction can occur only after phosphorylation of UNC76 by an autophagy-related kinase UNC51 (Toda et al., 2008).

Another way of the regulation of cargo-motor interaction can be Ca^{2+}-signalling. As mentioned above, KIF5 plays a role in mitochondrial transport (Tanaka et al., 1998). It was also found that Ca^{2+} significantly arrests mitochondrial motility (Yi et al., 2004). Recently it has been proved, that Ca^{2+}-binding permits Miro to interact directly with the motor domain of kinesin-1, preventing motor-microtubule interactions (Wang and Schwarz, 2009).

1.5. Annexins

1.5.1. Annexin family

Annexins are a family of Ca^{2+}-dependent phospholipid and membrane binding proteins. More than thousand proteins of the annexin superfamily have been identified so far (Moss and Morgan, 2004). In general, annexin consists of a conserved C-terminal core domain and a short variable N-terminal domain. The core domain is made up of four similar repeats approximately 70 amino acids long, each containing a characteristic "type 2" motif for calcium ions binding (Fig. 1.7). Thus, annexins provide a link between Ca^{2+} signalling and membrane dynamics, such as the regulated organization of membrane domains, membrane-cytoskeleton linkages and certain exocytic and endocytic transport steps. By forming networks on the membrane surface, annexins can function as organizers of membrane domains and membrane-recruitment platforms for proteins which they interact with.

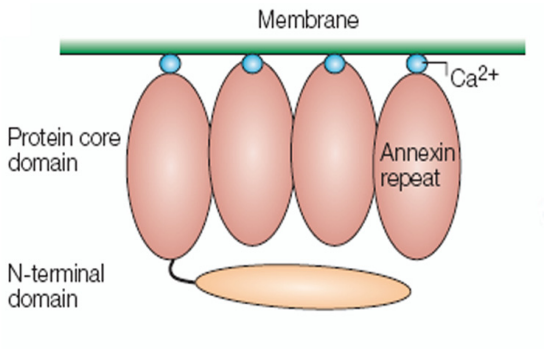

Figure 1.7. Annexin structure

A schematic drawing of an annexin that is peripherally attached to a membrane surface through bound Ca^{2+} ions.
(Modified from (Gerke et al., 2005))

Thus, for example, annexin A2 is implicated in the organization of membrane lipids at sites of actin cytoskeleton attachment. In the first studies it was identified as a component of the filamentous F-actin-rich comet tails that propel newly formed endocytic vesicles from the plasma membrane (Merrifield et al., 2001). Later, annexin A2 was shown to be a component of the F-actin pedestals that form the membrane-attachment sites of *E. coli* (Zobiack et al., 2002). These two processes are characterized by a dynamic reorganization of actin at membrane sites that are enriched in phosphatidylinositol 4,5-bisphosphate ($PtdIns(4,5)P_2$). Further studies on the specificity of annexin A2 interaction with lipids led to the idea that annexin A2 plays a role in the organization of lipid-raft-like membrane domains at sites of actin recruitment. In smooth muscle cells annexin A2 has been shown to be involved in the Ca^{2+}-dependent organization of lipid rafts (Babiychuk and Draeger, 2000). Moreover, annexin A2 is a component of mature cholesterol-rich junctions in endothelial cells. Here, it associates with the tyrosine phosphatise SHP2 (SH2-domain containing phosphatise-2) and

exists in complex with Rac1 at cell-cell contact sites between polarized epithelial cells (Hansen et al., 2002). Another example of the role of annexins in the membrane-cytoskeleton interaction is annexin A11. It is a midbody protein in cytokinesis and probably functions in the last step of cytokinesis, when abscission occurs and two daughter cells separate (Tomas et al., 2004).

Annexins also play an important role in exocytosis and endocytosis (Fig. 1.8). Several annexins, in particular annexins A1, A2 and A6 are present on endosomal compartments (Emans et al., 1993; Jost et al., 1997). Annexin A2 associates with endosomes at specific sites (possibly cholesterol-enriched domains) to provide a membrane scaffold that is required for the formation of elongated endosomal tubules and the detachment/biogenesis of certain regions (Gruenberg and Stenmark, 2004). Annexin A1 is involved in the inward vesiculation in multivesicular endosomes (Futter et al., 1993). By using a truncated annexin A6 mutant, Kamal et al. have shown that a cysteine-protease-dependent type of budding of clathrin-coated pits requires annexin A6 and its association with non-erythroid spectrin (Kamal et al., 1998). Another role of annexins is the ion channel regulation. Thus, for example, annexins A2, A4 and A6 function as modulators of plasma-membrane Cl^--channels and sarcoplasmic reticulum Ca^{2+}-release channels (Gerke and Moss, 2002). Annexin A2 in complex with S100A10 is required for the trafficking of various channels (e.g. TASK1, TRPV5) to the plasma membrane (Girard et al., 2002; van de Graaf et al., 2003). Annexin A7 was first discovered as a protein that promotes the contact and fusion of chromaffin granules, the secretory vesicles of adrenal medulla. Interestingly, it is not a fusogenic protein – it promotes only the close attachment of membranes (Creutz et al., 1978). Several studies have also demonstrated that annexin A2 is involved in Ca^{2+}-regulated exocytosis. Its activity in this case is regulated by PKC (Sarafian et al., 1991). In polarized epithelial cells annexin A2 associates with lipid raft-containing apical vesicular or tubulo-vesicular carrier populations, but is not involved in raft-independent apical trafficking (Jacob et al., 2004; Danielsen et al., 2003). Moreover, the interaction in a complex with S100A10 subunit with lipid rafts has been demonstrated (Oliferenko et al., 1999). The S100A10 subunit is also involved in trafficking of various channel proteins (Girard et al., 2002). All these data suggest that annexin A2-S100A10 complex forms a link between lipid raft carrying vesicles and cytoskeletal microfilaments (Jacob et al., 2004).

Thus, one of the main features of annexins is their unique mode of membrane interaction, which can influence many membrane-related processes. However, the precise function and mechanism of regulation of individual annexins is still not fully understood.

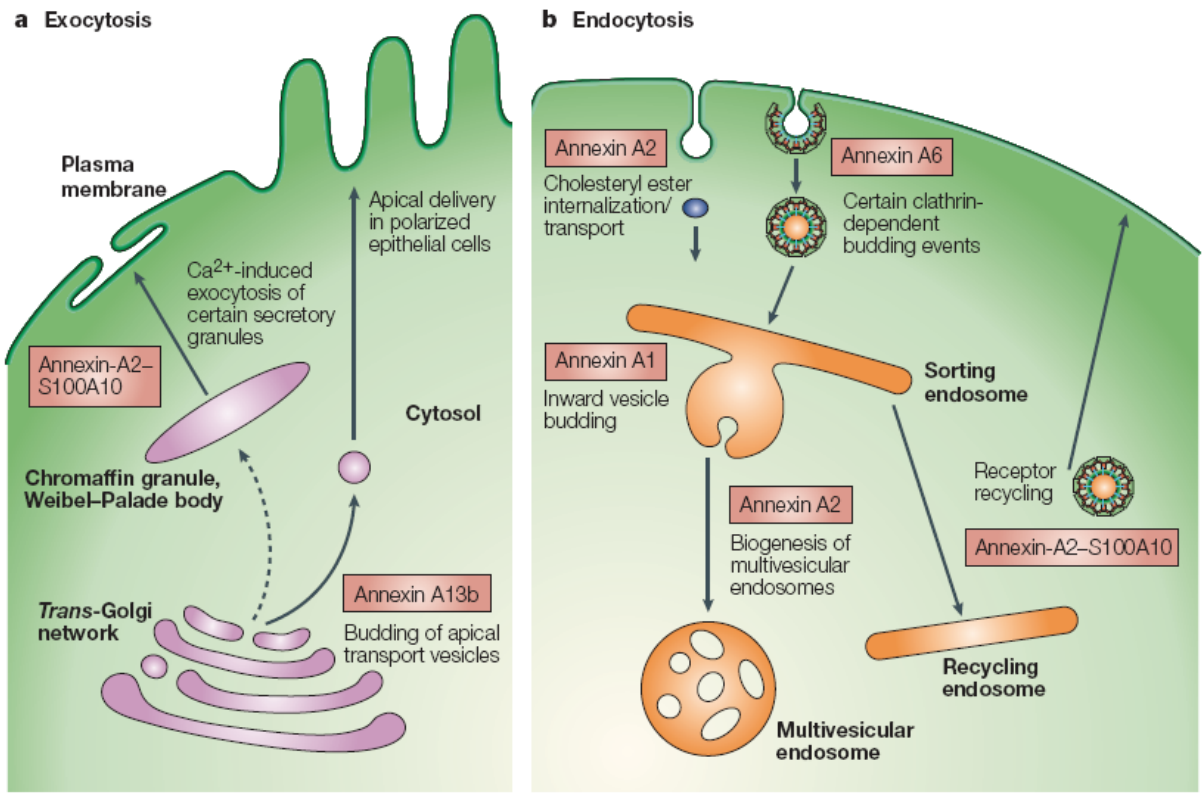

Figure 1.8. Annexins in membrane organization and trafficking

A schematic representation of various membrane-trafficking steps showing the involvement of annexins in the biosynthetic (a) and endocytic (b) pathways.
(Modified from (Gerke et al., 2005))

1.5.2. Annexin XIIIb

Annexin XIII is a key member of vertebrate annexins. The relationship of its gene organization with that of protists and plants indicates that it is the most ancient member of vertebrate annexins (Morgan and Fernandez, 1997). The annexin XIIIs are the only family members which are myristoylated on their N-terminal glycine residue (Wice and Gordon, 1992b). Two isoforms, annexin XIIIa and annexin XIIIb, are expressed in epithelial cells (Fiedler et al., 1995). Annexin XIIIa accumulates at the basolateral and apical plasma membrane (Lecat et al., 2000). This annexin, as well as annexin XIIIb, stimulates the apical transport of raft-associated hemagglutinin. However, only the basolateral pool of annexin XIIIa inhibits the transport of the vesicular stomatitis virus G protein (Lecat et al., 2000). Regarding their primary structure, annexin XIIIb differs from annexin XIIIa by an insertion of 41 amino acid residues after the first four residues of the amino-terminal domain (Fig. 1.9). Annexin XIIIb is expressed exclusively in the small intestine and in the kidney, where it concentrates preferentially in the apical brush border rather than in basolateral membranes (Lecat et al., 2000; Wice and Gordon, 1992a). Annexin XIIIb associates specifically with lipid raft domains of the *trans*-Golgi network, and the N-terminally

myristoylation of annexin XIIIb is required for the budding of these domains, which are then delivered to the apical surface (Lafont et al., 1998). The colocalization of annexin XIIIb with KIFC3, a minus end-directed motor, supports further the participation of this protein in the formation and docking of vesicles from the *trans*-Golgi network to the apical membrane (Noda et al., 2001). Moreover, annexin XIII knockdown causes also perturbations of epithelial 3D cyst morphogenesis and ciliogenesis (Torkko et al., 2008). Nevertheless, the role of annexin XIIIb in the apical trafficking of raft-independent cargo remains still unclear.

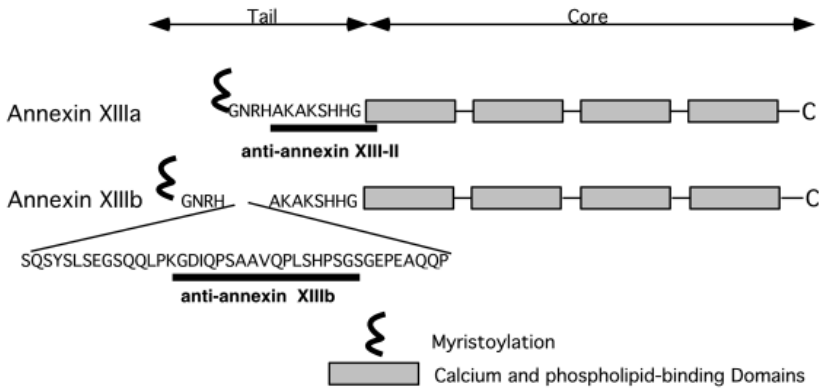

Figure 1.9. Comparison of the sequences of annexin XIIIa and XIIIb

The peptide sequences of the tails recognized by the specific antibodies are underlined. (Modified from (Lecat et al., 2000))

1.6. Aims of the study

Polarized epithelial cells are characterized not only by two separate membrane domains: apical and basolateral, but also by the intracellular sorting and trafficking machinery, which generates and maintains this epithelial asymmetry. This machinery forms a network of various pathways, signal-receptor interactions, membrane reorganization and intermediate compartments, traversed on the way to the final destination. Although some details of this process are already known (Delacour and Jacob, 2006; Weisz and Rodriguez-Boulan, 2009), the role of many proteins in apical trafficking remains still unclear.

The aim of the first part of the current study was to characterize novel motor proteins, which are involved in the *post*-Golgi protein transport. Untill now, only a few motor proteins have been known in apical trafficking and the function of each of them was restricted to the only one model protein studied (see Table 1.2). Thus, for example, in polarized MDCK cells KIF5B was shown to transport raft-independent p75 (Jaulin et al., 2007). Additionally, the role of dynein and two kinesins – KIFC3 and KIF5 – in the apical delivery of HA was demonstrated (Lafont et al., 1994; Noda et al., 2001). Nevertheless, no general motor protein for several pathways could have been identified so far. Also the exact steps on the way from the TGN to the apical membrane, where these motor proteins act, are still to be studied.

The second part was focused on the role of annexin XIIIb in apical transport. It has been known already that this protein associates with the raft-dependent pathway (Lafont et al., 1998). Recently, annexin XIIIb has been found by mass spectrometry in raft-independent p75-carrying vesicles (D.Delacour, (Astanina et al., 2010)). Thus, the aim of this part of the thesis was to characterize the role of annexin XIIIb in raft-independent pathway, as well as to clarify the mechanism of its functioning in apical trafficking in general.

2. Materials and methods

2.1. Materials

2.1.1. Laboratory equipment

- Incubators
  Cell culture CO_2 incubators (Heraeus, Newport Pagnell, UK), Forma series II Water Jacketed CO_2 incubator (Thermo Fischer Scientific, Schwerte, Germany)

- Laminar flow hood
  HeraSafe (Kendro Laboratory Products, Hanau, Germany)

- Centrifuges
  Ultracentrifuge Sorvall CombiPlus (rotor TH 641) (DuPont, Wilmington, USA), ultracentrifuge Optima LE-80K (rotor SW 41) and table cooling centrifuge Allegra X-22R (Beckman Coulter, Krefeld, Germany), table centrifuge Biofuge pico and cooling centrifuge Biofuge fresco (Heraeus, Newport Pagnell, UK), table centrifuge Rotofix 32A (Hettich, Tuttlingen, Germany), SpeedVac Univapo 100H (Uniequip, Leipzig, Germany)

- Heating blocks and shakers
  Thermomixer comfort (Eppendorf, Hanau, Germany), heating block UBD (Grant Instruments, Cambridge, UK), Mixing block MB-102 (BIOER, Hangzhou, P.R.China)

- Microscopes
  Confocal fluorescent microscope TCS SP2 and TIRF-microscope DMI 6000 B (Leica Microsystems, Wetzlar, Germany), optical microscope Axiovert 10 (Zeiss, Jena, Germany)

- Shakers
  Overhead shaker Reax 2 (Heidolph, Schwabach, Germany), platform shaker KS10 (Bühler, Tübingen, Germany), rocking shaker STR8 (Stuart Scientific, Essex, UK)

- Electrophoresis and blotting instruments
  Mini-VE system (Hoefer, San Francisco, USA), Trans-Blot SD semi-dry Transfer Cell (BioRad, Munich, Germany)

- MALDI-TOF

  Voyager DE STR instrument (PerSeptive Biosystems, Ramsey, USA), Ultraflex Instrument (Bruker Daltonik GmbH, Bremen, Germany)

- Other equipment

  Gel dryer model 583 (BioRad, Munich, Germany), analytical balances SBC 22 (ScalTec Instrument, Göttingen, Germany), precise balances APX-1502 (Denver Instrument, Göttingen, Germany), pH meter Cyberscan pH510 (Eutech Instruments, Nijkerk, Netherlands), phosphoimager FLA-3000 (Fujifilm, Tokio, Japan), magnetic stirrer Yellow Line MSH basic (Ika-Werke, Staufen, Germany), ChemiLux Imager (Intas, Göttingen, Germany), peristaltic pump Miniplus3 (Abimed/Gilson, Villiers-le-Bel, France)

2.1.2. Antibodies

Table 2.1. Primary antibodies

Antibody	Host	Clonality	Source
annexin XIIIb	rabbit	polyclonal	K. Simons (Max Planck Institute of Molecular Cell Biology and Genetics, Dresden, Germany)
dynein IC	mouse	monoclonal	Novus Biologicals (Cambridge, UK)
E-Cadherin	mouse	monoclonal	BD Biosciences (Heidelberg, Germany)
EEA1	mouse	monoclonal	BD Biosciences (Heidelberg, Germany)
galectin-3	rabbit	polyclonal	H.P. Elsaesser (University of Marburg, Germany)
GAPDH	mouse	monoclonal	Assay Designs (Ann Arbor, USA)
GFP (JL-8)	mouse	monoclonal	Clontech (Saint-Germain-en-Laye, France)
GM130	mouse	monoclonal	BD Biosciences (Heidelberg, Germany)
gp114	mouse	monoclonal	K. Simons (Max Planck Institute of Molecular Cell Biology and Genetics, Dresden, Germany)
gp135	mouse	monoclonal	G. Ojakian (State University of New York Health Science Center, New York, USA)
H1	mouse	monoclonal	Chemicon (Schwalbach, Germany)
H2	mouse	monoclonal	Abcam (Cambridge, UK)
KHC	mouse	monoclonal	US Biological (Swampscott, MA, USA)
KIF5A	rabbit	polyclonal	Abcam (Cambridge, UK)
KIF5B	goat	polyclonal	Everest Biotech (Upper Heyford, UK)
KIF5C	rabbit	polyclonal	Acris Antibodies (Hiddenhausen, Germany)
LPH	mouse	monoclonal	H. P. Hauri (Biocenter, University of Basel,

			Switzerland)
myc	mouse	monoclonal	Invitrogen (Darmstadt, Germany)
p230	mouse	monoclonal	BD Biosciences (Heidelberg, Germany)
p75 (ME20.4)	mouse	monoclonal	A. Le Bivic (Faculte des Sciences de Luminy, Marseille, France)
PDI	mouse	monoclonal	BD Biosciences (Heidelberg, Germany)
Rab10	rabbit	polyclonal	Sigma-Aldrich (Munich, Germany)
Rab7	rabbit	polyclonal	A. Wandinger-Ness (University of New Mexico Health Sciences Center, Albuquerque, New Mexico)
Rab8	mouse	monoclonal	BD Biosciences (Heidelberg, Germany)
SI	mouse	monoclonal	H. P. Hauri (Biocenter, University of Basel, Switzerland)

Table 2.2. Secondary antibodies

Antibody	Host	Conjugate	Source
anti-mouse	goat	HRP	Biorad (Munich, Germany)
anti-rabbit	goat	HRP	Biorad (Munich, Germany)
anti-goat	mouse	HRP	Antibodies-online (Aachen, Germany)
anti-mouse	goat	AlexaFluor 488	Invitrogen (Darmstadt, Germany)
anti-mouse	goat	AlexaFluor 546	Invitrogen (Darmstadt, Germany)
anti-rabbit	goat	AlexaFluor 488	Invitrogen (Darmstadt, Germany)
anti-rabbit	goat	AlexaFluor 546	Invitrogen (Darmstadt, Germany)

Table 2.3: Isotype-specific and non-specific antibodies directed against KIF5 kinesins.

Antibody	Immunogen, epitope	Specificity	Applications	Reference
H1	Bovine brain kinesin, N-terminus	KIF5A* KIF5C	WB	(Kanai et al., 2000; Cai et al., 2001)
H2	Bovine brain kinesin, N-terminus	KIF5A, KIF5B, KIF5C	IP	(Kanai et al., 2000; Cai et al., 2001)
KHC	Bovine brain kinesin, N-terminus	KIF5A, KIF5B, KIF5C	WB	
KIF5C	Synthetic peptide corresponding to amino acid residues 938-957 from human kinesin 5C. Amino acid sequence: C A(938)VHAIRGGGSSSNSTHY QK(957)	KIF5C	IP, IF	see Fig. 3.4
KIF5B	Peptide with sequence C-QPVAVRGGGGKQV, from the C-terminus of the KIF5B protein sequence according to NP_004512.1	KIF5B	IP, WB	see Fig. 3.4

* H1 antibody has very low affinity for canine KIF5A as depicted in Fig. 3.3. IF, immunofluorescence; IP, immunoprecipitation; WB, Western blot

Table 2.4. Plasmids

Plasmid	Source
pAnxXIIIb-DsRed-C1	Cloned by C. Delebinski (University of Marburg, Germany)
pLPH-cDNA3 Myc/His	(Jacob and Naim, 2001)
pSI-EYFP-C1	(Jacob and Naim, 2001)
p75-pEYFP-N1, -pDsRed-N1	(Kreitzer et al., 2000), recloned by D. Schneider (University of Marburg, Germany)
p50-Dynamitin-GFP	C. Hoogenraad (Erasmus MC, Rotterdam, Netherlands)

2.1.3. Buffers and Solutions

Where solvents are not specified, bidistilled water (ddH_2O) was used as a solvent.

- ATP-Regenerating System (RS) (100×)
  8 mg/ml creatine kinase, 1.6 M creatine phosphate were prepared separately in Buffer for Oxygen scavenging system/ATP-regenerating system (OSS/RS), frozen in 20-50 µl aliquots in liquid nitrogen and stored at -80 °C. Before use, the stocks were thawed on ice, the 10×RS was prepared and stored on ice for 1-2 h.

- Buffer for Oxygen scavenging system/ATP-regenerating system (OSS/RS)
  12 mM Pipes (pH 6.8), 2 mM $MgCl_2$, 1 mM EGTA

- Co-IP Lysis Buffer
  25 mM Tris-HCl (pH 7.5), 1 mM EDTA, 1 mM EGTA, 100 mM NaCl, 1% Triton X-100, 0.5% NP-40

- Destaining Solution
  50% CH_3CN, 0.5% $(NH_4)_2CO_3$

- Extraction Solution
  0.1% Trifluoracetic acid (TFA), 50% acetonitrile (ACN)

- Gel Fixation Solution
  10% CH_3COOH, 25% 2-propanol

- General Tubulin Buffer (GTB)
  80mM Pipes (pH 7.0), 1mM EGTA, 1mM $MgCl_2$

- IP Lysis Buffer
  25 mM Tris-HCl (pH 8.0), 50mM NaCl, 0.5% Sodium desoxycholate, 0.5% Triton X-100

- Laemmli Loading Buffer (3×)
  6% SDS, 30% glycerol, 150 mM Tris-HCl (pH 6.8), 0.02% Bromphenol blue, 150mM DTT

- Oxygen Scavenging System (OSS) (100×)
  50% β-mercaptoethanol, 20 mg/ml glucose oxidase, 3.5 mg/ml catalase, 450 mg/ml glucose
  The glucose oxidase and catalase were prepared in Buffer for OSS/RS, frozen in 20-50 µl aliquots in liquid nitrogen and stored at -80 °C. Before use, 50% β-mercaptoethanol solution was prepared and stored on ice. Thereafter, a 10×OSS was prepared on ice. The glucose was added the last, after mixing all other components. The 10×OSS was stored in tightly closed tube on ice for 2 h.

- Phosphate-buffered saline (PBS)
  137 mM NaCl, 2.7 mM KCl, 1.4 mM KH_2PO_4, 10 mM Na_2HPO_4

- PMEE Lysis Buffer
  35 mM Pipes (pH 7.4), 5 mM $MgCl_2$, 1 mM EGTA, 0.5 mM EDTA, 4 mM DTT, 250 mM sucrose

- PMEE Motility Buffer
  35 mM Pipes (pH 7.4), 10 mM $MgCl_2$, 1 mM EGTA, 0.5 mM EDTA, 4 mM DTT, 20 µM Taxol, 1×OSS, 1×RS, 2.5 mM MgATP

- PMEE Motility Washing Buffer
  35 mM Pipes (pH 7.4), 10 mM $MgCl_2$, 1 mM EGTA, 0.5 mM EDTA, 4 mM DTT, 20 µM Taxol, 5 mg/ml BSA

- PMEE Sucrose Gradient Solution
  35 mM Pipes (pH 7.4), 5 mM $MgCl_2$, 1 mM EGTA, 0.5 mM EDTA, 4 mM DTT, sucrose (0.8 M, 1.16 M, 1.3 M, 2 M)

- PMEE Washing Buffer
  35 mM Pipes (pH 7.4), 5 mM $MgCl_2$, 1 mM EGTA, 0.5 mM EDTA, 4 mM DTT, 250 mM sucrose

- Protease Inhibitors Mix
  1 µg/ml pepstatin (in DMSO), 1 µg/ml antipain (in DMSO), 5 µg/ml leupeptin (in PBS), 5 µg/ml aprotinin (in PBS), 5 µg/ml trypsin/chymotrypsin inhibitor (in PBS)

Protease Inhibitors Mix was prepared in PBS and stored at -20 °C in 500 µl aliquots. Directly before use, each aliquot was mixed with 25 µl of PMSF solution (3.4 mg/ml in DMSO).

- Roti-Blue Fixation Solution
  1% orthophosphoric acid (85%), 20% methanol

- Roti-Blue Stabilizing Solution
  20% $(NH_4)_2SO_4$

- Roti-Blue Staining Solution
  20% methanol, 20% Roti-Blue Dye (5×)

- Roti-Blue Washing Buffer
  25% methanol

- SDS Running Buffer
  25 mM Tris, 190 mM Glycin, 0.1% SDS

- Trypsin-mix (for MALDI-TOF)
  0.01 µg/µl Trypsin in 50 mM NH_4HCO_3 (pH 7.8)

- Washing Buffer I
  0.5% Triton X-100, 0.05% Sodium desoxycholate in 1×PBS

- Washing Buffer II
  500 mM NaCl, 125 mM Tris-HCl (pH 8.0), 10 mM EDTA, 0.5% Triton X-100

- Western Blot Blocking Solution
  5% skimmed milk in 1×PBS

- Western Blot Buffer
  25 mM Tris, 192 mM Glycin, 20% methanol

2.2. Methods

2.2.1. *In vitro* assays

- ***In vitro* microtubule polymerization**

Formation of Taxol stabilized microtubules was performed according to the manufacturer's protocol (Cytoskeleton, Denver, USA). Lyophilized rhodamine-tubulin (Cytoskeleton, Denver, USA) was reconstituted to final concentration 5 mg/ml in ice-cold General Tubulin Buffer (GTB) plus 10% glycerol and 1 mM fresh GTP (Cytoskeleton, Denver, USA). The aliquots were snap frozen in liquid nitrogen and stored at -70 ºC. To prepare the microtubules, GTB plus 10% glycerol was warmed up to 37 ºC. An aliquot of tubulin was quickly thawed and incubated at 37 ºC for 20 min to allow microtubules formation. After the tubulin has incubated for 15 min, the GTB plus glycerol was removed from 37 ºC and taxol (Cytoskeleton, Denver, USA) was added to give a final concentration of 20 µM. The GTB-glycerol-Taxol solution was left at room temperature. After the tubulin has incubated for 20 min, it was removed from the water bath and GTB-glycerol-Taxol solution was added immediately. The sample was mixed thoroughly but gently. Depending on the experiments, the microtubules were diluted in GTB-Taxol solution to the necessary concentration of microtubules. The microtubules were stored in darkness at room temperature and were stable for 2-3 days.

- ***In vitro* motility assay**

The *in vitro* motility assay was modified from Bananis et al. (Bananis et al., 2000) and from Mitchinson Lab protocols(http://mitchison.med.harvard.edu/protocols.html).

The assay was performed in self-made perfusion chambers, consisting of two coverslips (one round, 45 mm Ø, and a square one, 45×45 mm). The round coverslip was covered with 0.2 mg/ml DEAE-Dextran and dried. The square coverslip was fixed on the round one by two stripes of double-sided adhesive tape, so that the inner volume of the perfusion chamber was about 15-20 µl.

The vesicles were purified from $MDCK_{p75\text{-}GFP}$ cells as described below. After ultracentrifugation, vesicle-enriched fraction 9 was collected and fresh protease inhibitor-mix was added. The *in vitro* polymerized microtubules (see above) were added to the perfusion chamber and incubated at room temperature. After 3-5 min unbound microtubules were washed out with Motility Washing Buffer. Thereafter, the vesicle fraction was added to the chamber for 5-10 min. At this time, Oxygen Scavenging System and ATP-Regenerating System were prepared on ice. After thorough washing of the chambers with Motility Washing Buffer, Motility Buffer was prepared, warmed up to room temperature and added to the perfusion chamber. The chamber was put into the 37 ºC thermal-controlled chamber at the Leica DMI 6000 B Microscope (Leica Microsystems, Wetzlar, Germany) and the recording

was started. The velocity of the vesicles from 3 independent experiments was measured using Volocity software (Improvision)

- ***In vitro* binding assay**

The *in vitro* binding assay was modified from Blocker et al. (Blocker et al., 1996). Purified vesicles were heated to 80 ºC for 10 min or treated with trypsin (final concentration 100 µg/µl) at 37 ºC for 15 min. Trypsin was inactivated with 3,4-dichloroisocoumarin. The assay was performed in principle as *in vitro* motility assay (see above), but no ATP was added to the Motility Buffer. The proportion of bound vesicles to the total amount of vesicles in every microscope field was counted. At least three independent experiments were analyzed.

2.2.2. Immunoprecipitation

- **Vesicle immunoprecipitation**

Vesicle immunoprecipitation was performed essentially as published before (Cramm-Behrens et al., 2008). The cells were grown on 10 cm plates for 5 days after seeding to get full polarization. To accumulate newly synthesized material in TGN, the cells were incubated at 20 ºC for 4 h and then shifted to 37 ºC for various time intervals (TGN exit). The cell plates were put on ice, washed with PMEE Washing Buffer and scraped in PMEE Lysis Buffer. Cell suspension was homogenized by 20 passages through a 26-gauge needle. To get rid of nuclei and non-destroyed cells, the samples were centrifuged at 2000 g for 5 min at 4 ºC. The supernatant was loaded on the top of four-step sucrose density gradient (1 ml 2M, 4 ml 1.3M, 3.5 ml 1.16M, 2 ml 0.8M). The gradients were placed into a SW41 rotor (Beckman) and centrifuged for 2.5 h at 4 ºC at 47000×g in Beckman Optima LE-80k ultracentrifuge. The 1 ml fractions were collected from the bottom of the tube with glass micropipette and a peristaltic pump. The TGN-38-positive fractions 8, 9 and 10 were used for immunoprecipitation with monoclonal anti-GFP, monoclonal anti-myc or polyclonal anti-KIF5C antibodies. The samples were first precleared for 1 h at 4 ºC with Protein-A sepharose (PAS). The PAS was then pelleted and the supernatant was incubated for 1 h with specific antibody. PAS beads were added for overnight precipitation. Antigen-antibody complexes on PAS beads were pelleted by centrifugation at 2000×g and the samples were washed six times with PMEE Washing Buffer prior to SDS-PAGE analysis.

- **Surface immunoprecipitation**

$MDCK_{p75\text{-}GFP}$, $MDCK_{SI}$ or $MDCK_{LPH}$ cells were grown on *trans*-well filters and transfected with 100 pmol specific siRNA on the 1^{st} and 3^{d} day after seeding. On the 5^{th} day the cells were washed two times with PBS and incubated for 1.5 h at 37 ºC with methionine-free medium

("starvation"). Thereafter, the medium was replaced with fresh methionine-free medium and 40-60 µCi of [^{35}S]Methionine was added to the basolateral medium. After 2 h of labeling at 37 ºC the cells were washed with PBS and normal medium was added and the cells were incubated again at 37 ºC ("chase"). After 4 h the specific antibodies (monoclonal anti-p75, anti-SI or anti-LPH) were added either to the apical or to the basolateral medium and the cells were incubated at rocking shaker at 4 ºC. After 2 h the cells were washed 5 times with ice-cold 0.1% BSA PBS and one time with ice-cold PBS. To each filter 500 µl of IP Lysis Buffer was added, the cells were scraped and cell suspension was put in 1.5 ml tubes. The samples were put then in overhead shaker and incubated for 30 min. To get rid of cell debris, the samples were centrifuged at 4 ºC at 13000×g for 30 minutes. PAS beads were added to the supernatant for overnight precipitation. On the next day, PAS-antibody-protein complexes were spinned down by centrifugation at 4 ºC at 5000×g for 1 min. Cytosolic apical proteins were immunoprecipitated from the remaining supernatant for comparison. The samples were washed 2 times with Washing Buffer I and 2 times – with Washing Buffer II. The immunoprecipitates were subjected to SDS-PAGE, followed by phosphoimager analysis.

- **Surface immunoprecipitation – kinetics study**

Analysis of the kinetics of apical protein surface delivery was performed essentially as surface immunoprecipitation (see above), but the cells were labelled for 15 min only and thereafter the cells were incubated at 20 ºC for 4 h to accumulate newly synthesized material in the TGN. TGN release was performed at 37 ºC for different time intervals. The marker proteins were immunoprecipitated from apical, but not from the basolateral membrane.

- **Protein immunoprecipitation**

The cells were washed two times with ice-cold PBS scraped and lysed in IP Lysis Buffer. The samples were then incubated for 1 h at 4 ºC in overhead shaker. To remove insoluble material, the lysates were centrifuged at 13000×g for 5 min at 4 ºC. The PAS or PGS beads were added to the supernatants for preclearing for 1 h at 4 ºC. Thereafter, the beads were spinned down at 5000×g for 1 min at 4 ºC. Specific antibodies were added to the precleared cell lysates for overnight precipitation in overhead shaker at 4 ºC. As a negative control, no antibody was added. On the next day, the PAS or PGS beads were added for 2 h. The beads were spinned down at 5000×g for 1 min at 4 ºC, washed twice with ice-cold Washing Buffer I and twice with ice-cold Washing Buffer II. Samples were analyzed by SDS-PAGE and Western blotting.

- **Co-immunoprecipitation**

Co-immunoprecipitation was performed essentially as protein immunoprecipitation. Co-IP Lysis Buffer was used instead of IP Lysis Buffer. Beads were spinned down at 2000×g and

washed twice with ice-cold 0.1% NP-40 PBS and twice with ice-cold PBS. As a negative control, no antibody was added. As a positive control, co-immunoprecipitation of p75 and galectin-3 was used (Delacour et al., 2006).

2.2.3. Protein analysis

- **SDS-PAGE**

Denaturating Tris/Tricine SDS polyacrylamide gel electrophoresis was performed according to Laemmli (1970). The proteins were separated in 6-12% gels depending on the size of protein of interest. The gels were made according to the following schema.

Table 2.5. Resolving gel

	6%	8%	10%	12%
ddH_2O	4.13 ml	3.6 ml	3.08 ml	2.48 ml
30% PAA	1.55 ml	2.08 ml	2.58 ml	3 ml
1.5M Tris pH 8.8	1.93 ml	1.93 ml	1.93 ml	1.93 ml
20% SDS	38.75 µl	38.75 µl	38.75 µl	38.75 µl
TEMED	5.75 µl	5.75 µl	5.75 µl	5.75 µl
10% APS	77.5 µl	77.5 µl	77.5 µl	77.5 µl

Table 2.6. Stacking gel

ddH_2O	3.9 ml
30% PAA	0.98 ml
1M Tris pH 6.8	0.73 ml
20% SDS	28.75 µl
TEMED	5.75 µl
10% APS	57.5 µl

The samples were diluted in Laemmli Loading Buffer and boiled at 95 ºC for 5 min before loading. PageRulerPlus Prestained protein ladder solution (Fermentas, Burlington, Canada) was used in every gel as a marker for the size of proteins. Separation was performed in a discontinuous buffer system using the Mini-VE system (Hoefer, San Francisco, USA) in SDS Running Buffer.

- **Western Blot**

The proteins were transferred from SDS-PA gels to the nitrocellulose membrane using semi-dry transfer in *Trans*-Blot SD Transfer Cell (BioRad, Munich, Germany). The procedure was performed in a Western Blot Buffer, by 12 mV per blot for 1 h. The membrane was blocked thereafter in Blocking solution and then incubated overnight at 4 ºC with primary antibodies. After 3 wash steps (with PBS, 10 min each), the membrane was incubated with appropriate horseradish peroxidase-conjugated secondary antibody for 1 h at room temperature. Thereafter, the membrane was washed again three times with PBS and the signal was detected using the enhanced chemiluminiscence (ECL) system (Thermo Fischer Scientific, Schwerte, Germany) and INTAS Gel Imager charge-coupled device camera (Intas, Göttingen, Germany).

- **Coomassie staining**

After separating proteins by SDS-PAGE, the gels were stained with colloidal Coomassie dye Roti-Blue (Carl Roth, Karlsruhe, Germany) according to the manufacturer's protocol. The gel was first fixed in Roti-Blue Fixation Solution and then incubated overnight at room temperature in Roti-Blue Staining Solution. After 5 min washing in Roti-Blue Washing Buffer, the gel was transferred into Roti-Blue Stabilizing Solution.

- **Gel drying**

To dry the gel after SDS-PAGE, the gel was fixed in Gel Fixation Solution for 45 min at room temperature. Thereafter, the gel was transferred onto a whatman paper and dried in the vacuum gel dryer (BioRad, Munich, Germany).

- **MALDI-TOF**

After SDS-PAGE the gels were Coomassie stained and scanned. The gel parts with proper bands were cut out and put into the 1.5 ml tubes. Destaining Solution was added and the samples were incubated by rotation for 30 min. Destaining procedure was performed 2 or 3 times, until the gel part were destained. Thereafter, open tubes were put in the incubator at 37 ºC for 1-2 h, until the gel parts were dry. Trypsin digestion was performed by overnight incubation with Trypsin-mix at 37 ºC. On the next day, Trypsin-mix was removed from the samples and peptides were extracted from the gel with Extraction Solution at room temperature for 30 min. To reduce the volume of the samples and to eliminate acetonitrile (ACN), the tubes were centrifuged in SpeedVac for 15 min, until a final volume of 10-15 µl. Before target loading, ZipTips (Millipore, Schwalbach, Germany) were washed 3 times with 50% ACN and 3 times with 0.1% Trifluoracetic acid (TFA). Thereafter, the tips were incubated 10 times with the peptide solution and once more with 0.1% TFA. Then, matrix solution (α-Cyano-4-hydroxycinnamic acid) was loaded together with the peptide solution on

target. Finally, the proteins were analyzed by MALDI-TOF-TOF, using a Voyager DE STR instrument (PerSeptive Biosystems, Ramsey, USA) or an Ultraflex Instrument (Bruker Daltonik GmbH, Bremen, Germany) in the group of K. Lingelbach (SFB 593, Marburg, Germany). For protein identification, MALDI spectra were explored for database searches using the computer software Profound (http://prowl.rockefeller.edu/profound_bin/WebProFound.exe) and MASCOT (www.matrixscience.com).

2.2.4. Transfection

- **Lipofectamin transfection**

The transfection protocol was adapted from the manufacturer's instructions (Invitrogen, Darmstadt, Germany) and was used to transfect MDCK cells. On the day before transfection the cells were split on coverslips in a 1:4 dilution. For each transfection sample, DNA or siRNA was diluted in 1.5 ml of growth medium without serum and antibiotics. Therafter, 10 µl of Lipofectamin 2000 was added. The mixture was incubated at room temperature for 30 min. The cells were washed 2 times with PBS and the transfection mixture was added. After 6 h the medium was exchanged with normal growth medium.

- **DEAE transfection**

This type of transfection was used for COS cells. On the day before transfection the cells were split on coverslips in a 1:4 dilution. For each transfection sample, DNA was diluted in 1.5 ml of growth medium without serum and antibiotics. Thereafter, 9 µl of DEAE-Dextran solution (50 mg/ml) was added and the mixture was incubated for 15 min at room temperature. The cells were washed 2 times with PBS and the transfection mixture was added. After 1.5 h the transfection mixture was changed with 10 ml of growth medium with 10 µl Chloroquin solution (60 mg/ml). After 3-4 h incubation the medium was changed with normal growth medium.

- **siRNA protein knockdown**

For RNA-mediated interference (RNAi) experiments, specific siRNA duplexes were designed for each protein of interest.

For KIF5B:

5'-GAGCAAGUGUAUAAUGACUUU-3' / 3'-UUCUCGUUCACAUAUUACUGA-5'

5'-AAGCUGAGUGGAAAACUUUUU-3' / 3'- UUUUCGACUCACCUUUUGAAA-5'

5'-GGAGUAUGAAUUGCUUAGUUU-3' / 3'-UUCCUCAUACUUAACGAAUCA-5'

For KIF5C:
5'-UGCAGCAUCAAGGUGAUGUUU-3' / 3'-UUACGUCGUAGUUCCACUACA-5'
5'-AACCUAGAGUUUCACAUCAUU-3' / 3'-UUUUGGAUCUCAAAGUGUAGU-5'
5'-ACAAGACUCUGAAGAAUGUUU-3' / 3'-UUUGUUCUGAGACUUCUUACA-5'

For annexin XIIIb:
5´-AAACGAAAAUGGGCAAUCGUU-3´ / 5´-CGAUUGCCCAUUUUCGUUUUU-3´
5´-UCGUCAUAGCCAGUCUUACUU3´ / 5`-GUAAGACUGGCUAUGACGAUU-3´
5´-CUUCGAGAAGACAGCCUUGUU-3´ / 5´-CAAGGCUGUCUUCUCGAAGUU-3´

As a control, siRNA against luciferase was used (Genordia, Bromma, Sweden):
5'-CGUA CGCGGAAUACUUCGATT-3' / 5'-UCGAAGUAUUC CGCGUACGTT-3'

The efficiency of knockdown was checked by immunoblotting with specific antibodies of depleted cell lysate in comparison to control cell lysate.

2.2.5. Cell culture

- **Cell lines**

MDCK (Madin Darby Canine Kidney)
MDCK cell line originates from kidney of normal female adult Cocker Spaniel in 1958 by S.H. Madin and N.B. Darby. When grown on permeable supports, the cells form polarized epithelial monolayer. MDCKII strain, used in the current study, is thought to be derived from the distal tubule or collecting duct of the nephron. The cell line is usually used as an experimental model to study the generation and maintenance of cell surface polarity in epithelial cells (Gaush et al., 1966).

COS (CV-1 (simian) in Origin, and carrying the SV40 genetic material)
The COS cell line was obtained by immortalizing a CV-1 (Jensen et al., 1964) cell line derived from kidney cells of the African green monkey with a version of the SV40 genome that can produce large T antigen but has a defect in genomic replication (Gluzman, 1981). COS cells are suitable for microscopic studies because of their big size and flat topology
MDCK II (Madine Darby Canine Kidney) and COS-7 (CV-1, Origin, SV40) cells were cultured at 37 ºC under 5% CO_2 in specific growth medium:

Table 2.7. Cell culture conditions

Cell line	Medium	Fetal Calf Serum	Antibiotics	Selective antibiotic
COS	DMEM Low Glucose	10%	Penicillin (100 U/ml), Streptomycin (100 µg/ml)	—
MDCK	MEM	5%		G418 (0.5 mg/ml)
$MDCK_{AnxXIIIbDsRed}$				
$MDCK_{p75\text{-}GFP}$				
$MDCK_{SI}$				
$MDCK_{SI\text{-}YFP}$				
$MDCK_{LPH}$				
$MDCK_{LPHmyc}$				Zeocin

The cells were passaged every second day, or the medium was changed. All cell culture manipulations were done in laminal flow hood. DMEM Low Glucose, MEM, FCS, penicillin and streptomycin were from PAA (Pasching, Austria). G418 Geneticin was from Biochrom AG (Berlin, Germany). Zeocin was from Invitrogen (Darmstadt, Germany).

- **Immunofluorescence**

The cells were washed with PBS and fixed with 4% paraformaldehyde (PFA) for 20 min at room temperature. After three times washing with PBS, the cells were permeabilized either with 0.025% Saponin for 20 min, or with 0.01% Triton X-100 for 4 min at room temperature. Alternatively, the cells were fixed and permeabilized simultaneously by cold methanol for 20 min at -20 ºC. All further procedures were performed in wet chambers at room temperature. The cells were washed 3 times with PBS and incubated with 5% goat serum as blocking solution for 1 h. After 3 times washing with PBS the primary antibodies diluted in 5% goat serum were added. After 2 h the cells were washed 4 times with PBS and the secondary antibodies diluted in 5% goat serum were added for 1 h. Finally, the cells were washed again 4 times and mounted on glass slides with embedding medium.

2.2.6. Software

For the quantification of Western blots and phosphoimager screens the Gel-Pro Analyzer was used (Media Cybernetics, Marlow, UK). SiRNA duplexes were designed in siRNA Target Finder (http://www.ambion.com/techlib/misc/siRNA_finder.html). Microscopic data evaluation, *in vitro* assays analysis and colocolization analysis was performed with Leica software (Leica Confocal Software, Leica Application Suite Advanced Fluorescence, Leica Microsystems, Wetzlar, Germany) in combination with the Volocity (Improvision, Coventry, UK). MALDI

spectra were explored for database searches using the computer software Profound (http://prowl.rockefeller.edu/profound_bin/WebProFound.exe) and MASCOT (www.matrixscience.com).

3. Results

3.1. Characterization of motor proteins involved in apical protein trafficking

3.1.1. KIF5C, a kinesin motor involved in apical trafficking in MDCK cells

Polarized epithelial cells are characterized by two membrane domains: the apical and basolateral one. These two domains are separated by tight junctional complexes and are maintained by the intracellular trafficking machinery, which delivers, among others, *post*-Golgi cargo to their proper destination. Various trafficking routes use different cytoskeletal tracks and different motor proteins to be transported. Thus, delivery of raft-independent apical proteins requires only microtubules, whereas both microtubules and actin filaments are crucial for raft-dependent trafficking (Jacob et al., 2003). Several motor proteins have been identified already on *post*-Golgi carriers. The raft-independent neurotrophin receptor p75 is transported by kinesin-3 family motors in non-polarized MDCK cells and by a kinesin-1 familiy member, KIF5B, after polarization (Jaulin et al., 2007; Xue et al., 2010). Apical delivery of raft-associated hemagglutinin HA requires both dynein and minus-end directed kinesin KIFC3 (Lafont et al., 1994; Noda et al., 2001). On raft-associated SI-carrying vesicles myosin Ia was identified (Heine et al., 2005). Nevertheless, for many apical proteins the trafficking mechanism remains unclear. Also no general motor protein, common for several apical proteins or pathways, has been identified so far. The identification of new motor proteins can clarify the mechanism of apical protein transport and possible mechanisms of the regulation of this process.

3.1.2. Establishment of an *in vitro* motility assay

An *in vitro* motility assay is a nice tool to study the activity of motor proteins or the motility of organelles (vesicles, mitochondria etc.). This method was first invented by Kron and Spudich in 1986 to study the rate of myosin movement along actin microfilaments in a totally purified system *in vitro* (Kron and Spudich, 1986). This reconstitution of organelle movement allows not only the characterization of motility itself (direction, velocity etc.), but also the study of organelle-cytoskeleton interactions. For example, the role of Rab proteins in melanosome transport has been shown by using this method (Chabrillat et al., 2005).

The generation of the components which are necessary to perform an *in vitro* motility assay can essentially be split into two main parts. The first one is the isolation of organelles. Purification conditions, including buffers, pH etc., should preserve not only motor protein-organelle interaction, but also important biological functions, such as motor activities. The

second part is the generation of cytoskeletal tracks (microtubules) and assay perfusion chambers used in reconstituting *in vitro* organelle motility.

The motility assay protocol was modified from Bananis et al. (Bananis et al., 2000). As it was already shown that p75 requires only microtubules for its apical transport, this protein was chosen as a model protein for the establishment of a microtubule-based motility assay. *Post*-Golgi vesicles were purified essentially as described before (Cramm-Behrens et al., 2008), but the vesicle-enriched fractions were used directly in this assay without immunoisolation. As cytoskeletal tracks rhodamine-labeled microtubules were used. The rhodamine-tubulin was polymerized *in vitro* and stored at room temperature for several days.

As a buffering agent for all solutions (for vesicle purification and motility assay itself) piperazine-N,N′-bis(2-ethanesulfonic acid) (PIPES) has been chosen because of its midrange pKa (at 25 °C pKa = 6.8), maximum water solubility and minimal salt effects. Also minimal changes in pKa with temperature were important, because all motility assays were performed at 37 °C. It has been demonstrated that addition of PIPES during fixation of cells can increase the total microtubule contour length, the number of microtubules that are longer than 1 µm, and enhance the association of microtubules with cytoplasmic organelles (Luftig et al., 1977). As mentioned before, the working temperature was 37 °C, because both kinesin ATPase activity and mean gliding velocity reach their maxima at this temperature (Boehm et al., 2000a). Also magnesium, DTT and ATP concentrations were chosen according to the values known for the kinesin highest mean gliding velocity *in vitro* (Boehm et al., 2000b). As it was known that addition of EDTA to homogenization buffer significantly increases the fraction of kinesin bound to organelles (Tsai et al., 2000), EDTA has been used during vesicle purification and motility assays.

Perfusion chambers were made of two coverslips with stripes of double-sided adhesive tape in between. One of the coverslips was covered with DEAE-Dextran to get a positively-charged surface and to facilitate the binding of negatively-charged microtubules.

To scavenge oxygen in order to limit photodamage, an oxygen scavenging system (OSS) was added to the motility buffer. The principle by which a glucose oxidase/glucose/catalase mix scavenges oxygen is as follows:

catalase: $H_2O + O_2 \rightarrow H_2O_2$

glucose oxidase: D-glucose + H_2O_2 → D-glucono-1,4-lactone

To keep the ATP concentration high enough and to prevent motility inhibition by high ADP concentration, an ATP regeneration system was used. The mechanism of this reaction is as follows:

PCK + PC +ADP ↔ PKC + C + ATP, K_{eq} = 162

The abbreviations are as follows: ATP – Adenosine Tri Phosphate, ADP – Adenosine Di Phosphate, CPK – Creatine Phospho Kinase, PC – PhosphoCreatine, C – Creatine.

The assay was performed at 37 °C in thermal-controlled chamber. The video was recorded in general for 2-5 minutes, each frame every 2 seconds. *In vitro* binding assay was modified from motility assay.

3.1.3. Evidence for tubulin-dependent motors on purified p75-containing *post*-Golgi vesicles

To study the presence of motor proteins on apical *post*-Golgi vesicles, the isolated p75-GFP-carrying vesicles were analyzed in an *in vitro* binding and motility assays. $MDCK_{p75\text{-}GFP}$ cells, stably expressing raft-independent neurotrophin receptor p75, were grown until full polarization, then blocked for four hours at 20 °C and released for 10 minutes. This time point was chosen because it corresponds to the moment, when a lot of protein has already left the TGN and a great amount of vesicular carriers have been formed, but apical cargo has not reached the plasma membrane yet. At first, the binding of these vesicles to microtubules has been characterized. Purified vesicles were added to the perfusion chambers with microtubules, unbound material was washed out and the percentage of vesicles bound to microtubules was quantified. In average, 25-30% of all vesicles seen in a microscopic field were bound to the microtubules, whereas 70-75% of vesicles were bound to the coverslip itself (non-specific binding). To examine whether the interaction between p75-carrying vesicles and microtubules is specific, purified vesicles were heated to 80 °C or treated with trypsin before addition to the perfusion chamber (modified from (Blocker et al., 1996)). Both treatments should impair the proteins on the surface of vesicles without destroying the vesicle integrity. Indeed, preheating of vesicles reduced the binding efficiency to ~10%, in comparison to 30% in control experiments. Also protease digestion of surface proteins resulted in more than a 2-fold reduction of vesicle-microtubule interaction (Fig. 3.1A). These data prove that vesicle binding to microtubules *in vitro* is specific and that this interaction occurs in a protein-dependent manner.

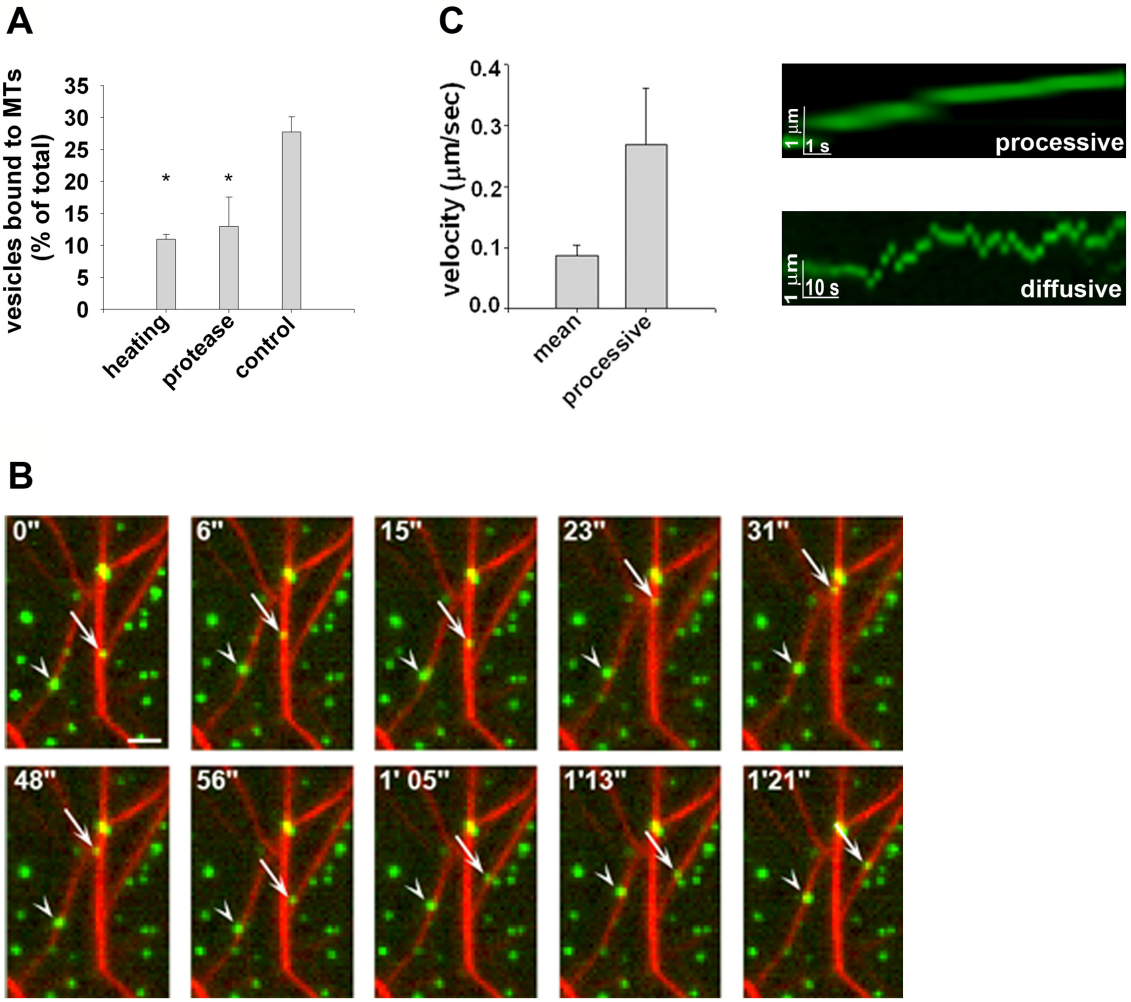

Figure 3.1. *In vitro* motility and binding assays of purified p75-GFP carrying vesicles

Purified p75-GFP vesicles were moving *in vitro* on rhodamine-labeled microtubules in an ATP-dependent manner. (**A**) Isolated vesicles were heated or subjected to protease digestion and the efficiency of vesicle binding to microtubules was compared to the control experiment. Statistically significant differences in the number of vesicles bound to microtubules are denoted by asterisks using paired Student's t-tests; * $p < 0.01$. Standard error bars are indicated. (**B**) Selected frames from a life cell time lapse series are shown. Moving vesicles are indicated by arrow or arrowhead. The movement is bidirectional, with a switch of microtubular tracks. The time is indicated in minutes (′) and seconds (″). Scale bar, 1 µm. (**C**) The velocity of p75-GFP vesicles was measured in three independent experiments. The mean velocity (depicted as "mean") was measured as a velocity of both types of movement: uni- ("processive") and bidirectional ("diffusive") (n=53). Additionally, the velocity of only unidirectional ("processive") movement was measured (n=16). Examples of kymographs of the processive and diffusive movements are shown on the right panel.

To assess if tubulin-dependent motors are involved in this binding capacity, the purified vesicles were tested in the motility assay. For this, purified p75-GFP vesicles were incubated with polymerized microtubules in perfusion chambers and motility buffer with ATP was added. The video recording was started directly thereafter. As shown at the Fig. 3.1B, some vesicles were bound to the coverslips and were motionless, others were attached to the microtubules and some of them were motile. In some cases vesicles detached from microtubules and stopped moving, while others attached to microtubules and started moving.

Also pauses occurred during the movements. Some of the vesicles were moving in both directions along microtubular tracks, the displacement of others was unidirectional. In Fig. 3.1C (right panel) the examples of kymograms for two types of movements (unidirectional, also called processive, and bidirectional, also called diffusive) are shown. Additionally, the velocities of vesicles were measured and revealed a mean vesicle speed of about 0.08 µm/s including uni- and bidirectional movements. Unidirectional (processive) movements displayed a significantly higher average velocity: 0.28 µm/s (Fig. 3.1A, left panel). Consequently, the observations indicate that purified apical *post*-Golgi vesicles still carry tubulin-dependent motor proteins and can thus be utilized for their biochemical characterization.

3.1.4. Vesicle-enriched fractions of p75-GFP preparations contain KIF5C

Bidirectional movement of p75-carrying vesicles along microtubules *in vitro* could be due to the presence of plus and minus end-directed vesicle-associated motor proteins (for example, plus-directed kinesin and minus-directed dynein). To confirm this hypothesis, it was decided to analyze immunoisolated *post*-TGN vesicles with anti-kinesin heavy chain (KHC) and anti-dynein intermediate chain antibodies. As depicted in Fig. 3.2A, p75-containing vesicles carried kinesin, but no dynein. To identify, which isoforms of kinesin heavy chain is associated with p75-GFP-carrying vesicles, kinesin heavy chain was immunoprecipitated from *post*-TGN vesicle-enriched fractions and the purified protein was subjected to proteomic analysis (Jacob and Naim, 2001;Cramm-Behrens et al., 2008). Apical vesicles were harvested 10 minutes after TGN release by differential sucrose density centrifugation. Kinesin heavy chain was immunoprecipitated from *post*-TGN vesicle-enriched fractions with H2 antibody, which interacts with all three isoforms of the kinesin-1 group (KIF5A, KIF5B and KIF5C) (for specificity of antibodies see Table 2.3). As depicted in Fig. 3.2B, several bands appeared in Coomassie stained gels: a major band about 56 kDa and minor bands at 36, 95, 120, 200 and 250 kDa. All these bands were cut out from the gels and the proteins were analyzed by MALDI-TOF. The major band (56 kDa) was identified as immunoglobulin heavy chain – the antibody which has been used for immunoprecipitation. From minor bands one (120 kDa) was identified as kinesin-1 isoform KIF5C. Other minor bands could not be identified with a significant MASCOT score. For verification, this experiment was performed three times with a MASCOT score in the range of 90-120 for KIF5C. Also immunoblotting of the gel with anti-KHC antibodies resulted in only two bands, corresponding to KIF5C and immunoglobulin heavy chain (Fig. 3.2B, right panel).

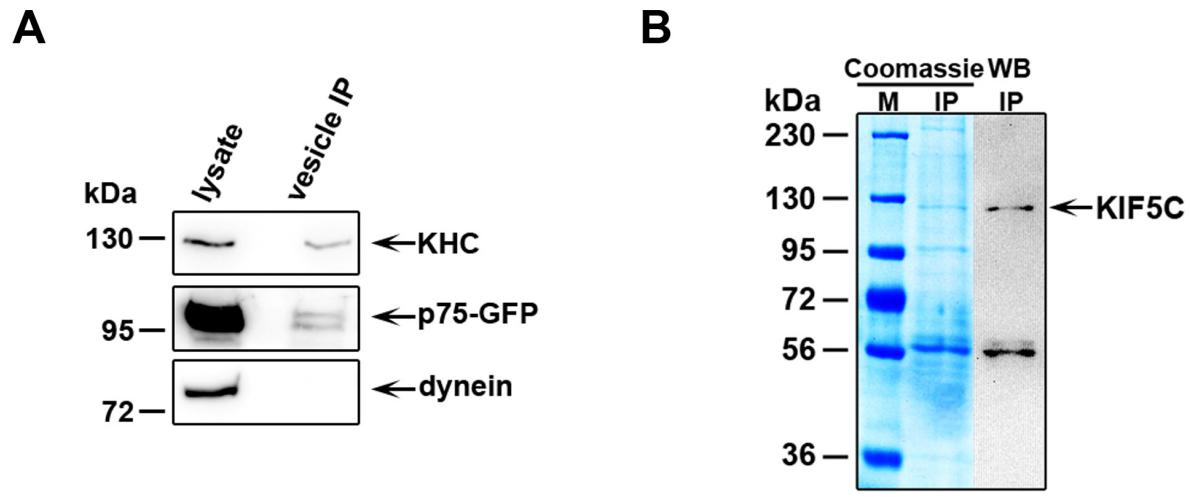

Figure 3.2. KIF5C is present in *post*-Golgi vesicle-enriched fractions.

(**A**) p75-GFP carrying *post*-Golgi vesicles were immunoisolated 10 minutes after TGN-release, separated by SDS-PAGE and immunoblotted with monoclonal anti-KHC (upper panel), anti-GFP (as a control for IP efficiency) and anti-dynein antibody (lower panel). (**B**) Cellular homogenates of $MDCK_{p75\text{-}GFP}$ cells were separated by density gradient centrifugation. Kinesin Heavy Chain was immunoprecipitated form the vesicle-enriched fractions with H2 antibody. The gel was stained with Coomassie (left panel) or immunoblotted with KHC (Kinesin Heavy Chain) antibody (right panel). KIF5C as identified by MALDI-TOF is indicated.

3.1.5. KIF5C is present on purified apical *post*-Golgi vesicle populations

To prove that KIF5C is present on immunoisolated p75-carrying apical vesicles, the proteins were blocked in the TGN by incubation at 20 °C and thereafter the TGN block was released at 37 °C for various time intervals (0, 5, 10, 15 and 20 minutes) and the *post*-TGN vesicles were harvested. To detect KIF5C on purified vesicles, a specific anti-KIF5C antibody (H1, see Table 2.3) was used. The specificity of antibodies was tested additionally by protein immunoprecipitation followed by Western blot analysis. Kinesin was immunoprecipitated from MDCK cells with KIF5C, KIF5A and H1 antibodies (Fig. 3.3C). As a negative control no antibody was added to the sample. The precipitated proteins were then immunoblotted first with H1 antibodies (Fig. 3.3C, upper panel). It resulted in a strong band in immunoprecipitate with KIF5C antibodies. This proves that H1 antibody detects KIF5C in Western blot, but is not efficient in immunoprecipitation. Thereafter, the same blot was incubated with KIF5A antibody and a new band appeared in KIF5A immunoprecipitates (Fig. 3.3C, lower panel). The detected protein, corresponding to KIF5A, has a significantly lower electrophoretical mobility and has a size about 130 kDa (data not shown). This KIF5A band could not be detected in the first lane (KIF5C immunoprecipitate), proving that KIF5C antibodies immunoprecipitate only the KIF5C isoform of kinesin-1 and not KIF5A. Altogether, this experiment proved that both H1 and KIF5C antibodies are specific to KIF5C with the only difference that H1 functions in Western blot, while the KIF5C antibody is suitable for immunoprecipitation.

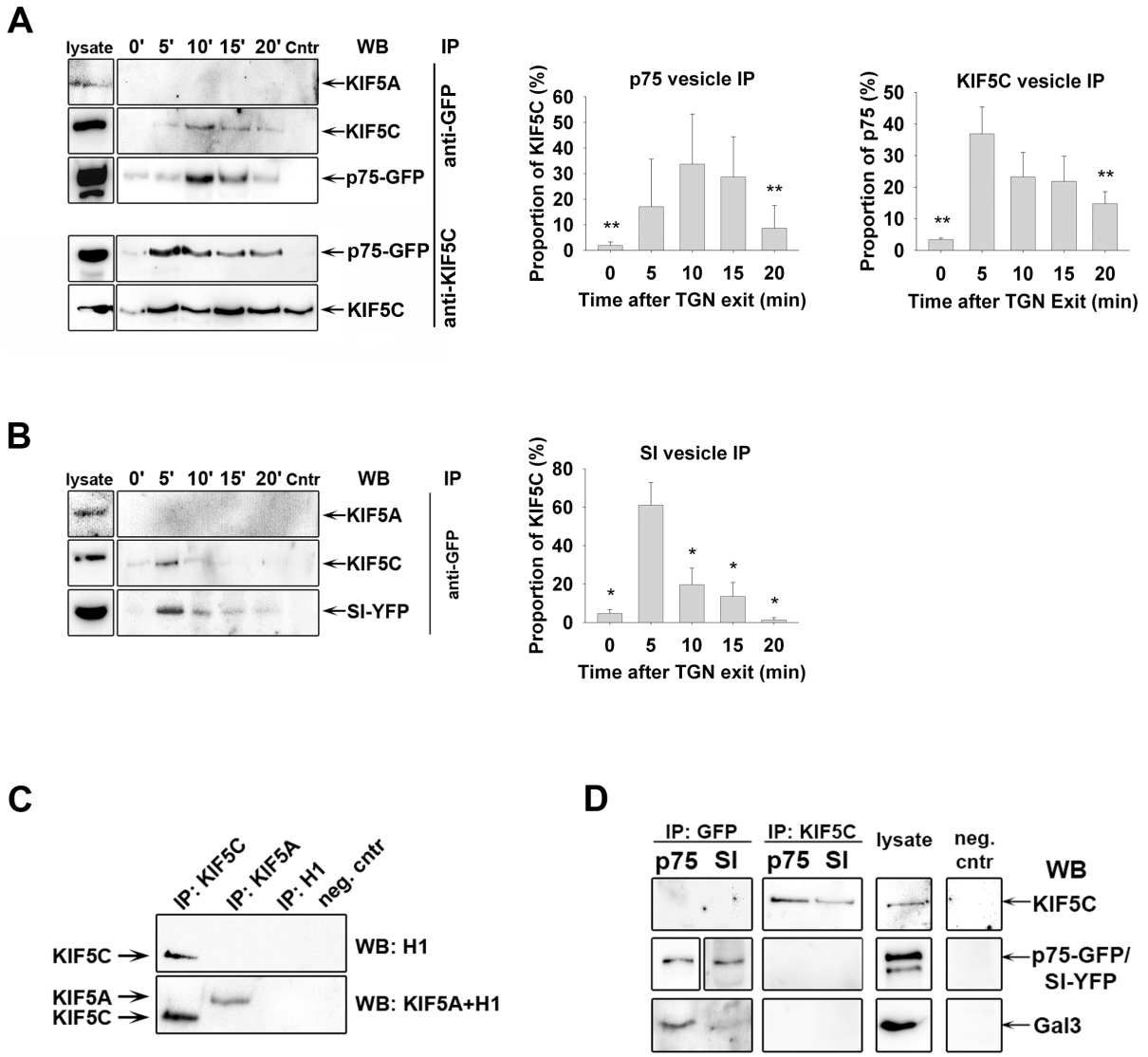

Figure 3.3. KIF5C is present on both p75- and SI-carrying vesicle populations.

(**A, B**) For a TGN accumulation of newly synthesized material, $MDCK_{p75\text{-}GFP}$, $MDCK_{SI\text{-}YFP}$ and MDCK (as a control, depicted as Cntr) cells were incubated at 20 °C for 4 h, followed by a TGN release at 37 °C for distinct time intervals (0, 5, 10, 15 and 20 minutes). Cell homogenates of $MDCK_{p75\text{-}GFP}$ (**A**), $MDCK_{SI\text{-}YFP}$ (**B**) and MDCK (**A, B**) cells were loaded onto a step sucrose gradient, and *post*-TGN vesicles were immunoisolated with anti-GFP (**A, B**) or anti-KIF5C antibody (**A**). The immunoprecipitates were separated by SDS–PAGE and labelled with anti-KIF5A, anti-KIF5C H1 (**A, B**) or anti-GFP (**A**) antibodies by Western blot. Immunoblots of cellular lysates are depicted as lysate. On the right panel the quantification of band intensities relative to the total amount of protein from four independent experiments is shown. Asterisks denote statistically significant differences between values from distinct time points and the maximum value using paired Student's t-tests; * $p < 0.01$, ** $p < 0.03$. (**C**) Kinesin immunoprecipitation from MDCK cell lysates was performed with anti-KIF5C, anti-KIF5A and H1 antibodies. For the negative control (neg. cntr) no antibody was added during immunoprecipitation. Immunoprecipitates were separated by SDS-PAGE and first immunoblotted with H1 antibodies (upper panel) and thereafter, without membrane stripping, with anti-KIF5A antibodies (lower panel). (**D**) P75-GFP was immunoprecipitated from $MDCK_{p75\text{-}GFP}$ and SI-YFP from $MDCK_{SI\text{-}YFP}$ cell lysates with anti-GFP antibodies, KIF5C was immunoprecipitated from $MDCK_{p75\text{-}GFP}$ and $MDCK_{SI\text{-}YFP}$ cell lysates. The immunoprecipitates were separated by SDS-PAGE and immunoblotted with H1 (anti-KIF5C), anti-GFP or anti-galectin-3 antibodies. $MDCK_{p75\text{-}GFP}$ cellular lysate is depicted as lysate. For the negative control (neg. cntr) no antibody was added during immunoprecipitation.

Nevertheless, as it was shown that this antibody can also detect truncated forms of KIF5A (Cai et al., 2001), the samples were additionally immunoblotted with anti-KIF5A antibody. As shown on Fig. 3.3A (upper left panel), vesicles were efficiently immunoprecipitated, as a signal of p75-GFP is seen at all time points and no signal could be detected in the negative control. The maximum signal intensity of p75-GFP was observed at 10 and 15 minutes after TGN exit. This corresponds to the moment, when a lot of protein has already left the TGN region, but still has not reached the plasma membrane, resulting in the maximum amount of vesicular carriers in the cell. Immunoblotting with anti-KIF5C antibodies revealed a signal at 5 – 20 minutes after TGN exit, with a maximum intensity at 10 and 15 minutes. This result correlates partially with the intensity of the p75-GFP band (amount of p75-carrying vesicles). Remarkably, at the first time point (0 minutes) just the p75-GFP signal could be detected, but there was no signal for KIF5C. The proportion of KIF5C present on p75-GFP vesicles was quantified (Fig. 3.3A, right panel) and it shows a significant increase of the KIF5C association with p75 vesicles at 5 – 15 minutes after TGN release. Immunoblotting of the samples with anti-KIF5A antibodies revealed no signal, proving that the signal of the H1 antibody corresponds to KIF5C, and not KIF5A.

To confirm the presence of KIF5C on p75 vesicles, vesicles were immunoprecipitated with anti-KIF5C antibodies, thus, all vesicles that carry KIF5C were isolated. As shown in Fig. 3.3A (lower left panel), immunoprecipitation was efficient at all time points. Immunoblotting with anti-GFP antibodies revealed a strong signal at 5 – 20 minutes after TGN exit. Thus, among KIF5C-associated *post*-TGN vesicles there is a significant population of p75-GFP-carrying vesicles. The quantification of p75 on KIF5C-associated vesicles is shown in Fig. 3.3A (right panel).

As p75 is a marker protein for raft-independent apical pathway, also raft-dependent SI-carrying vesicles were examined for their association with KIF5C. As described above, cells were incubated at 20 °C leading to a transport block at TGN and then released at 37 °C for various time intervals. SI-YFP-carrying vesicles were immunoprecipitated with anti-GFP antibodies and immunoblotted with anti-KIF5C (H1) and anti-KIF5A antibodies. SI-carriers were successfully isolated with the maximum at 5 min after TGN release (Fig. 3.3B, left panel). As for p75 (Fig. 3.3A), no signal could be observed after immunoblotting with anti-KIF5A antibody. In contrast, KIF5C was identified on SI-vesicles at several time points, with the strongest accumulation at 5 minutes after TGN exit (Fig. 3.3B, right panel).

The association of kinesin with organelles can occur through some adaptor proteins or by direct interaction with transported cargo. To study this interaction co-immunoprecipitation experiments were done: both marker proteins (p75 and SI) and KIF5C were isolated and the samples were immunoblotted with anti-KIF5C or anti-GFP antibodies, accordingly (Fig. 3.3D). As a negative control, no antibody was added during immunoprecipitation. As a positive control, the known interaction between p75 and galectin-3 was used (Delacour et al.,

2006). As shown in Fig. 3.3D, neither p75 nor SI co-immunoprecipitate with KIF5C. This suggests, that the association between KIF5C and apical cargo is not direct and may depend on specific attachment components present on the cytosolic side of vesicular carriers that exited from the Golgi.

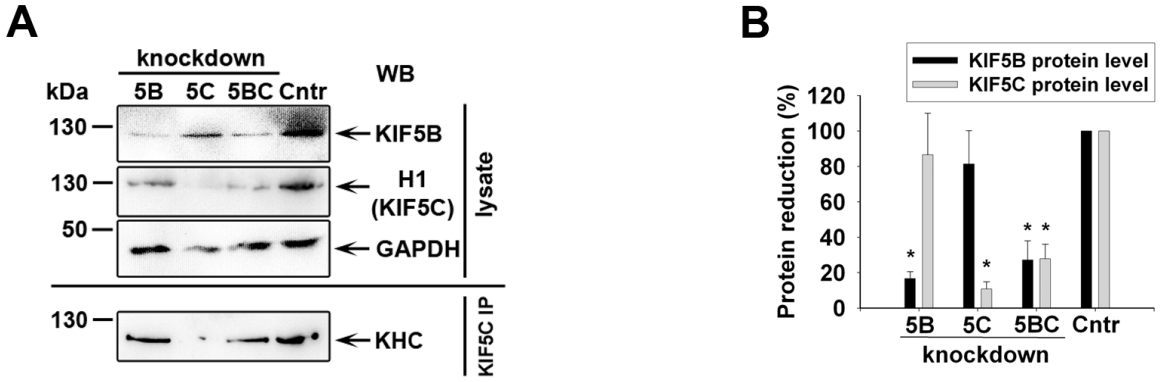

Figure 3.4. siRNA-mediated knockdown of KIF5B and KIF5C

MDCK cells were grown on *trans*-well filters and transfected two times with KIF5B- and/ or KIF5C-specific siRNA. (**A**) KIF5-depleted or control cellular lysates were analyzed by immunoblotting with specific KIF5B and H1 (anti-KIF5C) antibodies. Anti-GAPDH antibodies were used as loading control. To prove both, KIF5C knockdown efficiency and KIF5C antibody specificity, KIF5C was immunoprecipitated from the cell lysates with the specific anti-KIF5C antibodies. The immunoprecipitates were separated by SDS-PAGE and immunoblotted with KHC (Kinesin Heavy Chain) antibodies (**A**, lower part). (**B**) The quantifications of four independent experiments are shown. Asterisks denote statistically significant differences using paired Student's t-tests; * $p < 0.01$, ** $p < 0.03$.

3.1.6. Knockdown of KIF5C and KIF5B decreases the surface delivery of SI and p75

A functional role of KIF5C in apical transport was then studied by siRNA-mediated KIF5C depletion. In these experiments, KIF5B as a homologous member of the KIF5 group, which has been already characterized in *post*-Golgi transport in epithelial cells (Jaulin et al., 2007), was studied for comparison. First, the specificity and efficiency of knockdown for the two motor proteins was verified by immunoblotting and revealed a reduction of about 85% for each protein (Fig. 3.4). Not only lysates from depleted cells in comparison to control cells have been analyzed, but also immunoprecipitated KIF5C from KIF5-specific siRNA- and luciferase siRNA-transfected cells. Precipitated proteins were then immunoblotted with H1 antibody (KIF5C-specific, see Table 2.3; Fig. 3.4A, lower left panel). This experiment proves again that the protein level of KIF5C is significantly decreased in KIF5C siRNA-transfected cells. Moreover, as H1 antibody detects no signal in KIF5C-depleted samples, it confirms that

the H1 antibody is specific to KIF5C and does not cross-react with other isoforms of kinesin-1 (see also Table 2.3).

To assess the consequence of KIF5-specific knockdown on the polarized delivery of raft-associated SI and raft-independent p75 in MDCK cells, $MDCK_{SI}$ and $MDCK_{p75}$ cells were transfected with specific or control siRNA, biosynthetically labelled for 2 h and proteins from the apical or basolateral membranes were separately immunoprecipitated. As shown in Fig. 3.5, both apical markers preserve their apical distribution. Both forms: high mannose (SI_h and $p75_h$) and complex glycosylated (SI_c and $p75_c$) are seen in the lysates. Quantification revealed a significant reduction of p75 and SI at the apical membrane in KIF5B- and KIF5C-depleted cells. This indicates that both motors are involved in the intracellular transport of raft-associated SI and raft-independent p75 to the apical cell surface. When KIF5B and KIF5C were knocked down in a combined approach, the remaining protein level of each kinesin was twice as high as in single knockdown cells (Fig. 3.5). Nevertheless, the highest reduction in apical trafficking of the two markers was achieved by this double knockdown of the two kinesins (Fig. 3.5B).

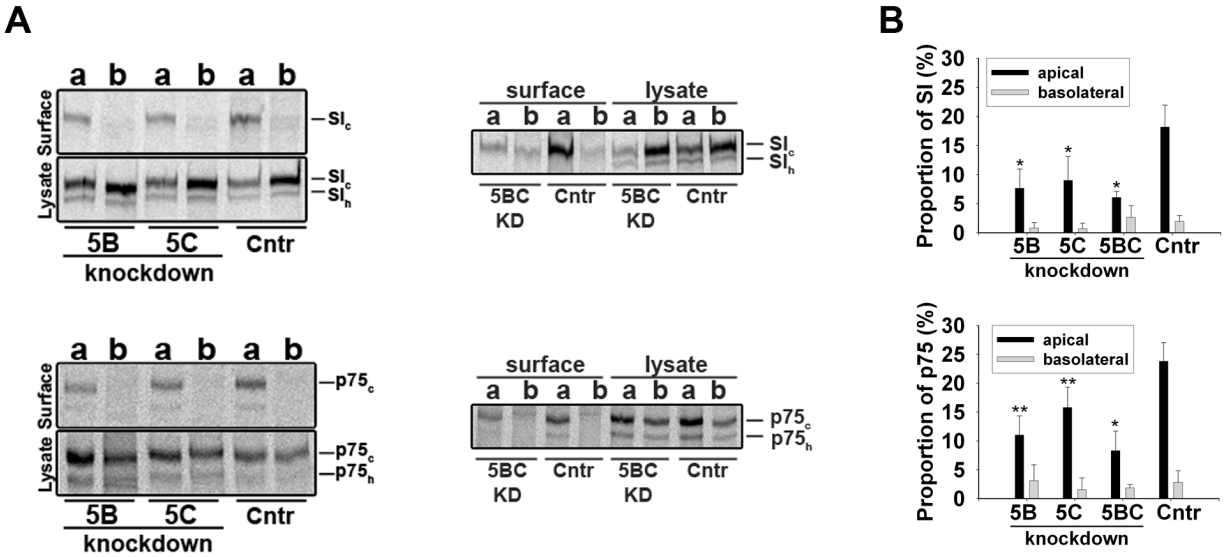

Figure 3.5. Impact of siRNA-mediated KIF5B and KIF5C depletion on apical trafficking of p75 or SI

(**A**)$MDCK_{p75\text{-}GFP}$ and $MDCK_{SI}$ cells were grown on *trans*-well filters and biosynthetically labelled with [^{35}S] methionine for 2 h in the presence of KIF5 isotype specific siRNA or luciferase siRNA for control. Cell surface immunoprecipitation of p75 or SI from the apical (a) or basolateral (b) surface was performed with the corresponding antibodies, and cytosolic p75 or SI was precipitated from the remaining cell lysates for comparison. The immunoprecipitates were subjected to SDS–PAGE, followed by phosphoimager analysis. The left panel shows representative gels of individual KIF5 knockdown experiments, middle panel – double knockdown of KIF5B and KIF5C together. High mannose ($p75_h$ and SI_h) or complex glycosylated ($p75_c$ and SI_c) forms are indicated. (**B**) The proportions of SI and p75 from three independent experiments were quantified. Asterisks denote statistically significant differences using paired Student's t-tests; * $p < 0.01$, ** $p < 0.03$.

The next question was then whether a trafficking delay in the absence of KIF5C was related to events following TGN exit by a transport kinetic study. Polarized KIF5C-depleted or control cells were labelled for 15 min with [^{35}S]methionine at 37 °C, rinsed with PBS and blocked for 4 h at 20 °C, so that all newly synthesized material accumulated in the TGN. Cells were then shifted to 37 °C for different periods of time (0, 20, 40, 60 and 120 min). Radioactively labelled polypeptides at the apical cell surface were then isolated by surface immunoprecipitation, cytosolic p75 and SI were precipitated from the remaining cell lysates for comparison (Fig. 3.6A). As quantification shows, the kinetics of surface delivery was significantly reduced for p75 and SI in KIF5C-depleted cells. Thus, 120 min after TGN release only 25% of p75 was transported to the apical membrane in comparison to control cells. Similarly, the efficiency of SI delivery to the apical membrane decreased from 60% in control cells to 45% in KIF5C-depleted cells. To prove that this effect was based on a delay after TGN exit and not on a decelerated passage from ER to Golgi, the kinetics of processing from high-mannose to complex glycosylated froms of p75 and SI were quantified. As indicated in Fig. 3.6B, no significant difference in p75 or SI processing between control and KIF5C-depleted cells could be observed. Thus, a cellular role of KIF5C in trafficking of the two model proteins concentrates on the passage from the TGN to the cell surface and not on earlier steps in the secretory pathway.

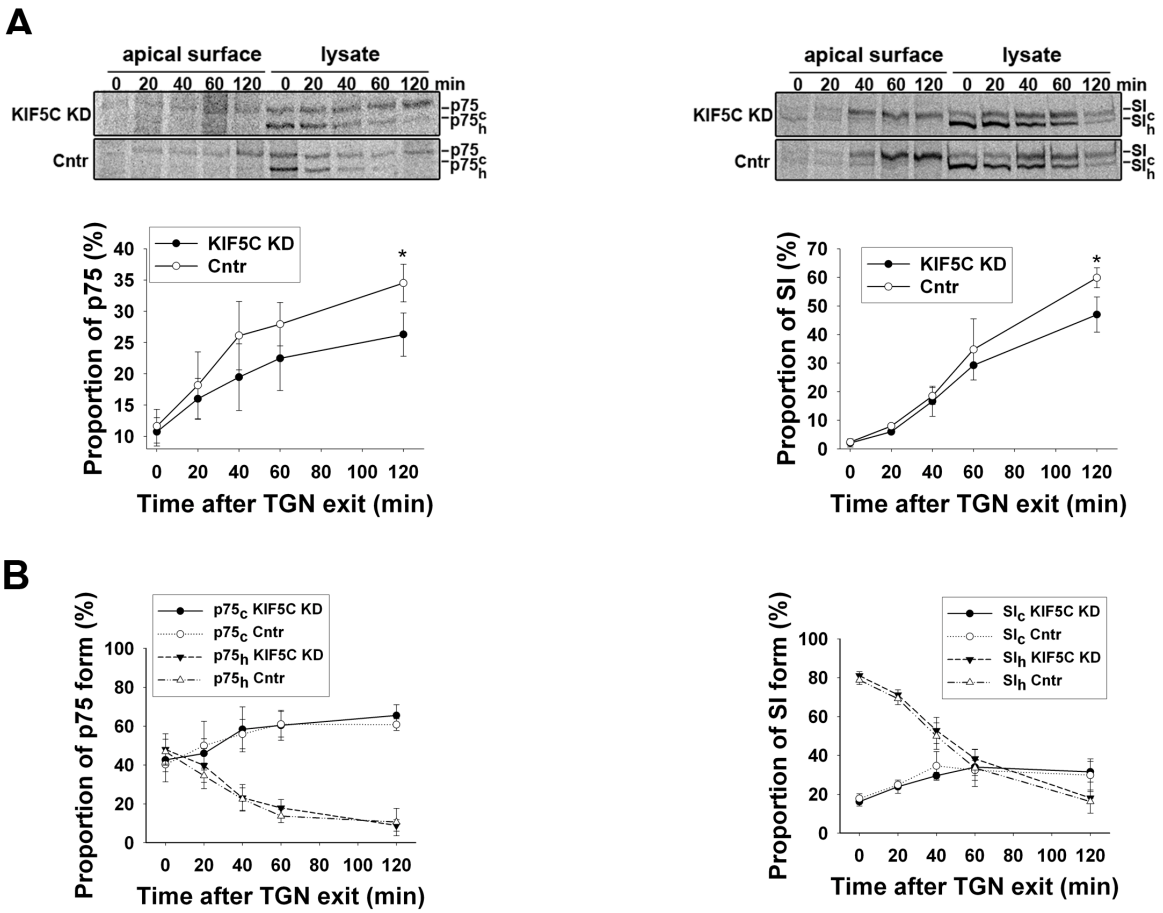

Figure 3.6. Kinetic studies of the role of KIF5B and KIF5C in the apical membrane delivery of p75 and SI

(**A**)Control or KIF5C-knockdown $MDCK_{p75\text{-}GFP}$ and $MDCK_{SI}$ cells were grown on *trans*-well filters and biosynthetically labelled with [^{35}S] methionine for 15 min. The cells were incubated at 20°C for 4 h to block newly synthesized proteins in the TGN. The cells were then shifted to 37 °C for various time intervals, followed by cell surface immunoprecipitation of p75 and SI from the apical surface. Cytosolic p75 and SI were immunoprecipitated from the remaining cell lysates for comparison. The immunoprecipitates were subjected to SDS-PAGE, followed by phosphoimager analysis. High mannose ($p75_h$ and SI_h) or complex glycosylated ($p75_c$ and SI_c) forms are indicated. The proportions of surface p75 and SI were quantified from four independent experiments. (B) The kinetics of processing from high-mannose to complex glycosylatated forms of p75 and SI in control and KIF5C-depleted cells as depicted in (**A**) was quantified. Asterisks denote statistically significant differences using paired Student's t-tests; * $p < 0.01$, ** $p < 0.03$.

3.1.7. KIF5C is colocalized with both p75 and SI after TGN release

The intracellular localization of KIF5C in polarized MDCK cells was studied by colocalization analysis with p75 and SI by confocal fluorescence microscope. $MDCK_{SI}$ cells or MDCK cells transiently transfected with p75-DsRed, $MDCK_{p75\text{-}DsRed}$, were immunostained for endogenous KIF5C. Anti-KIF5C antibody labeled intracellular vesicular structures close to the apical cell surface and also some basolateral staining could be observed. Some of the vesicles were colocalized with p75-DsRed or SI (data not shown). To study in detail when KIF5C

associates with *post*-TGN vesicles of both pathways (raft-dependent and raft-independent), kinetics analysis was performed. $MDCK_{SI}$ and $MDCK_{p75\text{-}DsRed}$ cells were blocked at 20 °C and released at 37 °C for 0, 5 and 20 minutes (Fig. 3.7A, B). At the first time point (0 min) both apical model proteins, p75 as well as SI, showed some overlap with KIF5C. At this moment, almost all p75 and SI are concentrated in the perinuclear region, which corresponds, presumably, to the TGN. Most likely, in this case a relatively high overlap coefficient of KIF5C with TGN-accumulated material is also due to their condensed residence in the perinuclear area. Following TGN-release, the overlap coefficient reaches a maximum after 5 minutes and drops down to a minimum after 20 minutes. Interestingly, the kinetics for both p75 and SI were quite similar, although biochemical studies revealed different results (see Fig. 3.3A, B). Nevertheless, both experimental approaches demonstrate that *post*-Golgi transport carriers for raft-dependent and non-raft-dependent apical cargo are at first decorated by the kinesin motor KIF5C followed by a switch to other motor proteins thereafter.

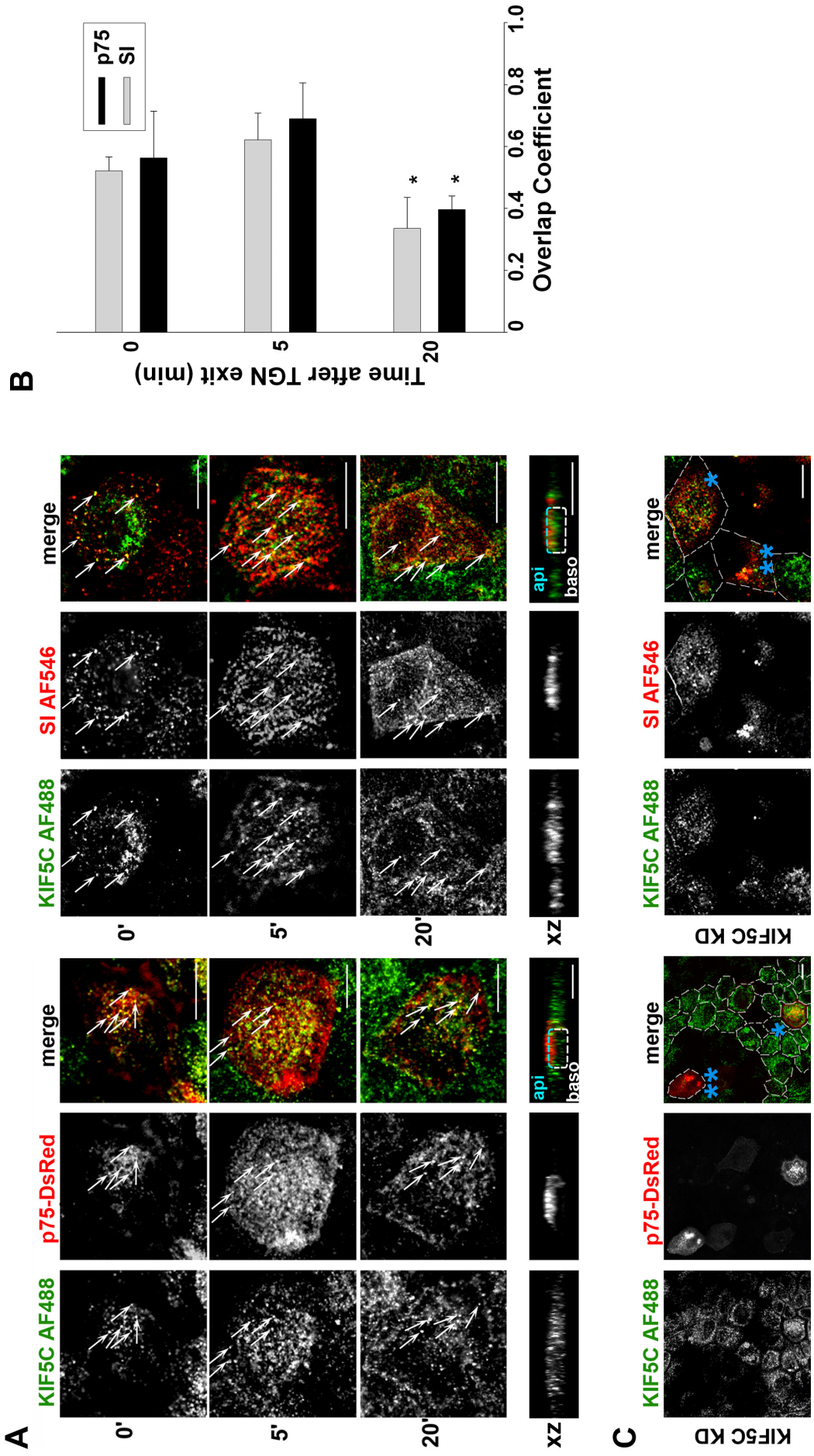

Figure 3.7. Figure legend on the next page

Figure 3.7. Confocal analysis of KIF5C colocolization with p75 and SI in MDCK cells

(**A**) MDCK cells were transiently transfected with p75-DsRed or the stable MDCK cell line expressing SI ($MDCK_{SI}$) was used. The cells were blocked for 4 h at 20 °C to accumulate newly synthesized proteins in the TGN. After TGN release at 37 °C for 0, 5 and 20 minutes, cells were fixed and stained for endogenous KIF5C (with Alexa Fluor 488 as secondary antibody) and SI (with Alexa Fluor 546 as secondary antibody). Confocal sections were recorded from regions just beneath the apical membrane. Colocalized structures are indicated by arrows. At the lower panel the xz views are shown. The apical region is depicted as api, the basolateral – as baso. (**B**) Overlap coefficients between KIF5C- and p75- or SI-fluorescence were quantified from 20 cells for each time point after TGN release. Asterisks denote statistically significant differences between time points 5 and 20 minutes using paired Student's t-tests; * $p < 0.001$. (**C**) MDCK cells stably expressing SI or transiently transfected with p75-DsRed were transfected twice with KIF5C-specific siRNA. On the 5th day after seeding the cells were fixed and stained specifically for endogenous KIF5C (with secondary Alexa Fluor 488 antibodies). Images were taken from the apical area and dashed lines roughly indicate cell borders. The cells with high levels of KIF5C expression are depicted with one blue asterisk, the KIF5C-depleted cells – with two blue asterisks. In the merged images KIF5C is shown in green, p75 and SI - in red colour. Scale bars, 10 µm.

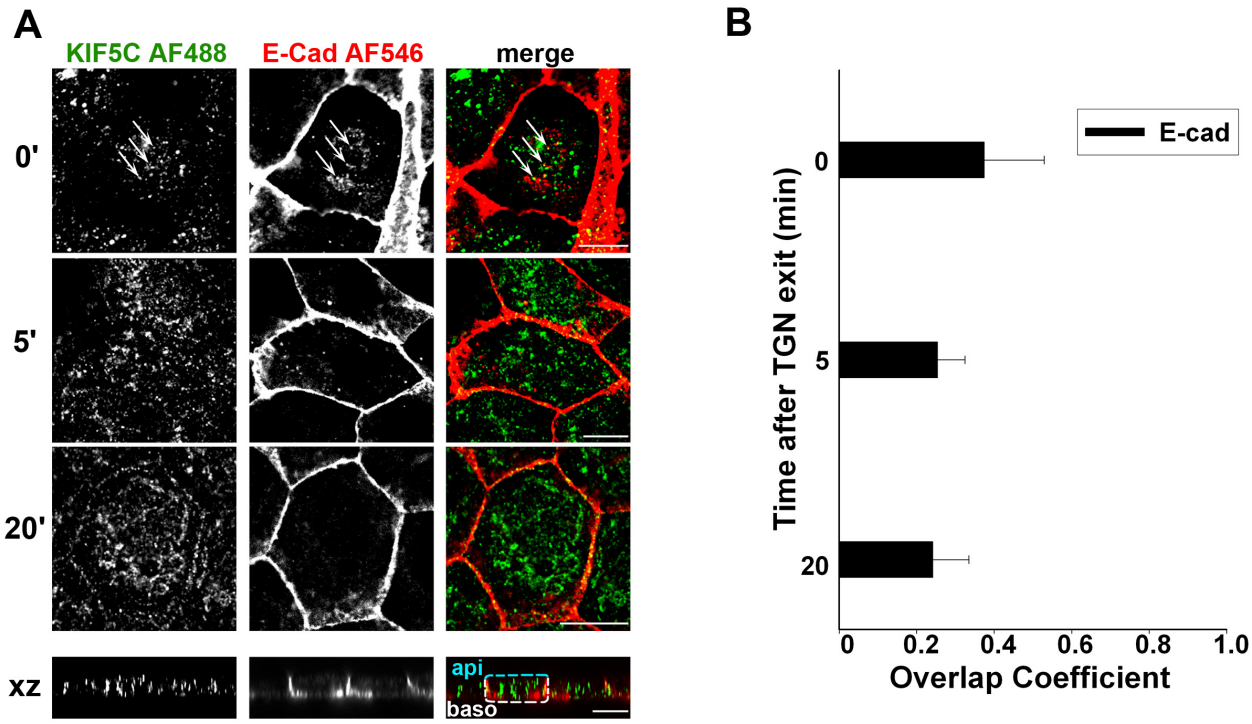

Figure 3.8. Confocal analysis of KIF5C colocalization with E-cadherin in MDCK cells

(**A**) TGN-release experiments were performed with polarized MDCK cells as indicated in Fig. 3.7. Following fixation the cells were immunostained with anti-KIF5C (with Alexa Fluor 488 as secondary antibody) and anti-E-cadherin (with Alexa Fluor 546 as secondary antibody). Colocalized structures are indicated by arrows. At the lower panel xz views are shown. The apical region is depicted as api, the basolateral – as baso. (**B**) The quantification of overlap coefficients between KIF5C- and E-cadherin-fluorescence from 20 cells for each time point after TGN release is shown. In the merged images KIF5C is depicted in green, E-cadherin in red colour. Scale bars, 10 µm.

Remarkably, not all KIF5C-positive structures colocalize with apical marker proteins. At 5 and 20 minutes after TGN release also a basolateral localization of KIF5C was observed.

Consequently, the question rises, whether KIF5C has other functions in the cell, for example, as a motor protein for other cargo. To prove this hypothesis the cells were stained for KIF5C and basolateral cargo E-cadherin. The experiment was performed as described above. As shown in Fig. 3.8A, 0 min after TGN exit E-cadherin localized not only to basolateral membrane, but also some vesicles are observed in the perinuclear region. At this time point KIF5C showed a weak overlap with E-cadherin (Fig. 3.8B). The overlap coefficient of KIF5C with basolateral E-cadherin dropped down to a minimum directly after TGN-exit (Fig. 3.8B).

Thereafter, the role of KIF5C in cellular trafficking of p75 or SI was checked by fluorescence microscopy. $MDCK_{SI}$ and $MDCK_{p75\text{-}DsRed}$ cells were transfected with KIF5C-specific siRNA. Since KIF5C expression was transiently depleted, the specific knockdown was visible in some unevenly distributed cells of a polarized epithelium, while other cells still expressed normal levels of the motor. Fig. 3.7C shows that p75-DsRed or SI accumulated in relatively large vesicles in KIF5C-depleted cells thus suggesting that their transport was blocked intracellularly. On the other hand, the distribution of p75 or SI in KIF5C-expressing cells was normal.

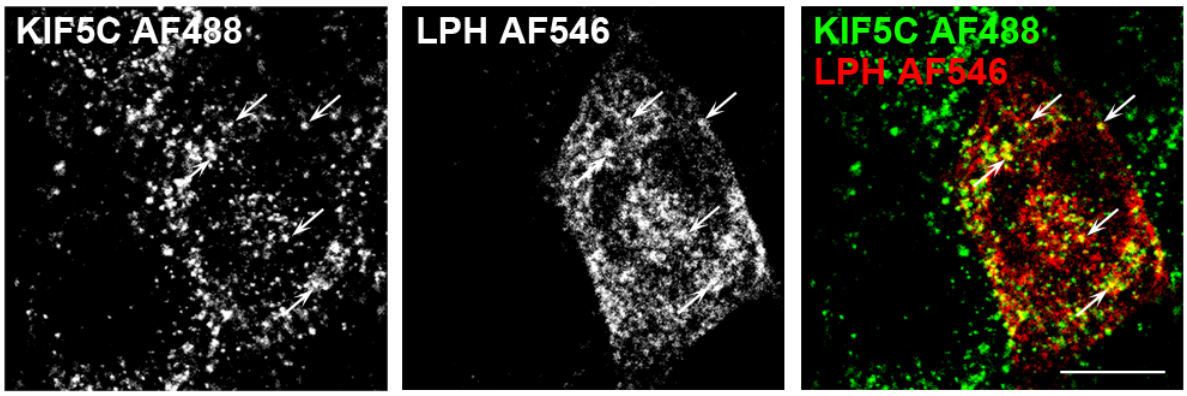

Figure 3.9. Colocalization analysis of endogenous KIF5C and LPH in polarized MDCK cells

MDCK cells, stably expressing LPH, were fixed and stained with anti-KIF5C (with Alexa Fluor 488 as secondary antibody) and anti-LPH (with Alexa Fluor 546 as secondary antibody) antibodies. Colocalized structures are indicated by arrows. In the merged image KIF5C is depicted in green, LPH – in red colour. Scale bar, 10 µm.

To confirm that KIF5C is a general motor protein for different apical proteins, endogenous KIF5C was immunostained in a MDCK cell line, stably expressing LPH, $MDCK_{LPH}$, 10 minutes after TGN release. This time point was chosen because it corresponds to the highest level of KIF5C association with p75. In fact, endogenous KIF5C colocalized to some extent with LPH-carrying vesicles (Fig. 3.9). This result corroborates with the idea that KIF5C is a motor protein not only for p75 and SI, but for the *post*-Golgi trafficking in general.

3.1.8. Intracellular localization of KIF5C in polarized MDCK cells

To understand better the roles of KIF5C in the intracellular transport, colocalization studies with various cellular compartment markers were performed. Anti-GM130 antibody was used to label the Golgi region and anti-TGN38 antibody – to visualize the TGN. To show a possible accumulation of KIF5C in some endosomal compartments, polarized MDCK cells were stained with anti-Rab4 and anti-Rab8 antibodies. As shown in Fig. 3.10, KIF5C does not colocalize with the Golgi. In contrast, some vesicular structures were double-stained with anti-KIF5C and anti-TGN38 antibodies. However, only moderate association of KIF5C with *post*-TGN cargo at 0 min after TGN exit has been observed. Immunostaining with anti-Rab4 and anti-Rab8 antibodies revealed some colocalization with KIF5C (Fig. 3.10). Although the double-stained vesicles are clearly seen, there are a lot of Rab-positive vesicular compartments which are not labeled with KIF5C.

3.1.9. KIF5C tends to localize to tyrosinated microtubules in polarized MDCK cells

It was published before that KIF5C demonstrate preferential binding to detyrosinated microtubules in COS cells (Dunn et al., 2008). It is also known that *post*-translationally modifications of microtubules can play an essential role in the establishment of cell polarity (on the example of neuron development (Konishi and Setou, 2009). To analyze if KIF5C binds to tyrosinated microtubules in polarized MDCK cells, we co-labelled the cells with anti-KIF5C and anti-tyrosinated tubulin (anti-TyrTub) antibodies. As tubulin antibody stains filamentous structures in the cells and KIF5C – vesicular structures, we could see no strong colocalization of these two proteins. Nevertheless, most of the KIF5C-positive vesicles were bound to the TyrTub-microtubules (Fig. 3.11).

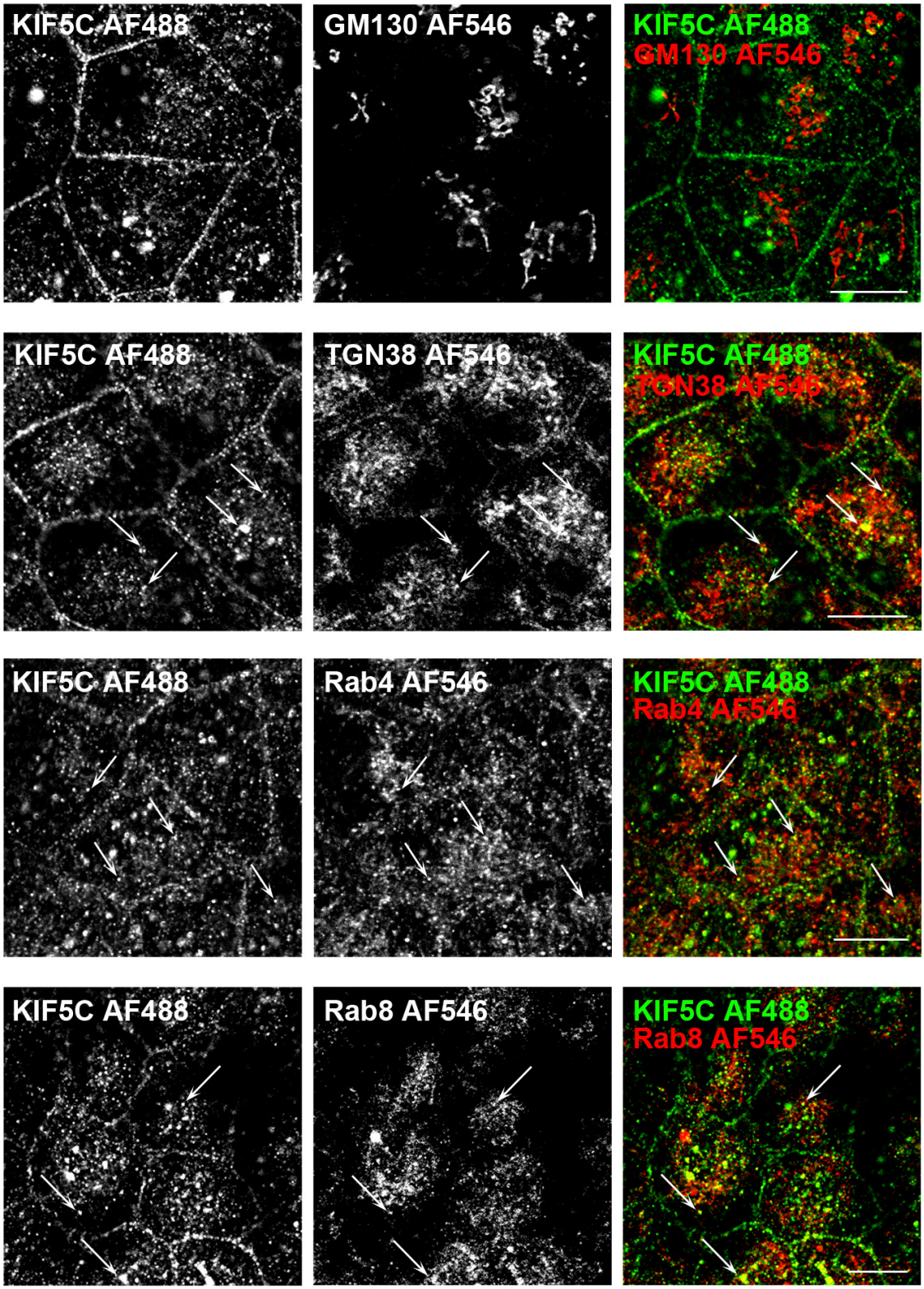

Figure 3.10. Intracellular localization of KIF5C in polarized MDCK cells

MDCK cells were grown to fully polarized state, fixed and stained with KIF5C antibody (Alexa Fluor 488 as secondary antibody) and GM130, TGN38, Rab4 or Rab8 antibody (Alexa Fluor 546 as secondary antibody). Colocalized structures are indicated by arrows. In the merged image KIF5C is depicted in green, GM130, TGN38, Rab4 and Rab8 – in red colour. Scale bars, 10 μm.

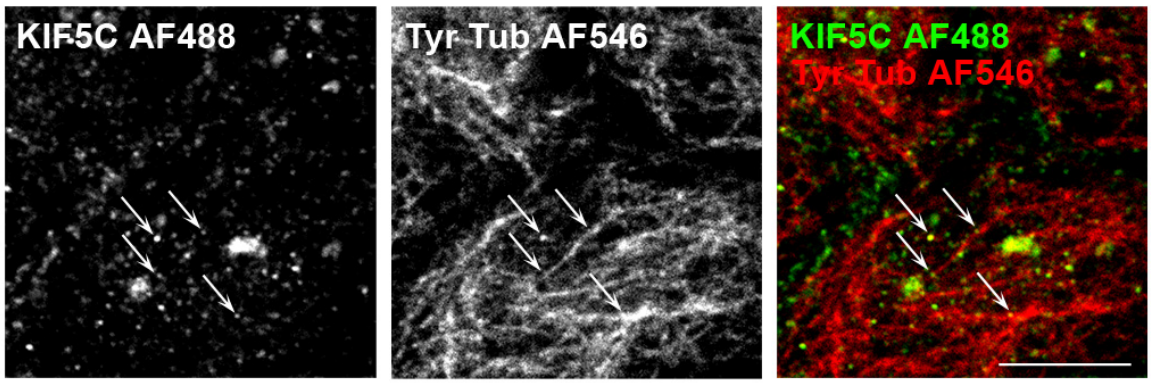

Figure 3.11. KIF5C localizes to tyrosinated microtubules in polarized MDCK cells.

MDCK cells were fixed and immunolabeled with KIF5C (Alexa Fluor 488 as secondary antibody) and TyrTub (Alexa Fluor 546 as secondary antibody) antibodies. KIF5C-positive structures, which localize to tyrosinated microtubules, are indicated by arrows. Scale bar, 10 µm.

3.1.10. Intracellular localization of KIF5C in non-polarized COS cells

MDCK cells are a nice model for studying trafficking processes in polarized epithelial cells. Nevertheless, after polarization the cells are tall and narrow, and this makes microscopy studies more complicated. COS cells are a good alternative for this approach, because of their big size and flat topology. To study the intracellular localization of KIF5C in COS cells, fluorescently labeled KIF5C-GFP was overexpressed. As already published before, overexpressed KIF5C-GFP shows different distributions depending on the level of expression (Dunn et al., 2008). After transfection of COS cells with KIF5C-GFP, four main types of its localization were observed (Fig. 3.12). First of all, a more or less diffusive distribution with some strong peripheral accumulations was detected (Fig. 3.12a). In other cells KIF5C-GFP localized to vesicular structures distributed evenly in the cytoplasm (Fig. 3.12b). In many cells KIF5C-GFP decorated microtubules, additionally forming clusters in the cortical region of the cell (Fig. 3.12c-f), whereas just in a few cells KIF5C-GFP formed also vesicle-like structures along KIF5C-decorated microtubules (Fig. 3.12f).

To prove the specificity of the overexpressed KIF5C-GFP function in COS cells, we co-transfected the cells with the mitochondrial marker Mito-DsRed. As shown in Fig. 3.13 (upper panel), the majority of KIF5C-GFP-positive organelles are mitochondria. Additionally, in contrast to the studies in MDCK cells, KIF5C also shows a colocalization with Golgi in COS cells (Fig. 3.13, lower panel).

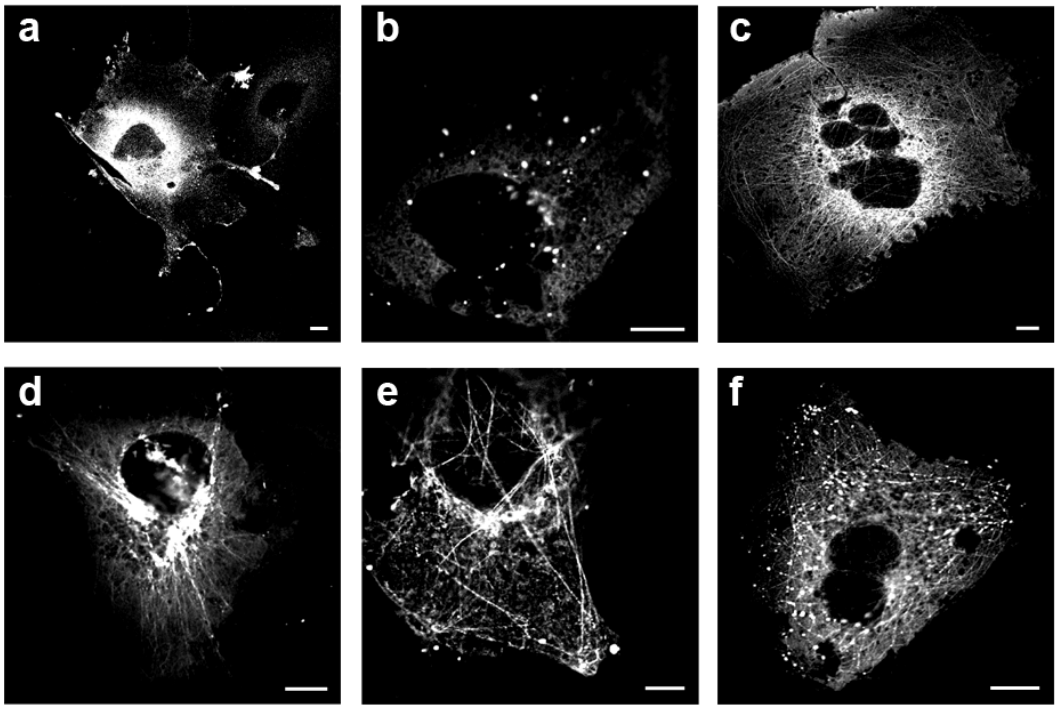

Figure 3.12. Intracellular distribution of overexpressed KIF5C-GFP in COS cells

COS cells were transfected with KIF5C-GFP and after 48 h the cells were fixed. (**a-f**) Different types of intracellular localization of KIF5C-GFP have been seen. Scale bars, 10 μm.

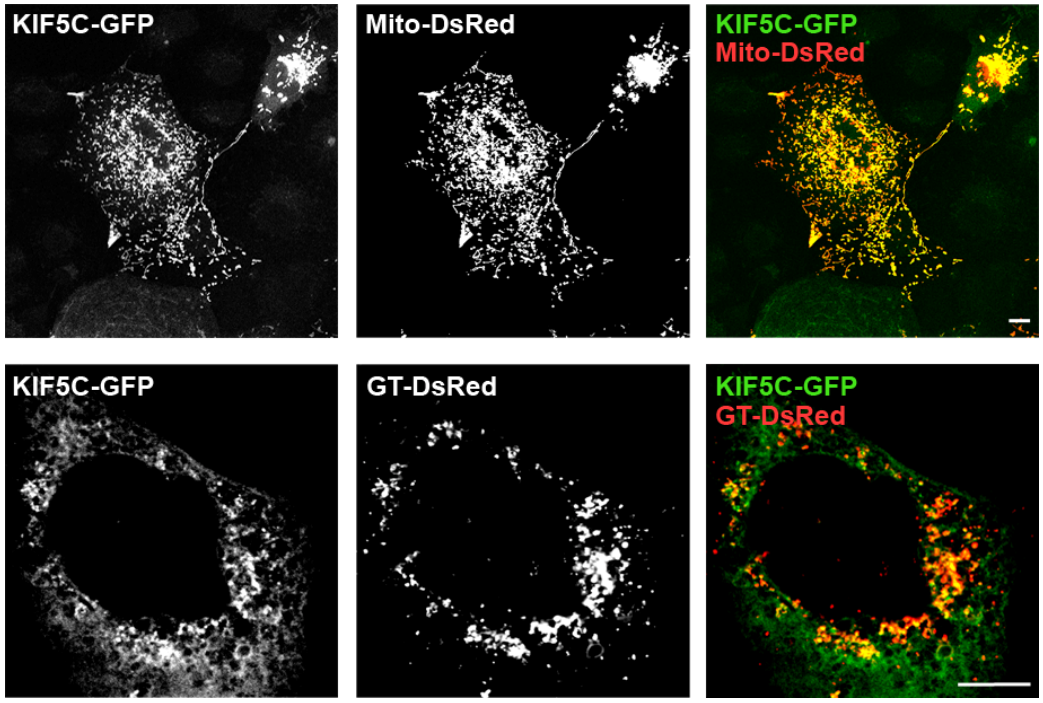

Figure 3.13. KIF5C-GFP colocalizes with mitochondria and Golgi in COS cells.

COS cells were co-transfected with KIF5C-GFP and either mitochondrial marker Mito-DsRed or Golgi marker GT-DsRed. In the merged images KIF5C-GFP is depicted in green, Mito-DsRed and GT-DsRed – in red colour. Scale bars, 10 μm.

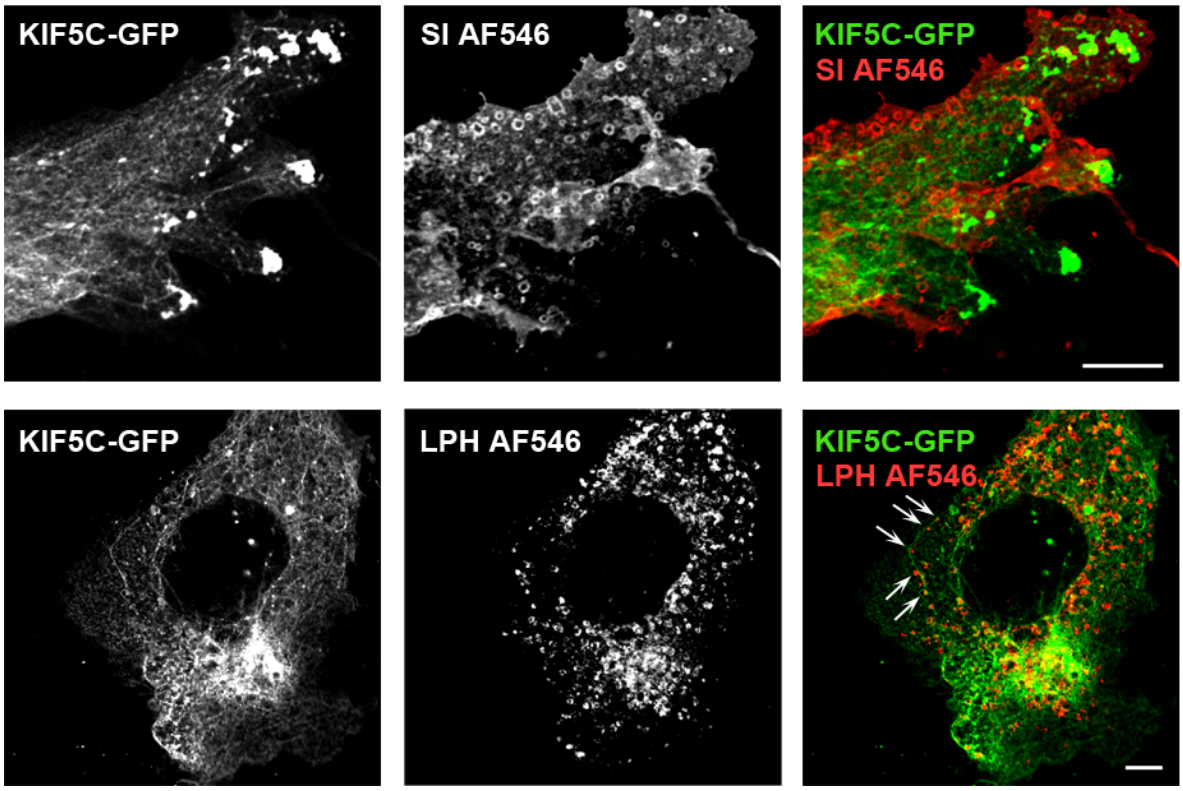

Figure 3.14. KIF5C does not colocalize with apical marker SI and LPH in COS cells.

COS cells were co-transfected with KIF5C-GFP and an apical marker: either raft-associated SI or non-raft-associated LPH. Arrows indicate sites of localization of LPH-carrying vesicles to KIF5C-GFP-decorated microtubules. In the merged images KIF5C-GFP is depicted in green, SI and LPH – in red colour. Scale bars, 10 μm.

To test whether KIF5C-GFP colocalizes with apical markers, either raft-dependent SI or raft-independent LPH were co-expressed with KIF5C-GFP in COS cells. Both apical markers form vesicular structures inside the cell, almost no colocalization was observed (Fig. 3.14). This fact can be explained by the non-polarized organization of the COS cells. Similarly, in non-polarized MDCK cells apical marker p75 is transported by KIF1A/B, whereas after polarization – by KIF5B (Jaulin et al., 2007;Xue et al., 2010).

3.1.11. Dynein is present on the vesicles of raft-associated pathway

As already demonstrated, dynein is not present on raft-independent p75-carrying vesicles (see Fig. 3.2A). To examine if it is also absent on raft-associated pathway, we immunoblotted purified vesicles of both pathways with anti-dynein intermediate chain (IC) antibody. Surprisingly, a strong signal of dynein was seen in SI vesicle preparations (Fig. 3.15A, left panel). To confirm this observation the protein transport in $MDCK_{SI}$ cells was blocked in the TGN region and thereafter released for various time intervals. Purified raft-associated SI-carrying vesicles, corresponding to each time point (0, 5, 10, 20 min), were analyzed by Western blot with anti-dynein IC antibody (Fig. 3.15A, right panel). As expected, dynein is

present on SI-associated vesicles with the highest intensity at 0, 5 and10 minutes after TGN exit. The blot was stained with anti-SI antibodies to check the efficiency of vesicle precipitation.

3.1.12. Interfering dynein function by p50-dynamitin results in decreased apical protein delivery

P50-dynamitin is one of the dynactin subunits and its overexpression disrupts the dynactin complex, which leads to the interference of dynein functions in the cell (Burkhardt et al., 1997). To study the role of dynein in apical protein transport, the cells were transfected with p50-dynamitin-GFP plasmid. The efficiency of transfection was controlled by immunoblotting of lysates with anti-GFP antibodies (Fig. 3.15B, right panel). Both transfected cell lines, $MDCK_{p75}$ and $MDCK_{SI}$ (depicted as “p75” and “SI”, accordingly) expresses p50-GFP, while in control (non-transfected cells) no GFP signal could be detected. Surface delivery of apical markers in p50-transfected cells in comparison to control cells was examined by surface protein immunoprecipitation. The cells were biosynthetically labeled and the p75 or SI were precipitated from either apical or basolateral surface (Fig, 3.15B, left panel). Unexpectedly, the quantifications of three independent experiments revealed the influence of dynein interfering not only on SI trafficking, but also – even stronger – on the apical surface delivery of p75 (Fig. 3.15C). Thus, dynein interference results in the decreased delivery of the marker proteins to the apical membrane, although, whether it is caused by perturbations in *post*-Golgi trafficking, is not clear.

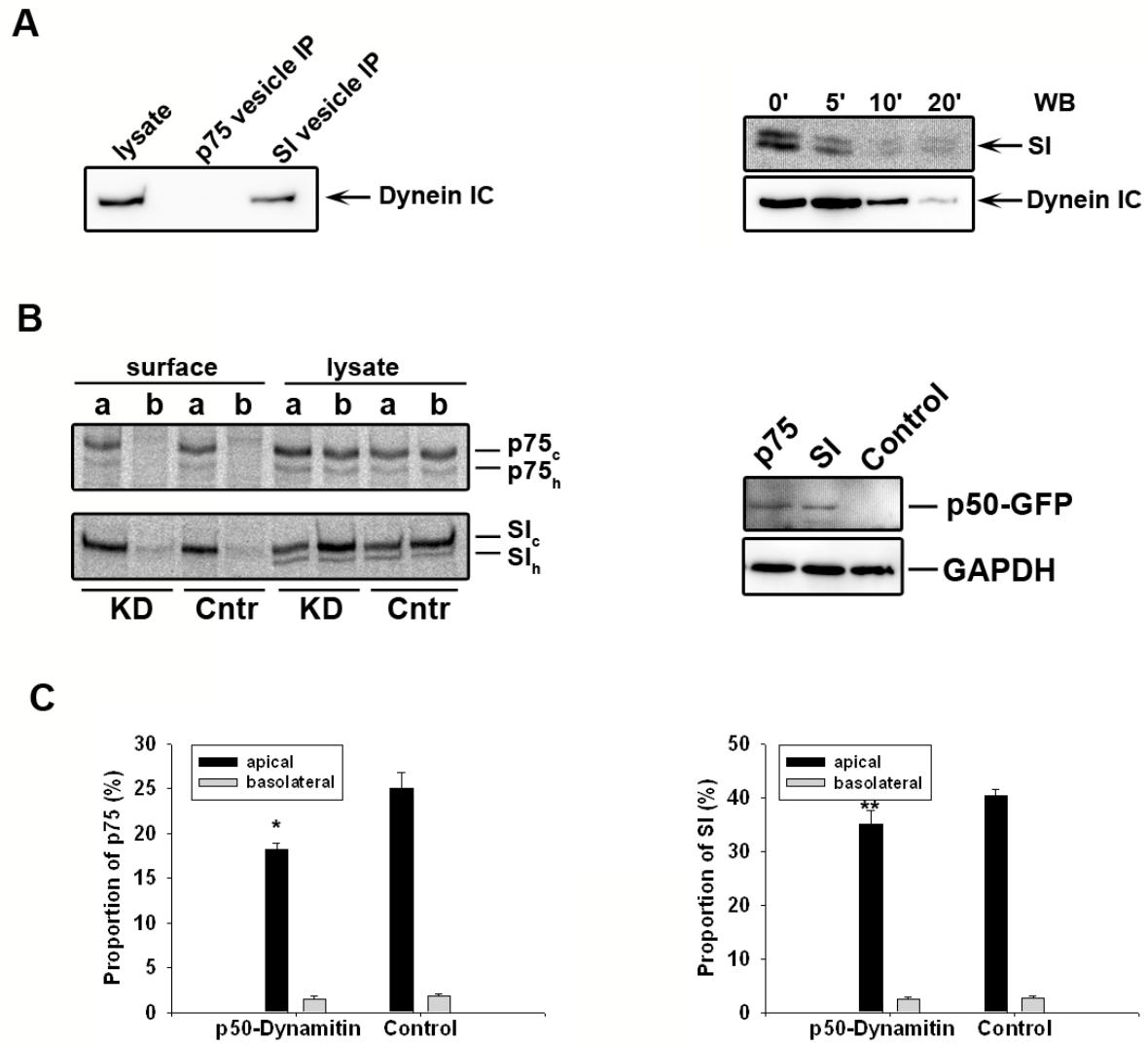

Figure 3.15. The role of dynein in *post*-Golgi trafficking of apical markers SI and p75 in polarized MDCK cells

(**A**) *Post*-Golgi vesicles were purified from either $MDCK_{p75\text{-}GFP}$ or $MDCK_{SI\text{-}YFP}$ cells and analyzed by SDS-PAGE and immunoblotting with dynein IC antibody. Additionally, $MDCK_{SI\text{-}YFP}$ cells were blocked at 20°C and thereafter a TGN release was performed for various intervals (**A**, right panel). To check the efficiency of vesicle immunoprecipitation, the samples were immunoblotted with SI antibody. $MDCK_{SI\text{-}YFP}$ cellular lysate is depicted as lysate. (**B, C**) $MDCK_{p75\text{-}GFP}$ and $MDCK_{SI}$ cells were grown on *trans*-well filters, transfected with p50-GFP and biosynthetically labelled with [^{35}S] methionine for 2 h. The efficiency of p50-GFP transfection was confirmed by Western blot analysis. GAPDH was used as a loading control (**B**, right panel). Cell surface immunoprecipitation of p75 or SI from the apical (a) or basolateral (b) surface was performed with the corresponding antibodies, and cytosolic p75 or SI was precipitated from the remaining cell lysates for comparison. The immunoprecipitates were subjected to SDS–PAGE, followed by phosphoimager analysis. High mannose ($p75_h$ and SI_h) or complex glycosylated ($p75_c$ and SI_c) forms are indicated. (**C**) The proportions of SI and p75 from three independent experiments were quantified. Asterisks denote statistically significant differences using paired Student's t-tests; * $p < 0.01$, ** $p < 0.05$.

3.2. The role of annexin XIIIb in apical protein transport

3.2.1. Annexin XIIIb guides raft-dependent and raft-independent apical traffic in MDCK cells

Annexins are a family of thirteen Ca^{2+}-dependent phospholipids and membrane binding proteins that contain a C-terminal core domain and a short, variable N-terminal domain. Annexins play major roles in many membrane related events such as the organization of membrane domains and the regulation of the activity of several ion channels (Nilius et al., 1996; Kaetzel et al., 1994). Two isoforms, annexin XIIIa and annexin XIIIb, are expressed in epithelial cells (Fiedler et al., 1995). Annexin XIIIb is expressed exclusively in the small intestine and in the kidney, where it concentrates preferentially in the apical brush border rather than in basolateral membranes (Lecat et al., 2000; Wice and Gordon, 1992). It has been demonstrated, that annexin XIIIb plays an essential role in *post*-Golgi lipid raft-dependent protein trafficking to the apical membrane. The role of annexin XIIIb in raft-independent apical transport remained unclear and was a subject of the following study.

3.2.2. Association of annexin XIIIb with non-raft associated vesicles

The first evidence that annexin XIIIb can play a role in raft-independent apical trafficking came from a proteomic analysis (D. Delacour; (Astanina et al., 2010)). To identify protein components which are specifically involved in the transport and sorting of non-raft-associated apical glycoproteins, LPH-positive *post*-Golgi vesicles were isolated from $MDCK_{LPH}$ cells (Jacob et al., 2003). The samples were subjected to 2D gel electrophoresis and were silver stained. The spot pattern was compared with the silver stained 2D gel of SI, corresponding to the raft-associated vesicle population. The spots which were present only in LPH vesicles, and not in SI samples, were cut out and analyzed by MALDI-TOF-TOF. Tandem mass spectrometry revealed galectin-3 (Delacour et al., 2006), as well as annexin XIIIb in raft-independent LPH vesicles, but not in raft-associated SI vesicles.

3.2.3. Annexin XIIIb colocalizes with LPH, p75 and SI in COS cells

To assess if annexin XIIIb is involved in transport routes that are concurrently used by raft-associated and non-raft-associated apical cargo, the intracellular distribution of annexin XIIIb in comparison to raft-associated SI and raft-independent LPH or p75 has been studied in COS cells. This analysis was done by C. I. Delebinski (Astanina et al., 2010). To visualize the intracellular localization of annexin XIIIb, the cDNA of canine annexin XIIIb was amplified from an MDCK cDNA library and ligated into the DsRed-C1 vector. The cells were transiently co-transfected with annexin XIIIb-DsRed and either SI-YFP and LPH-CFP or p75-YFP and

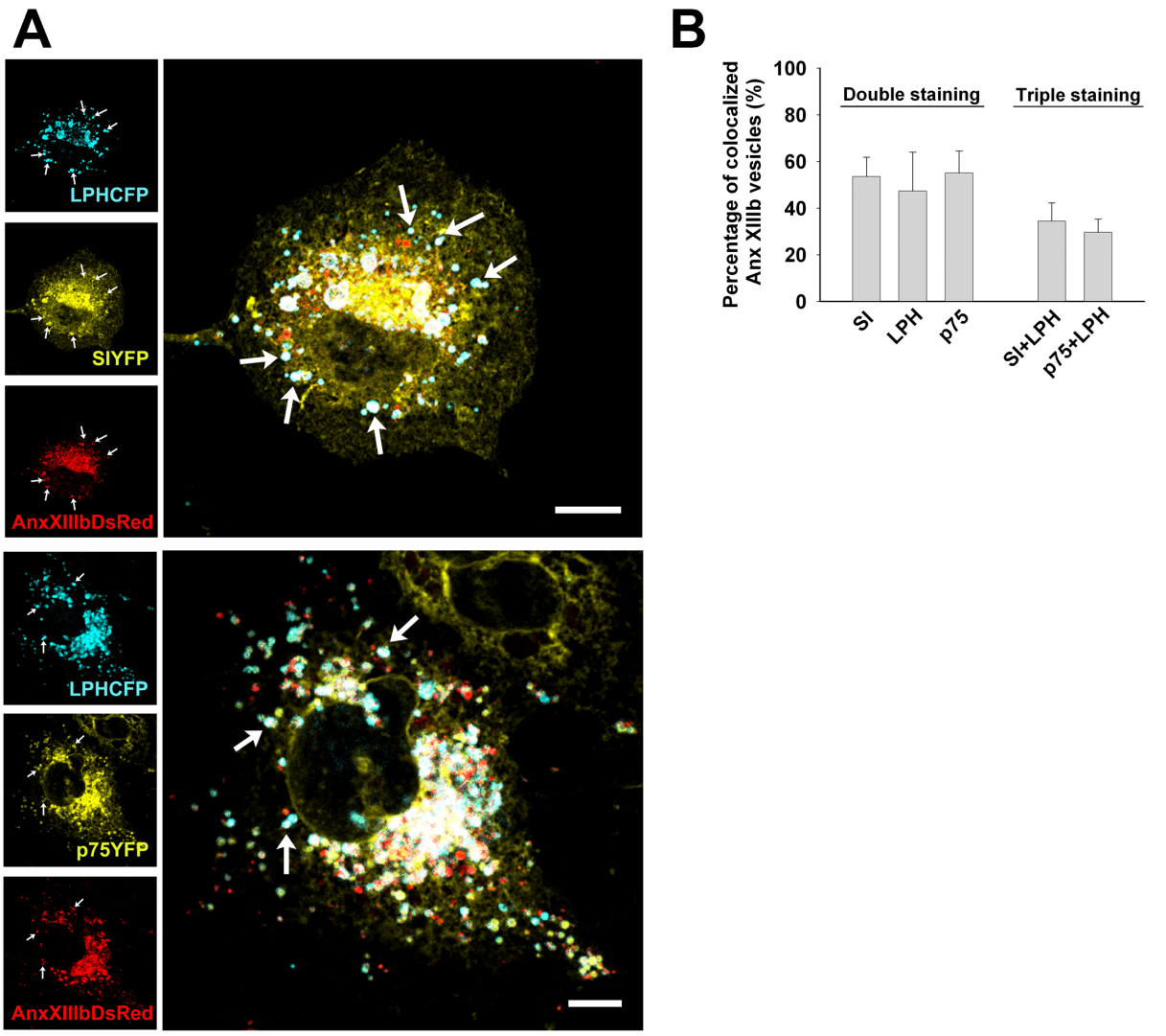

Figure 3.16. Co-staining of p75, SI and LPH with annexin XIIIb in COS cells

(**A**) COS cells were co-transfected with AnxXIIIb-DsRed and SI-YFP/LPH-CFP (upper panel) or LPH-CFP/p75-YFP (lower panel). 48 h after transfection the cells were blocked in TGN and released for 10 min. After fixation the cells were analyzed by confocal microscopy. Arrowheads depict AnxXIIIb-positive structures stained by LPH and SI or LPH and p75, which are also indicated by arrows in the single fluorescence images. Scale bars, 10 µm. (**B**) Quantification of the colocalization of annexin XIIIb with apical markers SI, p75 and LPH. The percentage of annexin XIIIb positive vesicles, colocalized with either SI, LPH, p75 (double staining) or with SI and LPH or p75 and LPH (triple staining) is depicted.

LPH-CFP. After 48 hours the accumulation of newly synthesized material in the TGN was stimulated. The TGN block was then released by incubation at 37 ºC for 10 minutes followed by fixation of the cells with paraformaldehyde. Confocal microscopy analysis of the intracellular distribution of annexin XIIIb revealed that it concentrates in small vesicular

structures, mostly located in the perinuclear region. Fig. 3.16 indicates that about 50% of the annexin XIIIb-positive vesicles colocalized with the raft-independent markers p75 and LPH, as well as with the raft-dependent SI. Moreover, these triple-stained vesicles containing annexin XIIIb, LPH and SI or p75 were found in the perinuclear region of transfected COS cells and constitute about 30% of all annexin XIIIb-positive vesicles. Altogether, these data suggest that in COS cells annexin XIIIb as well as LPH, p75 and SI accumulate to a notable extent in identical compartments 10 minutes after TGN-exit.

3.2.4. Annexin XIIIb colocalizes with apical marker proteins in polarized cells

Next, together with C.I.Delebinski the subcellular localization of annexin XIIIb was examined in polarized epithelial MDCK cells. Stable MDCK cell lines expressing SI-YFP or p75-GFP were transiently transfected with annexin XIIIb-DsRed. The TGN block and release was performed as described above. The cells were immediately fixed and their apical regions were analyzed by confocal microscopy. As expected, in accordance with a previously described role of annexin XIIIb in the raft-dependent apical pathway (Lafont et al., 1998), annexin XIIIb colocalized with SI-YFP-containing structures (Fig. 3.17A). Furthermore, significant quantities of raft-independent p75-GFP positive vesicles were co-stained with annexin XIIIb. To confirm the role of annexin XIIIb in apical protein transport, co-staining of annexin XIIIb with endogenous apical markers of both pathways was examined. Gp135 was immunolabeled for raft-dependent (Ojakian and Schwimmer, 1988) and gp114 for raft-independent apical pathways (Le Bivic et al., 1990; Verkade et al., 2000) (Fig. 3.17B). Again, annexin XIIIb colocalized with markers for both apical pathways, which corroborates our findings in COS cells and indicates that annexin XIIIb is involved in raft-dependent as well as in raft-independent apical trafficking in polarized MDCK cells.

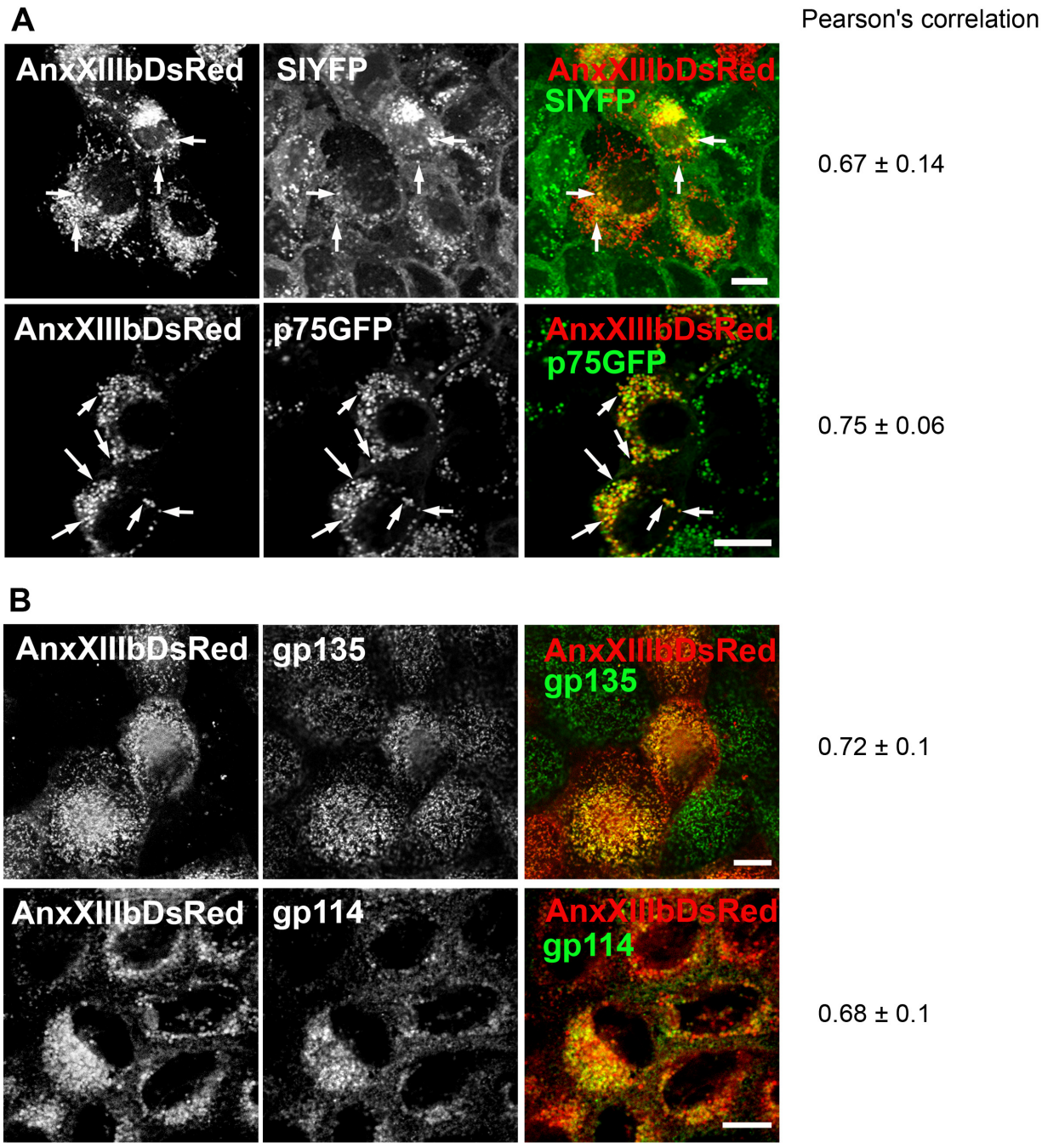

Figure 3.17. Co-staining of p75 and SI with annexin XIIIb in MDCK cells

$MDCK_{SI\text{-}YFP}$ and $MDCK_{p75\text{-}GFP}$ cells were grown on coverslips and transfected 2h after seeding with AnxXIIIb-DsRed. After five days the cells were fixed and stained for gp114 and gp135 with specific antibodies. The cells were analyzed by confocal microscopy. In the merged image AnxXIIIb-DsRed is shown in red, and SI-YFP, p75-GFP (A), gp114 or gp135 (B) in green. Some colabelled structures are indicated by arrows. Pearson's correlations were quantified for 10 cells and are indicated on the right panel. Scale bars, 10 µm.

3.2.5. Characterization of annexin XIIIb positive structures in MDCK cells

The following study was done in collaboration with C. I. Delebinski (Astanina et al., in press). To further characterize subcellular compartments of polarized MDCK cell monolayers enriched in annexin XIIIb, an MDCK cell line, stably expressing annexin XIIIb-DsRed was generated ($MDCK_{AnxXIIIb\text{-}DsRed}$). The cells were grown for five days on coverslips and the distribution of annexin XIIIb-DsRed, in comparison to subcellular marker proteins, was analyzed by immunocytochemistry and confocal microscopy. Annexin XIIIb-DsRed forms vesicular structures, which distributed evenly in the cytosol (data not shown). As a marker for early endosomes *Early Endosome Antigen 1* (EEA1) was used – a membrane bound protein component, which is specific to early endosomes and essential for fusion between early endocytic vesicles (Mu et al., 1995). Rab7 has been used as a marker for late endosomes, as it is known to be localized to this organelle and to play an important role in the late endocytic pathway. Both antibodies, as expected, (anti-EEA1 and anti-Rab7) labelled vesicular structures in the cytosol of polarized MDCK cells. The TGN region was labelled with anti-p230 antibody because it was shown that p230 is associated with vesicles budding from the *trans*-Golgi network (Gleeson et al., 1996). This antibody stained characteristic membrane accumulation in the perinuclear region, which corresponds to the TGN. As a marker for the Golgi apparatus anti-GM130 antibody was used. GM130 is a member of the Golgin protein family and is localized to the Golgi. Annexin XIIIb-positive vesicles did not co-stain with the early endosomal marker EEA1 or the late endosomal marker Rab7 (Pearson's correlation 0.08 and 0.07). Furthermore no colocalization could be observed either with the TGN marker p230 or Golgi GM130 (Pearson's correlation 0.09 and 0.07) (Fig. 3.18). However, significant quantities of vesicular structures were positive for both annexin XIIIb and Rab8 or Rab10 (Pearson's correlation 0.77 and 0.44) (Fig. 3.18), which suggests that annexin XIIIb is localized to Rab-positive endosomal organelles.

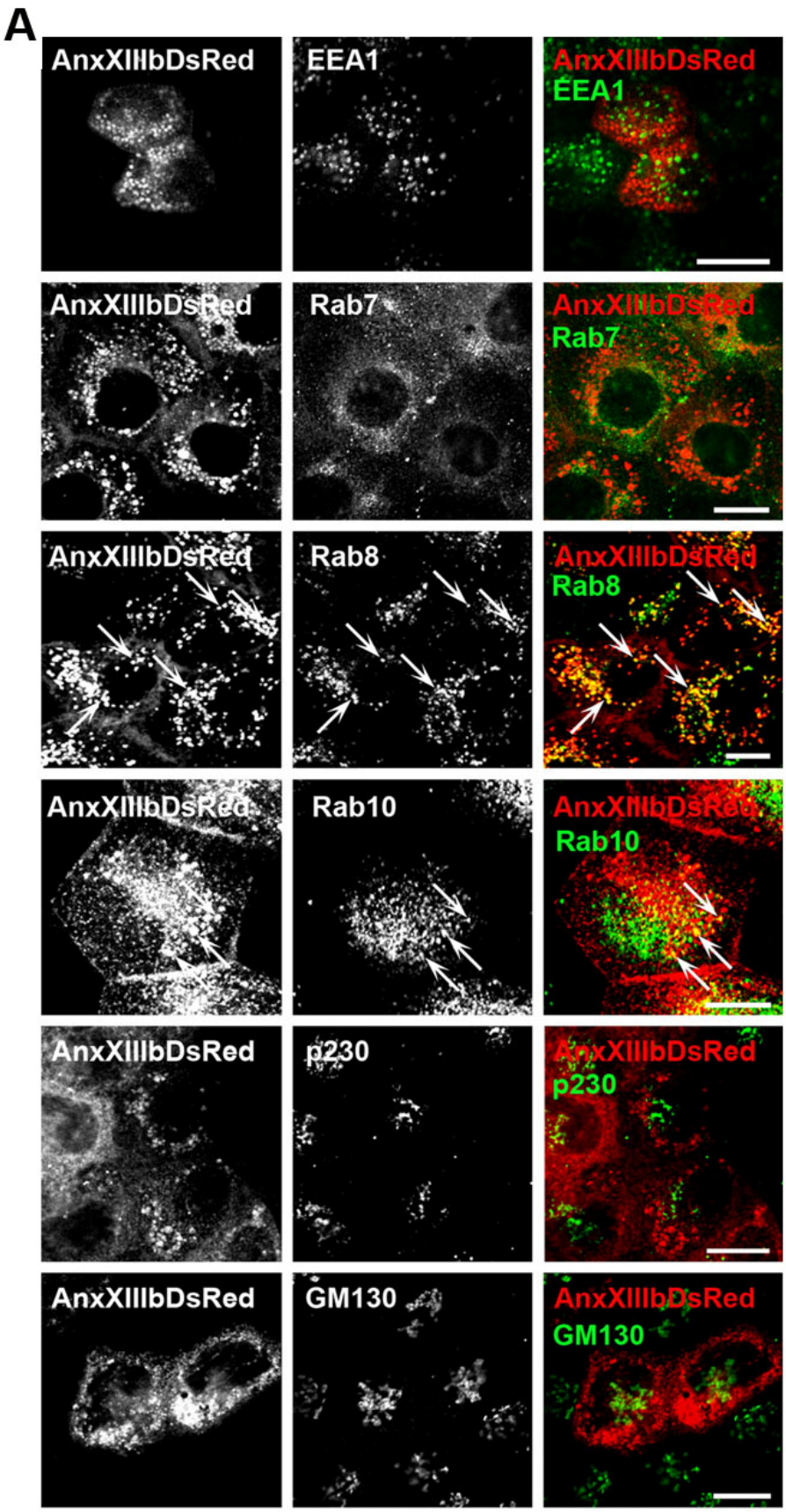

Figure 3.18. Characterization of annexin XIIIb-DsRed in MDCK cells

Continued on the next page

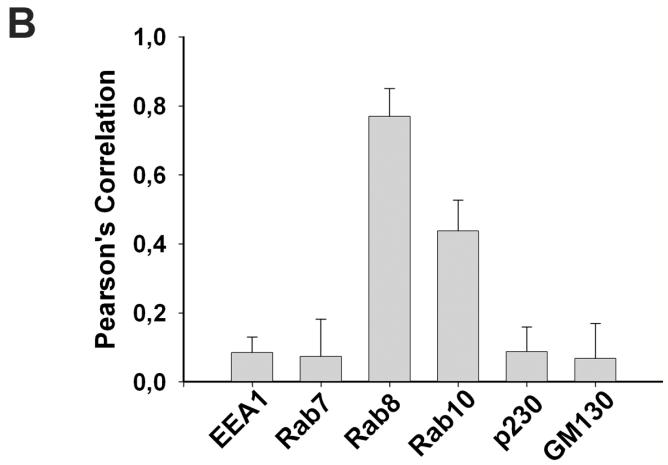

Figure 3.18. Characterization of annexin XIIIb-DsRed in MDCK cells

(**A**) $MDCK_{AnxXIIIb\text{-}DsRed}$ cells were grown on coverslips for five days. The cells were fixed and stained for immunofluorescence with antibodies directed against the TGN (p230), the Golgi region (GM130) or against endosomal EEA1, Rab7, Rab8, Rab10. Alexa-fluor 488 (green) was used as secondary antibody. No co-staining between AnxXIIIb-DsRed and the TGN, Golgi, early or late endosomes could be detected. AnxXIIIb-DsRed and Rab8 or Rab10 colabelled structures are indicated by arrows. Scale bars, 10 µm. (**B**) Pearson's correlations quantified from 10 cells are indicated.

3.2.6. Endogenous annexin XIIIb colocalizes with apical markers and endosomal Rab8

To prove that annexin XIIIb colocalization with apical and endosomal markers is not caused by overexpression, the intracellular distribution of endogenous annexin XIIIb was studied. MDCK cells, or cells stably expressing p75-GFP or SI-YFP, were fixed and stained with polyclonal anti-annexin XIIIb antibody. Similar to overexpressed annexin XIIIb-DsRed, endogenous annexin XIIIb localized to vesicular structures, distributed evenly in cytosol with a weak bias to the apical region (Fig. 3.19A, B). Annexin XIIIb colocalized with both apical markers: raft-associated SI and raft-independent p75, with a Pearson's correlation 0.49 and 0.73, respectively (Fig. 3.19A). This corroborates with our findings for overexpressed annexin XIIIb-DsRed (Fig. 3.17). The endogenous annexin XIIIb colocalized also with Rab8, although to a lesser extent than by overexpressed annexin XIIIb: The Pearson's correlation for overexpressed annexin XIIIb was 0.77, in comparison with only 0.4 for endogenous protein (Fig. 3.17, 3.19). Nevertheless, analysis of the intracellular distribution of the endogenous annexin XIIIb confirms that it is present on apical vesicles of both – raft-dependent and -independent – pathways, as well as on the Rab8-positive endosomal compartment.

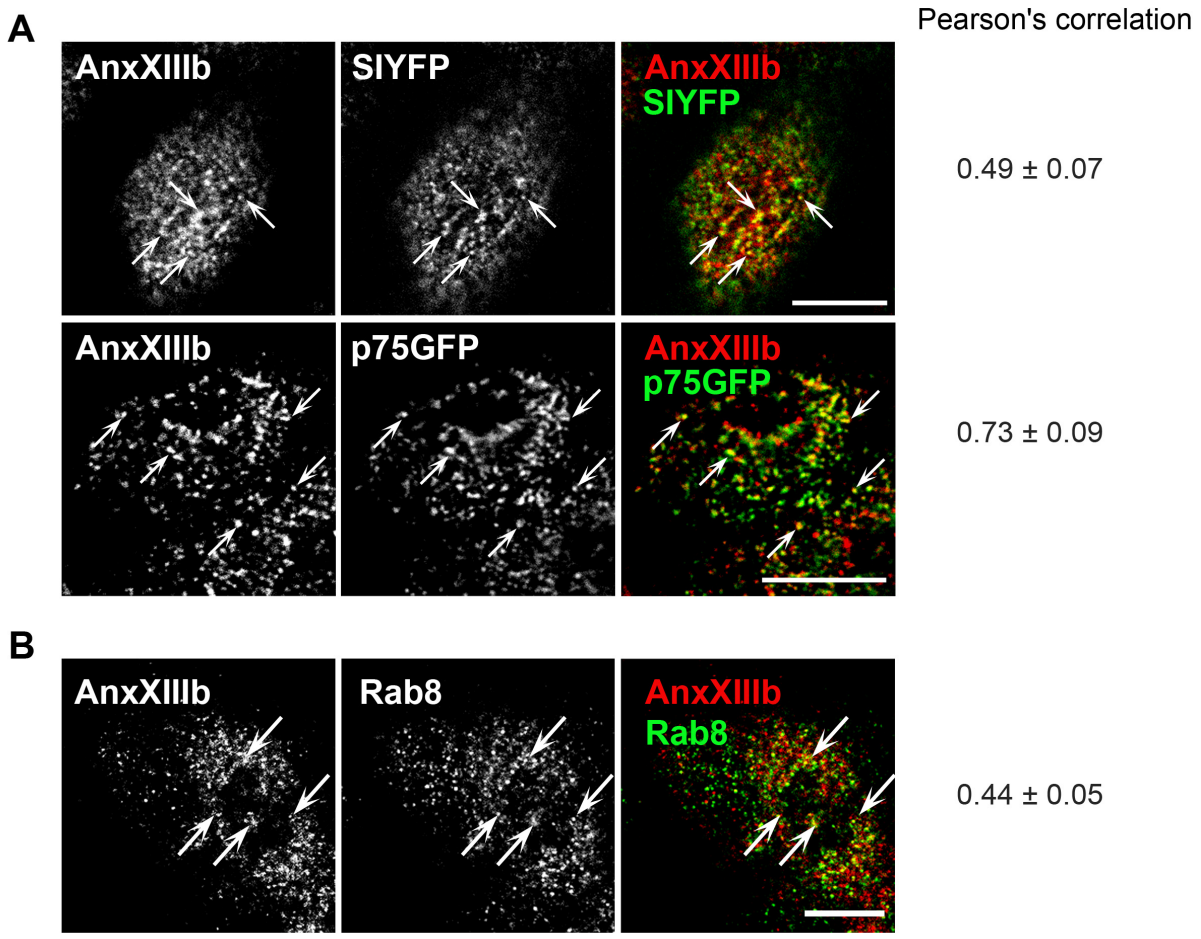

Figure 3.19. Endogenous annexin XIIIb colocalizes with apical markers and Rab8.

(**A**) $MDCK_{SI\text{-}YFP}$ (upper panel) and $MDCK_{p75\text{-}GFP}$ (lower panel) cells were grown on coverslips and fixed on the fifth day. The cells were stained with polyclonal anti-annexin XIIIb antibodies (with Alexa Fluor 546 as secondary antibody). (**B**) MDCK cells were grown on coverslips, fixed and stained with polyclonal anti-annexin XIIIb (secondary antibody Alexa Fluor 546) and monoclonal anti-Rab8 antibodies (secondary antibody Alexa Fluor 488). Confocal sections were recorded from regions just beneath the apical membrane. Colocalized structures are indicated by arrows. Pearson's correlations quantified from 10 cells are indicated on the right panel. Scale bars, 10 µm.

3.2.7. Annexin XIIIb is present on immunoisolated apical *post*-Golgi vesicles

Previous studies have shown that annexin XIIIb is enriched in TGN-derived apical carriers of the raft-associated hemagglutinin glycoprotein in MDCK cells (Lafont et al., 1998). To assess the presence of annexin XIIIb on immunoisolated apical *post*-Golgi carriers for raft-associated and non-raft-associated transport, purified vesicles from $MDCK_{SI\text{-}YFP}$ and $MDCK_{p75\text{-}GFP}$ cells were examined (Delacour et al., 2006). The cells were blocked at 20 ºC for 4 hours followed by a TGN release at 37 °C for various time intervals. The cells were lysed and *post*-Golgi vesicles were fractionated by sucrose density centrifugation and immunoisolated with monoclonal anti-GFP antibody. Following gel electrophoresis the samples were analyzed by immunoblotting with polyclonal anti-annexin XIIIb antibody. As

shown in Fig. 3.20, annexin XIIIb could not be detected on immunoisolated vesicles carrying SI-YFP or p75-GFP 5 min after TGN-release. However, 10 min after TGN-release annexin XIIIb was present on both SI-YFP- and p75-GFP-carrying vesicular structures. Thereafter, at 20 min after TGN release, annexin XIIIb almost disappeared from both vesicle populations. Immunobloting with anti-Rab8 antibodies revealed that annexin XIIIb association with *post*-Golgi vesicles occurs simultaneously with the Rab8 association on immunoisolated vesicles (Fig. 3.20). This observation is corroborated by the endosomal accumulation of annexin XIIIb in MDCK cells (Fig. 3.18, 3.19). By using anti-PDI (protein disulfide isomerase – marker protein for endoplasmic reticulum) antibody as a negative control, we could exclude the presence of ER-derived membranes in these vesicle preparations (Fig. 3.20).

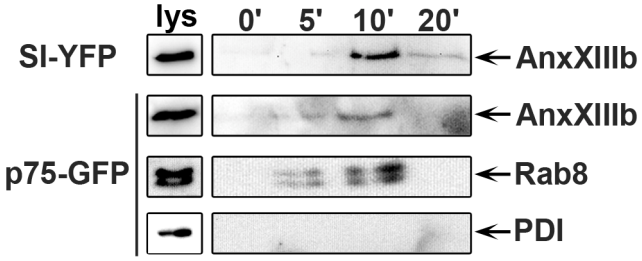

Figure 3.20. Annexin XIIIb is present on immunoisolated *post*-Golgi.

Newly synthesized material was accumulated in the TGN of $MDCK_{p75\text{-}GFP}$ and $MDCK_{SI\text{-}YFP}$ cells at 20 °C followed by a release at 37 °C for 0, 5, 10 and 20 minutes. Cell homogenates were loaded onto a step sucrose gradient and *post*-TGN vesicles were immunoisolated with monoclonal anti-GFP antibodies. The immunoprecipitates were separated by SDS-PAGE and immunoblotted with anti-annexin XIIIb, anti-Rab 8 and anti-PDI antibodies. Immunoblots of cellular lysates are depicted as lys.

3.2.8. Depletion of annexin XIIIb decreases the apical surface delivery of SI, p75 and LPH

Having identified annexin XIIIb in an endosomal compartment that resembles a crossroad between raft-dependent and raft-independent apical trafficking, now the function of this annexin was examined in both pathways. Therefore, annexin XIIIb was depleted by RNA interference. Three siRNA duplexes were designed to specifically target the annexin XIIIb mRNA. The efficiency of knockdown in MDCK cells was over 95% (Fig. 3.21A). This was determined by Western blot analysis of cell lysates from annexin XIIIb depleted and control cells transfected with luciferase siRNA. Remarkably, annexin XIIIb depletion had no influence on the polarization of the cells: E-cadherin localizes to basolateral membrane, p75 – to the apical membrane (Fig. 3.21B). To evaluate the efficiency of surface delivery of SI, p75 and

LPH in annexin XIIIb depleted MDCK cells, the cells were grown on *trans*-well filters and biosynthetically labeled with [^{35}S]methionine. The marker proteins were immunoprecipitated separately from the apical or basolateral surfaces and their levels were compared to the quantities isolated from control cells (Fig. 3.21C). This experiment revealed a reduction in apical surface delivery, after annexin XIIIb knockdown, of all three transmembrane proteins studied.

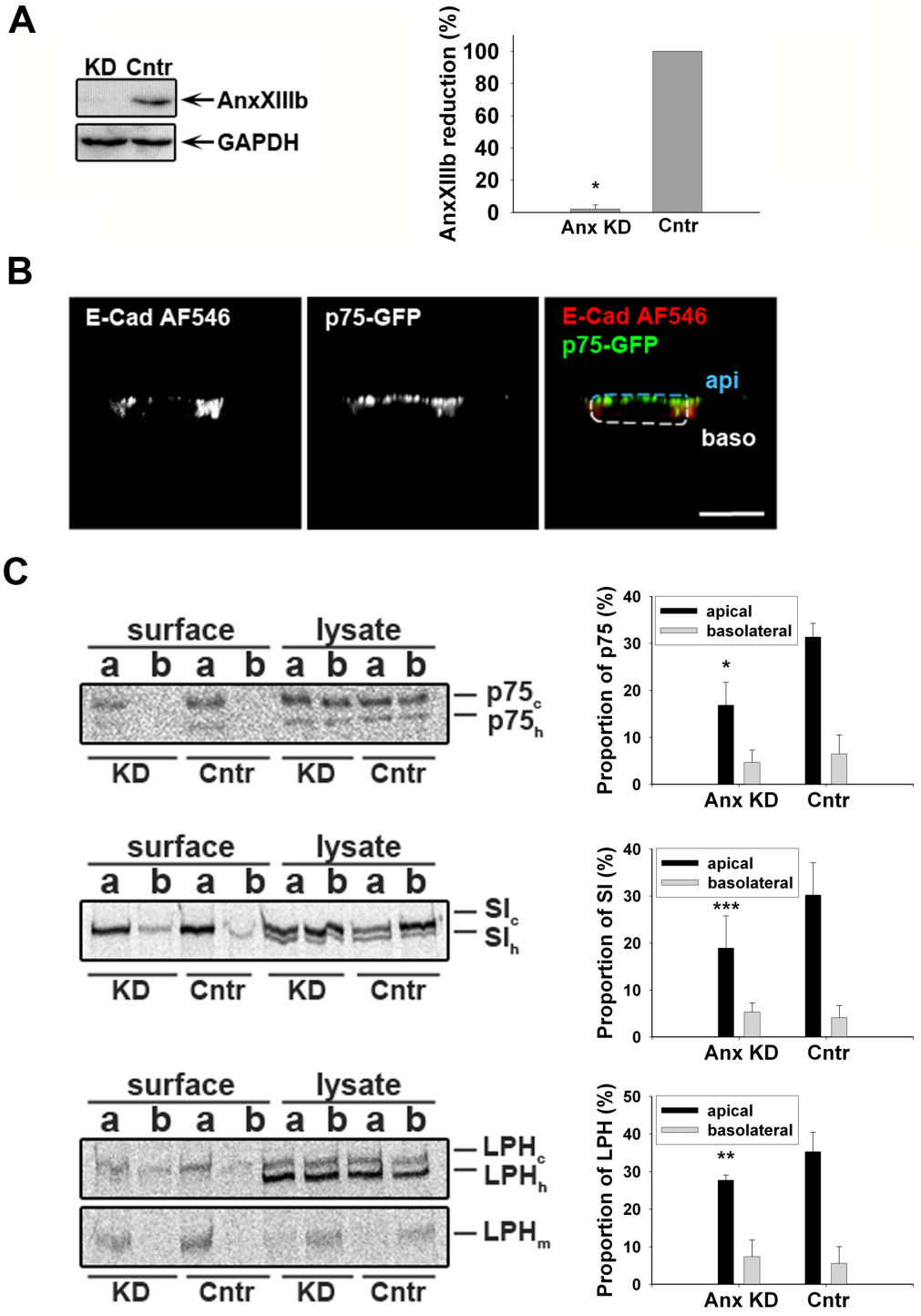

Figure 3.21. Figure legend on the next page

Figure 3.21. Annexin XIIIb is involved in surface delivery of apical markers.

(**A**) MDCK cells were transfected with annexin XIIIb-specific siRNA-duplexes (KD) or luciferase siRNA as control (Cntr). 48h after transfection, the knockdown was analyzed by Western blotting using anti-GAPDH antibodies (as a loading control) or anti-annexin XIIIb (**A**, left panel). Quantification of the knockdown efficiency is shown (**A**, right panel). (**B**) MDCK $_{p75\text{-}GFP}$ cells were transfected with annexin XIIIb-specific siRNA-duplexes. 48 hours after transfection the cells were fixed and stained with anti-E-cadherin antibody. The xz view is shown; the apical region is depicted as api, the basolateral – as baso. Scale bar, 10 µm. (**C**) $MDCK_{LPH}$, $MDCK_{p75\text{-}GFP}$ and $MDCK_{SI}$ cells were grown on *trans*-well filters, transfected with annexin XIIIb or control siRNA and biosynthetically labelled for 2h with [^{35}S]methionine, followed by incubation for 4 h at 37 °C. Cell surface immunoprecipitation of LPH, p75 or SI from the apical ("a") or basolateral ("b") membranes (depicted as "surface") was performed with the corresponding antibodies. Cytosolic LPH, p75 or SI were precipitated from the remaining cell lysates for comparison (depicted as "lysate"). The immunoprecipitates were subjected to SDS-PAGE followed by phosphoimager analysis. High-mannose (LPH_h, SI_h, $p75_h$) or complex glycosylated forms (LPH_c, SI_c, $p75_c$) are indicated. LPH_m, mature form of LPH. The proportions of p75, SI and LPH from four independent experiments were quantified (**C**, right panel). Asterisks denote statistically significant differences using paired Student´s t tests; * = $p<0.001$, ** = $p<0.01$, *** = $p<0.05$.

To prove that the trafficking delay in the absence of annexin XIIIb is related to events following TGN-exit, the transport kinetics of apical cargo molecules was studied as described before (Astanina and Jacob, 2010; Cramm-Behrens et al., 2008). Here, after siRNA-depletion of annexin XIIIb radioactively labeled p75, SI and LPH were isolated from the apical cell surface in a pulse-chase experiment after different time intervals of chase (Fig. 3.22). The quantification revealed a significant delay in apical surface delivery of both raft-dependent SI and raft-independent p75 in the absence of annexin XIIIb. The difference between p75 and SI proportion at the apical surface in annexin XIIIb-depleted and control cells was in both cases about 15%.

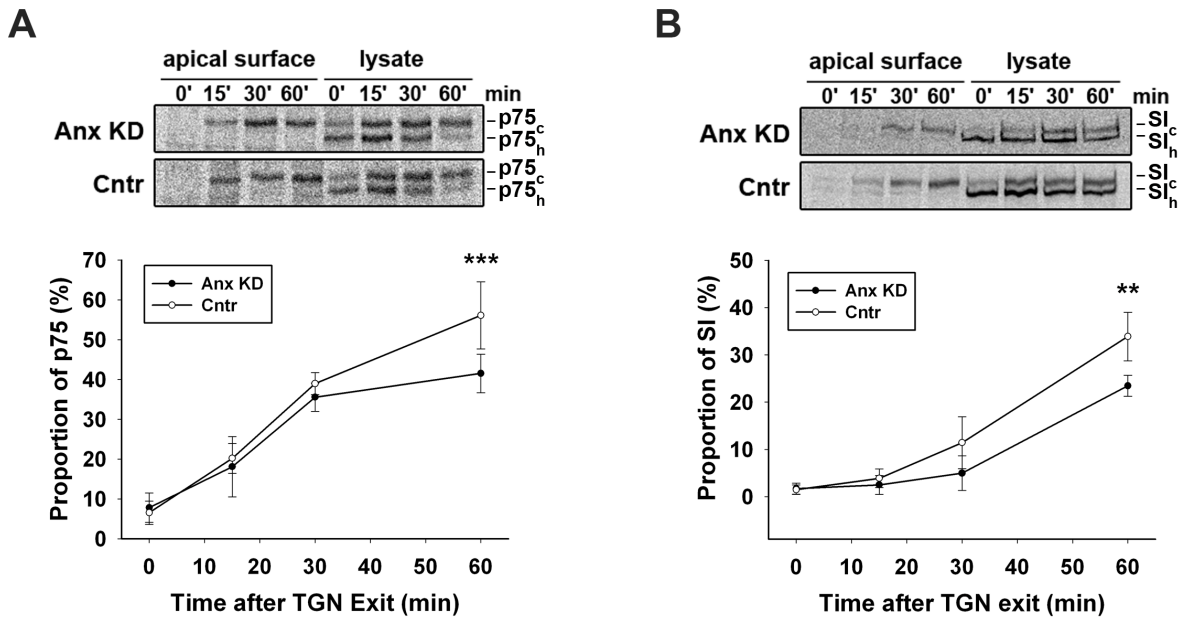

Figure 3.22. Transport kinetics of p75 and SI after depletion of annexin XIIIb

Control or annexin XIIIb-depleted $MDCK_{p75\text{-}GFP}$ (**A**) and $MDCK_{SI}$ (**B**) cells were grown on *trans*-well filters and biosynthetically labelled with [^{35}S]methionine for 15 min. The cells were incubated at 20 °C for 4 h to block newly synthesized proteins in the TGN. Temperature was shifted to 37 °C for various time intervals (0, 15, 30 and 60 minutes), followed by cell surface immunoprecipitation of p75 and SI from the apical surface. Cytosolic p75 and SI were immunoprecipitated from the remaining cell lysates for comparison. The immunoprecipitates were subjected to SDS-PAGE, followed by phosphoimager analysis. Mannose-rich ($p75_h$ and SI_h) or complex glycosylated ($p75_c$ and SI_c) forms are indicated. The proportions of surface p75 and SI were quantified from three independent experiments (**A**, **B**, bottom panel). Asterisks denote statistically significant differences using paired Student´s t tests; ** = $p<0.01$, *** = $p<0.05$.

4. Discussion

4.1. Characterization of motor proteins involved in apical protein trafficking

4.1.1. Purified vesicles bind and move along microtubules *in vitro*.

Microtubule-based *in vitro* motility and binding assays allow to study interaction of motor proteins with cytoskeletal filaments and to characterize movement of purified organelles along microtubules. In the current study, *in vitro* assays have been used to adjust the vesicle immunoprecipitation procedure and to confirm the presence of molecular motors on purified vesicles, which were examined thereafter biochemically. *In vitro* binding assays have revealed first evidence that purified *post*-TGN vesicles carry proteins that form a link between a vesicle itself and a microtubule. Most probably, this interaction is carried out by motor proteins. In fact, the motility assay showed that the purified vesicles do not only bind to microtubules, but also move along them (Fig. 3.1). Remarkably is, that the vesicles were moving in both directions on microtubular tracks and this fact can have several explanations. First of all, bidirectional movement can be carried out by at least two types of motor proteins (plus and minus end-directed) present on the motile organelle. For example, this could be the plus end-directed kinesin and minus end-directed dynein, as in the case of *in vitro* reconstitution of ATP-dependent movement of endocytic vesicles (Murray et al., 2000). On the other hand, the normal diameter of a single microtubule is 25 nm, whereas the measured diameter of microtubules in the current assay was 100-200 nm (data not shown), which means that several microtubules could have formed a bundle, probably with even orientations of plus and minus ends. Thus, the vesicles were moving always in one direction (plus or minus), but they were changing the microtubular filament within the bundle. Another possibility for bidirectional movement is so called “diffusive” movement of motor proteins. This type of motion has been shown, for example, for kinesin-13, which uses a one-dimensional diffusive search to rapidly target microtubule ends where it binds and depolymerises microtubules (Helenius et al., 2006). Recently, diffusive *in vitro* movement has been demonstrated also for processive kinesin-1 (Lu et al., 2009).

In general, the velocities of organelle movement *in vitro* may vary depending on the motor protein itself and the study approach. For example, for gliding assays the pace of KIF1B was about 0.66 µm/sec (Nangaku et al., 1994), whereas KIF1B-coated beads were transported in the motility assay with a velocity up to 0.82 µm/s (Wozniak et al., 2005). In cells, the organelle speed can be significantly higher, for example, KIF5B-dependent movement of apical cargo in living cells is about 1.4 µm/s (Jaulin et al., 2007). In the present study the mean velocity of vesicles was quite low (0.08 µm/s, see Fig. 3.1), although, when only unidirectional processive movements was quantified, the mean value was 0.28 µm/s. A

plausible reason for this variability can be the presence of cofactors that substantially influence the kinesin velocity and thus vesicle movement. Also the purification procedure itself can lead to the detachment of molecular motors from some vesicles or to their inactive state. In agreement with this idea is the fact that a lot of vesicles do not bind to microtubules in perfusion chambers *in vitro*: these vesicles either stick non-specifically to the DEAE-Dextran-covered glass surface, or do not carry any motor protein to bind specifically to microtubules. Although, 100% binding of vesicles to microtubules can be also interfered by the motility buffer itself. For example, it is known that kinesin undergoes a salt-dependent transition from an extended active to a folded inactive molecule (Hackney et al., 1992).
Another interesting point is that in motility assays the vesicles have often changed the microtubular tracks and continued their movement on another microtubular filament (Fig. 3.1). Most probably it can be realized if the motor protein remains bound to the organelle during detachment from microtubule. In fact, similar mechanism was shown for mitochondria, where the kinesin heavy chain remains associated with cargo regardless of whether they are moving to plus or minus end, or even when the mitochondria is not motile (Wang and Schwarz, 2009). In the living cell, the strong association of the motor protein with specific cargo is important for processive directed transport of organelles to their destination, in spite of possible microtubular interruption or trafficking jams on trafficking pathways.

4.1.2. KIF5C is present on purified p75-carrying vesicles.

To check the hypothesis about presence of two types of motor proteins on vesicles, biochemical studies have been performed. Immunoprecipitated *post*-TGN vesicles were tested whether they carry kinesin heavy chain or dynein (Fig. 3.2). KHC has been chosen because, first of all, it is one of the most important motor protein in intracellular organelle trafficking, and, second, one member of KHC group – KIF5B – has been already identified to be essential for *post*-Golgi transport of p75 in polarized epithelial cells (Jaulin et al., 2007; Hirokawa et al., 2009). Dynein was another candidate because it is a member of minus end-directed class of motor proteins and, thus, could provide bidirectional vesicle movement *in vitro*. For dynein detection specific antibody against intermediate chain have been chosen because of the size of detected protein (72 kDa) and because the dynein intermediate chain is relatively conserved between different dynein types (Ogawa et al., 1995). Although, the possibility, that the antibody does not recognize one or another type of IC, should not be excluded. Immunoblotting of p75 vesicle samples revealed no signal for dynein, at the same time kinesin heavy chain has been detected (Fig. 3.2). This data proved that p75 vesicles carry no dynein, but kinesin heavy chain. Nevertheless, it remained unclear, which member of KHC group is present on p75-carrying vesicles, because KHC antibody reacts with all

three members of this group: KIF5A, KIF5B and KIF5C (see Table 2.3). For proteomic analysis KHC was immunoprecipitated from *post*-TGN vesicle-enriched fractions and subjected to MALDI-TOF. The immunoprecipitated protein was identified as KIF5C. The probability based MOWSE (MOlecular Weight SEarch) score in all experimental sets was about 80-120, while protein scores greater than 68 are significant.

KIF5C is a motor protein of KHC group and it was thought to be expressed exclusively in neurons, preferentially in motor neurons. In the absence of this motor, KIF5C knockdown mice exhibit smaller brain size, but were viable with a relative loss of motor neurons to sensory neurons (Kanai et al., 2000). Moreover, KIF5C plays a role in morphogenetic processes, as shown in chicken embryos (Dathe et al., 2004). Here, the KIF5C expression during embryo development is not restricted to neuroectoderm-derived structures, but was additionally found in epithelial somites. Furthermore, Jaulin et al. detected KIF5C in epithelial A549 and MCF-7 cells (Jaulin et al., 2007). Recently, KIF5C was detected in the acrosome of spermatozoa (Mannowetz et al., 2010). The concrete function of KIF5C in non-neuronal tissues, however, has not been described so far. In neurons this motor plays a role in anterograde traffic of mitochondria and vesicles. KIF5C can bind its cargo at the C-terminus of kinesin heavy chain or by association with two kinesin light chains. This interaction is mediated by the adaptor protein GRIP1, which forms a ternary complex with the two KIF5C heavy and light chains (Smith et al., 2006). GRIP1 also forms a complex with GluR2, a subunit of the AMPA (α-amino-3-hydroxy-5-methylisoxazole-4-propionate) receptor (Setou et al., 2002), and thus KIF5C is linked to synaptic vesicle components in neuronal cells.

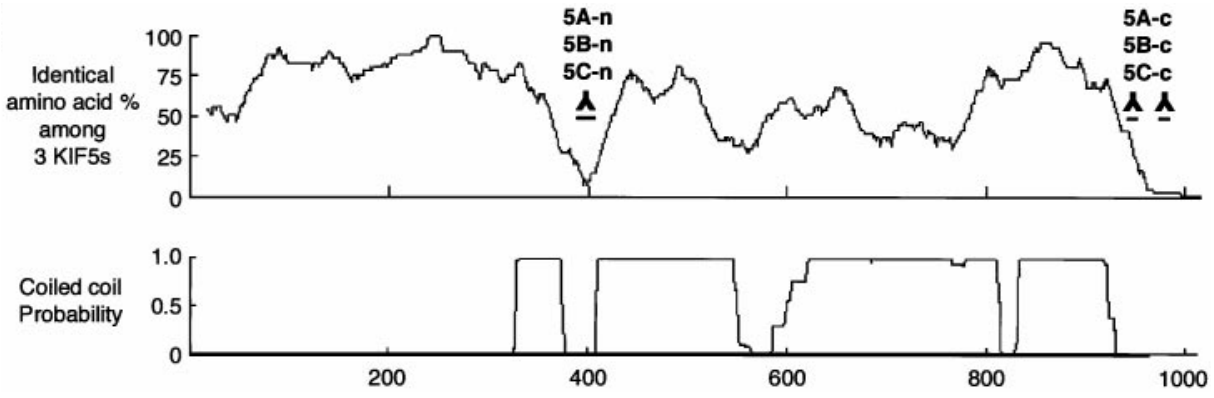

Figure 4.1. Homology among the three KIF5s and coiled-coil probability of KIF5C
(Modified from (Kanai et al., 2000))

KIF5C consists of 956 amino acids and shows a high degree of similarity to KIF5A or KIF5B (60% identical), especially in its motor domain (KIF5C: 9–321, 80%) and in the C-terminal coiled coil region (KIF5C: 829–908, 90%). There are also two short regions with very few

similarities and low coiled-coil probabilities (see Fig. 4.1). These regions were used for generation of KHC isoforms-specific antibodies (Kanai et al., 2000). Nevertheless, the specificity of each antibody used in the current study has been checked additionally for verification (see Table 2.3).

4.1.3. KIF5C transports both raft-associated and non-raft-associated vesicles.

The presence of KIF5C on *post*-TGN p75-carrying vesicles was proved also by immunoblotting of p75-GFP carrying vesicles with specific anti-KIF5C antibody (Fig. 3.3A). The maximum of KIF5C association with *post*-TGN p75-carrying vesicles was observed at 5 – 10 minutes after TGN exit. According to previous studies, this point of time corresponds to the moment when both pathways (raft-associated and non-raft-associated) are transported in common vesicles from TGN. It was shown, that distinct endosomal compartments, positive for Rab4, Rab8 and Rab11, are traversed en route to the apical plasma membrane (Cramm-Behrens et al., 2008). In fact, analysis of raft-associated SI-carrying *post*-TGN vesicles revealed that KIF5C is a motor protein also for this pathway. The highest association of KIF5C with SI carrying vesicles was observed 5 minutes after TGN exit (Fig. 3.3B). Remarkably, the amount of KIF5C on SI vesicles decreased dramatically after 5 minutes TGN release, whereas for p75 vesicles this parameter declined moderately until 20 minutes.
Similar kinetics of KIF5C association with apical cargo was observed by immunostaining of endogenous KIF5C in polarized MDCK cells (Fig. 3.7). Though, here already at 0 minutes after TGN exit quite high overlap coefficient was reached. Possibly, it is partly due to the condensed residence of apical proteins in the perinuclear area directly after TGN block. Immunofluorescence studies of the intracellular distribution of KIF5C in polarized MDCK cells revealed also that this motor protein colocalizes with TGN, Rab4- and Rab8-positive endosomes, but not with the Golgi (Fig. 3.10). Moderate levels of colocalization with TGN, Rab4 or Rab8 suggest that KIF5C is not strictly associated with certain membrane compartments, but is rather shuttling between them, providing apical protein trafficking to its final destination.
Thus, according to biochemical and immunofluorescence studies, KIF5C transports apical proteins of both pathways (raft-associated and non-raft-associated), possibly in the same vesicular carriers, from TGN to some endosomal compartments (Jacob and Naim, 2001; Cramm-Behrens et al., 2008). At this point of time the apical cargo is finally sorted, the two pathways are divided and transported thereafter separately. Presumably, KIF5C stays then longer associated with raft-independent vesicles (maybe even until the cargo reaches plasma membrane), whereas its role for raft-dependent trafficking finishes at 10 minutes after TGN exit. This hypothesis corroborates with previous studies, which showed that at the cell periphery raft-associated vesicles are transported by myosin I along actin filaments (Jacob et

al., 2003; Heine et al., 2005). Additionally; to prove the general role of KIF5C in *post*-Golgi apical trafficking, another model protein – LPH – has been studied. As shown in Fig. 3.9, non-raft-associated LPH colocalizes with KIF5C, as well as another model protein of this pathway – p75 (Fig. 3.7).

4.1.4. KIF5C interaction with *post*-TGN vesicles and possible regulation mechanisms.

To understand the mechanism of KIF5C interaction with vesicles, co-immunoprecipitation analysis was performed (Fig. 3.3D). As expected, no direct interaction of kinesin with either SI or p75 was detected. Both apical markers are heterologously expressed in MDCK cells, therefore it was unlikely that a general motor for both pathways will bind directly to the transported proteins. Probably, this interaction occurs either through some adaptor proteins or there are other interaction partners that direct cargo molecules into a vesicle and also recruit specific motor proteins to this vesicle.

Several adaptor proteins have been reported to interact with KIF5C. Thus, it binds to Ran-binding protein 2 (RanBP2) during mitochondria transport (Cho et al., 2007). In neurons, KIF5C, as well as KIF5A and KIF5B, are steered to dendrites via their association with alpha-amino-3-hydroxy-5-methyl-4-isoxazolepropionate (AMPA) receptor subunit-GluR2-interacting protein (GRIP1) (Setou et al., 2002). Another possibility of cargo binding is the interaction through kinesin light chains, as shown for amyloid precursor protein transport (Kamal et al., 2000). Interestingly, link proteins between kinesin and cargo provide not only binding itself, but also a hot point for regulatory mechanisms. Thus, for example, mitochondrial movement is regulated by local Ca^{2+} concentration through conformational changes in kinesin-1 adaptor proteins: Milton-Miro complex (Wang and Schwarz, 2009). Here, Ca^{2+} binding to the Rho-like GTPase Miro permits its interaction directly with the motor domain of kinesin-1, preventing motor-microtubule interaction and, hence, mitochondrial transport.

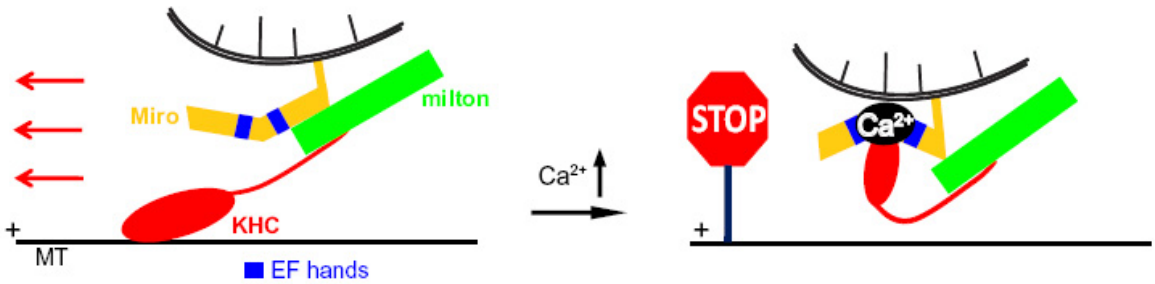

Figure 4.2. Schematic model of the means by which Ca^{2+} interacts with Miro to regulate the anterograde motility of mitochondria

(Modified from (Wang and Schwarz, 2009))

Another way of regulation of kinesin-cargo interaction is phosphorylation. Thus, it was shown that kinesin-1 is a phosphoprotein and that phosphorylation can modulate intracellular transport (Stagi et al., 2006). It has also been demonstrated that KIF5C is a binding partner of protein kinase CK2, although the physiological role of this interaction is still unclear (Schäfer et al., 2009). Many motor protein complexes include also compartment-specific Rab GTPases, which frequently associate with the motor protein through a specialized adaptor protein (Akhmanova and Hammer III, 2010). Recently it has been shown that Rab3A is an essential protein component of amyloid precursor protein vesicles for their interaction and trafficking by KIF5C (Szodorai et al., 2009).

Recently it has been demonstrated that also kinesin light chains (KLC) can regulate the activity of KHC (Wong and Rice, 2010). Here, the authors presented that the kinesin light chains reduce head-tail interaction of the heavy chain, preventing its self-inactivation. Moreover, the light chains inh ibit tainl-microtubule binding as well. Thus, it is proposed that KLCs promote recruitment of kinesin-1 complex to a cargo by simultaneously suppressing tail-head and tail-microtubule interactions (Fig. 4.3).

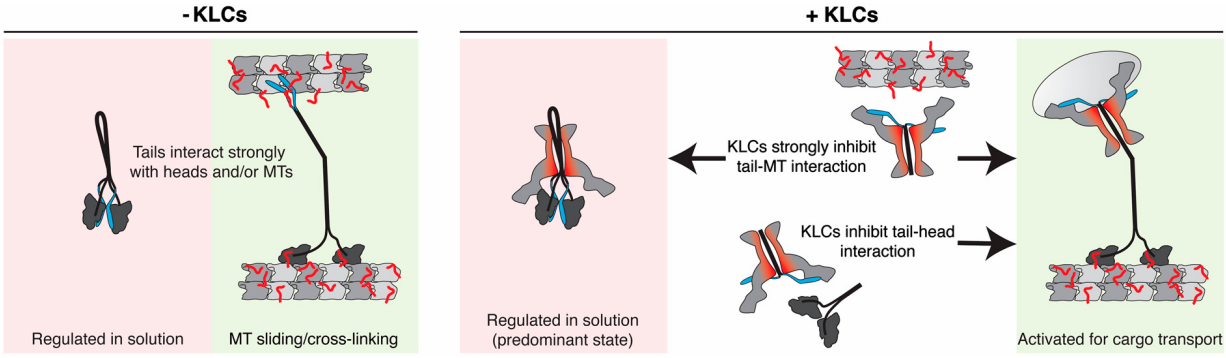

Figure 4.3. A model for KLC-mediated regulation of the kinesin-1 tail.

Without KLCs (Left), kinesin-1 would be either regulated in solution or bound to MTs with the tail tethered. Due to the high affinity of tails for heads/MTs, the motor cannot access its cargo transport-competent state. In the presence of KLCs (Right), tail-head and tail-MT interactions are inhibited. Strong inhibition of tail-MT binding means that the regulated conformation of kinesin-1 becomes the predominant form, but tail-head affinity is also reduced such that the motor is in a poised state that can be easily activated for cargo transport. The identification of adaptor proteins for KIF5C and the regulation mechanisms in apical trafficking in polarized epithelium are a subject of future studies.
(Modified from (Wong and Rice, 2010))

The identification of adaptor proteins for KIF5C and the regulation mechanisms in apical trafficking in polarized epithelia are a subject of future studies.

4.1.5. KIF5C is a motor protein only for apical and not for basolateral cargo.

To prove that KIF5C is specific for apical protein transport and not a general motor protein for *post*-Golgi trafficking, the interaction of KIF5C with basolateral E-cadherin has been checked (Fig. 3.8). Although most of E-cadherin was located to the basolateral membrane, after accumulation of newly synthesized proteins in the TGN, E-cadherin-positive vesicles were observed in the cytoplasm. Nevertheless, no colocalization was seen between basolateral transport vesicles and KIF5C. Also the overlap coefficient was quite low at all time points. Although 0 minutes after TGN exit a small increase in the overlap coefficient value, which can be explained by the high accumulation of both proteins in the perinuclear area at this point of time. Remarkably, 20 minutes after TGN exit a certain amount of KIF5C localizes to the basolateral membrane. Previously, it has been shown that kinesin-1 is enriched in apical junctional complexes of polarized epithelial cells (Ivanov et al., 2006). Probably, kinesin-1 takes a part in cytoskeletal reorganization and trafficking of apical junctional complexes proteins. Although which isoforms of kinesin-1 play a role in junctional complexes formations, have not been identified.

Nevertheless, form the data presented in the current study, it can be concluded that the role of KIF5C in *post*-TGN trafficking is restricted to apical, and not basolateral cargo. Similar result has been reported for KIF5B inhibition, which did not affected *post*-Golgi transport of E-cadherin in polarized MDCK cells (Jaulin et al., 2007).

4.1.6. KIF5C knockdown decreases the efficiency of apical protein surface delivery.

The presence of KIF5C on purified *post*-Golgi vesicles, as well as colocalization of KIF5C with apical proteins in immunofluorescence studies does not prove the physiological role of this kinesin in apical trafficking. It is known that some motor proteins can be recruited to the organelle even if they are not functional at this moment. Thus, dynein is always present on mitochondria, also when it is moved by kinesin in the plus end direction of microtubules or when the microtubule is inmotile (Wang and Schwarz, 2009). To study the physiological importance of KIF5C in *post*-TGN trafficking, siRNA-mediated knockdown experiments were performed. Although siRNA duplexes were designed against regions of KIF5C with low similarity to KIF5B, the homology between the two proteins is quite high (Fig. 4.1). Moreover, KIF5B has been demonstrated to transport p75 in polarized MDCK cells (Jaulin et al., 2007). KIF5 antibodies have been shown to block the apical transport of HA (Lafont et al., 1994). To avoid non-specific side effects in the current study KIF5B knockdown experiments were performed for comparison.

KIF5C depletion in MDCK cells resulted in a significant decrease of the delivery to the apical membrane of both marker proteins: raft-associated SI and non-raft-associated p75 (Fig. 3.5).

This effect can be enhanced by double knockdown of both kinesins, KIF5B and KIF5C. It is possible that KIF5B and KIF5C act in concert and have equivalent functions in apical trafficking. This kind of redundant kinesin association with cargo has ben demonatrated for mitochondrial transport (Cho et al., 2007). Thus, although the presence of KIF5A on *post*-TGN vesicles could be excluded (Fig. 3.3), KIF5C is not the only KIF5-isotype involved in apical trafficking. Also knockdown experiments in MDCK cells never resulted in a total block of apical transport (Fig. 3.3). This view is supported by the description of relatively mild phenotypes in KIF5C-knockout mice (Kanai et al., 2000). Perhaps, a lack of KIF5C in intracellular trafficking could be compensated by some other alternative motor proteins. In fact, a lot of organelles such as mitochondria, synaptic and exocytic vesicles are probably transported by several redundant kinesins whose cooperation makes trafficking more robust (Akhmanova and Hammer III, 2010).

Remarkably, the amount of apical proteins in the basolateral membrane has not increased, thus, KIF5 depletion influences only transport, but not the sorting process. As the role of kinesin-1 in in ER-to-Golgi transport was known before (Gupta et al., 2008), it was additionally shown that a trafficking delay after KIF5C depletion is related to events following TGN exit (Fig. 3.6A). For both proteins, raft-associated SI and non-raft-associated p75, a deceleration of the rate of their delivery to the apical membrane was demonstrated. Remarkably, KIF5C knockdown had no influence on the p75 and SI processing from high-mannose to complex glycosylated forms (Fig. 3.6B). It proves that the effect of KIF5C depletion on apical surface delivery is based on a delay after TGN exit and not on a decelerated passage from ER to Golgi.

Additionally, the physiological role of KIF5C in apical transport has been studied *in vivo* in MDCK cells. Here, depletion of KIF5C resulted in a strong intracellular accumulation of the apical markers SI and p75 (Fig. 3.7C). These data prove that KIF5C knockdown blocks specifically the apical protein trafficking in polarized epithelial cells. Most likely, this accumulation occurs in some endosomal compartments that are traversed on the way to the apical membrane. Whether the transport of apical cargo is blocked in TGN already, or late, for example, in Rab8-positive endosomal compartments, still has to be clarified.

4.1.7. KIF5C binds to tyrosinated microtubules.

It is known that motor proteins can bind preferentially to some types of *post*-translationally modified microtubules (Fukushima et al., 2009). Moreover, tubulin modifications are essential for normal tissue development and organization of polarized trafficking in neurons. It is suggested that *post*-translational modifications of tubulin are important in directing trafficking to specific regions of the cell and in regulating efficiency of this transport (Lakämper and Meyhöfer, 2006). Thus, for example, tubulin tyrosination navigates the kinesin-1 motor domain to axons (Konishi and Setou, 2009). The pattern of *post*-translational modifications of

microtubules in polarized epithelia and its possible role in polarization and intracellular trafficking remains unknown.

Immunofluorescence study of tyrosinated tubulin in MDCK cells revealed that apical marker protein p75 tends to localize to tyrosinated microtubules (Fig. 3.11). Tyrosinated tubulin usually forms dynamic microtubules, in contrast to stable detyrosinated microtubules (Fukushima et al., 2009). Remarkably, the role of dynamic microtubules in polarized apical trafficking has been already reported (Jaulin et al., 2007). Thus, probably this type of microtubules forms the tracks for apical surface cargo delivery by KIF5C. Nevertheless, to prove KIF5C preference to tyrosinated microtubules in MDCK cells and to clarify the possible role of other *post*-translational tubulin modifications in apical trafficking, further studies have to be done.

On the other hand, it was demonstrated that KIF5C-GFP preferentially moves along detyrosinated microtubules in COS cells (Dunn et al., 2008). This opposite result could be caused by side effects of overexpression of tagged KIF5C or by difference in motor-microtubule interaction in polarized and non-polarized cells.

4.1.8. Intracellular localization of KIF5C-GFP in non-polarized cells.

Cell polarization influences not only the plasma membrane organization, but also the intracellular trafficking machinery. Thus, it has been demonstrated that apical protein p75 is transported by KIF5B, but only in fully polarized cells (Jaulin et al., 2007). Before, when the cells are non-polarized, the same protein is transported by KIF1 family (Xue et al., 2010). To examine whether KIF5C plays the same role in protein trafficking in non-polarized COS cells as in polarized MDCK cells, the tagged version of KIF5C, KIF5C-GFP has been used. This construct has been already characterized in COS cells (Dunn et al., 2008).

First of all, the intracellular localization of overexpressed KIF5C in COS cells has been studied (Fig. 3.12). Thus, KIF5C-GFP localizes not only to vesicles, but also to filamentous structures, presumably, microtubules, and forms peripheral accumulations. Several different phenotypes can be caused by the side effects of the overexpression and made further analysis more complicated. Although, these phenotypes are in agreement with previously published data (Dunn et al., 2008).

Nevertheless, KIF5C-GFP demonstrated normal function in COS cells, while almost all KIF5C-GFP was colocalized with mitochondrial marker (Fig. 3.13), as expected from the reported role of KIF5C in mitochondria transport (Cho et al., 2007). Though, if the majority of KIF5C-GFP is present on mitochondria, the question rises, whether other functions of KIF5C in the cell are feasible. It is possible that overexpression of mitochondrial marker itself recruits KIF5C to the higher range that in normal, non-transfected cells, where KIF5C transports not only mitochondria, but other cargo as well.

The difference of the KIF5C role in intracellular transport between polarized and non-polarized cells came also from colocalization analysis of KIF5C-GFP and Golgi marker GT (Fig. 3.13). As described before, KIF5C showed no co-staining with Golgi in polarized MDCK cells (Fig. 3.10). At the same time, in COS cells KIF5C colocalizes with Golgi. This data suggest that in non-polarized cells KIF5C plays a role in Golgi membrane dynamics, whereas in polarized cells its role was restricted to *post*-Golgi trafficking (Fig. 3.10, 3.6).
Furthermore, colocalization analysis of KIF5C-GFP with apical marker proteins revealed no association with either raft-dependent SI or raft-independent LPH (Fig. 3.14) in COS cells. Only a few LPH-carrying vesicles were located at KIF5C-GFP-decorated microtubule. Thus, KIF5C-GFP showed different intracellular localization in non-polarized COS cells in comparison to endogenous KIF5C in polarized MDCK cells. Moreover, no colocalization with apical marker proteins in COS cells could be observed. Probably, previously described role of KIF5C in *post*-TGN trafficking is either restricted to polarized cells, or to endogenous kinesin. The study of the role of endogenous KIF5C in non-polarized COS cells could not be performed, because no KIF5C antibody detected any protein in COS cells. KIF5C function in non-polarized MDCK cells is a subject of future studies.

4.1.9. Dynein plays a role in *post*-Golgi apical protein trafficking.

As described before, dynein was not present on raft-independent p75-carrying *post*-Golgi vesicles (Fig. 3.2). Nevertheless, it has been demonstrated that dynein plays an essential role in apical delivery of raft-associated hemagglutinin (Lafont et al., 1994). To examine, whether this motor protein is also involved in *post*-Golgi trafficking of SI, the biochemical analysis of raft-associated vesicles was performed (Fig. 3.15A). In fact, dynein was present on purified SI-carrying vesicles at all point of times after TGN exit, with maximum intensity at 0 and 5 minutes. These data do not corroborate with the hypothesis that both vesicle populations – raft-associated and non-raft-associated are transported in the same vesicular carriers the first 10 minutes after TGN exit (Jacob and Naim, 2001). One possible explanation can be that dynein interacts directly with SI, thus, $MDCK_{p75}$ cells, which do not express SI, do not carry dynein on *post*-TGN vesicles. To prove this hypothesis, co-immunoprecipitation of SI with dynein should be performed. On the other hand, targeting of motors to membranes often depends on the formation of large multiprotein assemblies and can be influenced by membrane lipid composition. Thus, for example, in late endosomes cholesterol can regulate the architecture of the dynein-dynactin binding complex through the cholesterol sensor ORP1L (Rocha et al., 2009). Probably, dynein interacts through large protein complexes specifically with lipid rafts. By overexpression of raft-associated SI, the amount of typical raft lipids in transport vesicles increases, thus, resulting in higher rates of

dynein recruitment. In contrast, in p75-expressing cells the initial amount of vesicle-bound dynein is less and it is lost from the vesicles during purification procedures.

To study the physiological role of dynein in apical protein trafficking in polarized epithelial cells, the overexpression of p50-dynamitin has been used. It was published before, that overexpression in mammalian cells of one dynactin subunit, dynamitin, results in dissociation of cytoplasmic dynein from prometaphase kinetochores and dynein-dependent maintenance of membrane organelle organization (Burkhardt et al., 1997). After transfection of p50-dynamitin-GFP in MDCK cells, a moderate decrease in apical surface delivery of both p75 and SI was observed (Fig. 3.15C). Surprisingly, the effect on p75 trafficking was even stronger, than on SI. Although dynein was found only on SI-carrying vesicles, as discussed before, it is possible that it plays a role in the trafficking of both *post*-TGN pathways. Moreover, it has been demonstrated, that dynamitin-overexpressing cells, early endosomes, as well as late endosomes and lysosomes, were redistributed to the cell periphery. Also the Golgi stack, was dramatically disrupted into scattered structures, although Golgi-to-ER traffic was not inhibited (Burkhardt et al., 1997). Thus, the p50-dynamitin overexpression effect on the apical protein surface delivery is due to the side effects of interference of dynein functions in the cells, for example, on the level of ER-to-Golgi trafficking.

Nevertheless, it is quite possible that some additional minus end-directed motor proteins will be found on *post*-Golgi apical vesicles. It was shown that opposite polarity motors might help each other to avoid roadblocks or activate each other through the generation of mechanical strain (Ally et al., 2009). Additionally, minus end-directed motor proteins (dynein, for example) could provide the retrograde transport of some essential components of the trafficking machinery from the apical membrane back to the TGN. Moreover, by linking to apical *post*-TGN vesicles, dynein might be able to be transported to distal cell areas where it cannot be synthesized but need to function (for example, the tip of the cilium).

Thus, in the current study KIF5C has been identified as a novel kinesin motor involved in the apical trafficking of polarized MDCK cells. This motor protein is required for raft-associated, as well as for non-raft-associated pathways. Most likely, KIF5C transports *post*-Golgi cargo directly after TGN exit through Rab4- and Rab8-positive compartments. KIF5C acts together with another kinesin-1 group member, KIF5B, and, probably, with some other, still non-identified motors.

4.2. The role of annexin XIIIb in apical protein transport

Annexin XIIIb has been reported to play a role in apical trafficking of the raft-associated hemagglutinin glycoprotein (Lafont et al., 1998). In the present study it was demonstrated that annexin XIIIb is essential not only for raft-dependent, but also for raft-independent trafficking. Additionally, it was shown that in polarized MDCK cells annexin XIIIb localizes preferentially to the Rab8-positive endosomal compartment.

4.2.1. Annexin XIIIb associates with *post*-Golgi vesicles.

The first evidence of the possible role of annexin XIIIb in raft-independent apical trafficking came from proteomic analysis of *post*-Golgi LPH-carrying vesicles (D. Delacour, Astanina et al., submitted). Thereafter, the studies of overexpressed annexin XIIIb in non-polarized COS cells revealed that it colocalizes with apical markers of both raft-associated (SI), as well as non-raft-associated (p75 and LPH) pathways (Fig. 3.16). Moreover, these marker proteins (of both pathways) were localized together to the annexin XIIIb-positive vesicles 10 minutes after TGN exit. Although COS cells allow detailed microscopic analysis of intracellular localization of protein of interest, they do not possess polarized organization of membrane compartments and protein trafficking machinery. And it is known, that the transport mechanisms in polarized and non-polarized cells can differ significantly (Jaulin et al., 2007;Xue et al., 2010). Therefore, the colocalization of annexin XIIIb-DsRed with apical markers was examined in polarized MDCK cells. In fact, both p75 and SI showed a relatively high Pearson's correlation value with annexin XIIIb (Fig. 3.17A). The same result was observed also for endogenous proteins of both *post*-TGN trafficking pathways: gp135 as raft-associated and gp114 as non-raft-associated markers (Fig. 3.17B). Thus, overexpressed annexin XIIIb localizes to apical *post*-TGN vesicles in polarized MDCK cells. The co-staining could not be a side effect of annexin overexpression, because endogenous protein showed colocalization with apical markers as well (Fig. 3.19A). Moreover, the presence of annexin XIIIb on purified *post*-Golgi carriers of both pathways was proved by vesicle immunoprecipitation (Fig. 3.20). Here, the maximum intensity of annexin XIIIb-apical cargo association was observed at 10 minutes after TGN exit. This result corroborates with the observation for COS cells (Fig. 3.16). Moreover, it has been demonstrated before, that apical cargo of both pathways is transported in the same vesicular compartments after TGN exit. Thereafter, the cargo is sorted into two distinct vesicular populations (Jacob and Naim, 2001).

4.2.2. Annexin XIIIb accumulates in Rab8- and Rab10-positive endosomal compartments.

To understand, which intracellular membrane compartment is enriched in annexin XIIIb and where the colocalization of annexin XIIIb with SI and LPH takes place, colocalization studies with various markers has been performed (Fig. 3.18). First of all, no co-staining was seen with either early endosomes, late endosomes, TGN or Golgi. In contrast, annexin XIIIb accumulated in Rab8- and Rab10-positive compartments. The same result showed colocalization studies with endogenous annexin XIIIb (Fig. 3.19B). Association of annexin XIIIb with apical cargo in Rab8-positive endosomal compartments was confirmed additionally by vesicle isolation and immunoblotting (Fig. 3.20).

Rab8, Rab10 and also Rab13 belong to a subfamily of Rab proteins that represents the closest mammalian relatives of yeast Sec4p (Chen et al., 1993; Pereira-Leal and Seabra, 2001). In yeast, Sec4p mediates polarized transport from the TGN to the site of bud formation (Salminen and Novick, 1987; Walworth et al., 1989). In MDCK cells, Rab8 as well as Rab10 are concentrated in common endosomes that mediate polarized trafficking to the basolateral cell surface (Babbey et al., 2006; Schuck et al., 2007). However, based on recent data, Rab8 is also required for apical protein trafficking and accumulates in compartments that are traversed in biosynthetic apical trafficking pathways (Cramm-Behrens et al., 2008; Sato et al., 2007).

Nevertheless, the exact role of annexin XIIIb in these endosomal compartments remains unclear. For other annexins, various functions in membrane reorganizations have been demonstrated. Thus, for example, annexin 6 plays a role in clathrin-coated vesicle formation, whereas annexin A2 has been implicated in internal vesicle formation within multi-vesicular bodies (Turpin et al., 1998; Mayran et al., 2003). Another interesting mechanism of annexin function is raft clustering. This was shown for annexin A2, which is first targeted to the membranes by a binding to phospholipids and then is recruited to rafts by the specific interaction with PtdIns(4,5)P_2 (Hayes et al., 2004; Rescher et al., 2004). Most likely, by engaging in homophilic lateral interactions, annexin A2 could induce and/or stabilize raft clustering (Rescher and Gerke, 2004). Thus, it can be speculated, that the annexin XIIIb acts in a similar way. Moreover, it was shown that annexin XIIIb accumulates in raft clusters of the membrane (Lafont et al., 1998). Probably, annexin XIIIb provides the primary segregation of raft-associated and non-raft-associated cargoes within the endosomal compartments.

4.2.3. Depletion of annexin XIIIb decreases protein delivery to the apical membrane.

The physiological role of annexin XIIIb in polarized MDCK cells was studied by siRNA-mediated knockdown and surface protein immunoprecipitation. Depletions itself had no influence on polarized organization of membrane compartments in MDCK cells (Fig. 3.21B). Nevertheless, surface immunoprecipitation revealed a significant reduction in apical delivery of all three marker proteins (Fig. 3.21C). Importantly, no shift towards the basolateral membrane was observed for any of our model proteins. This data suggests that the loss of annexin XIIIb affected their intracellular transport rather than their sorting to the apical plasma membrane. Remarkably, an influence on apical trafficking was not only demonstrated for the raft-associated marker protein SI, which is congruent with previously published data (Fiedler et al., 1995), but also for the two raft-independent proteins, p75 and LPH. Kinetic studies have proven that the trafficking delay occurs after TGN exit and not at the ER-to-Golgi transport step (Fig. 3.22).

In conclusion, the above discussed results suggest, first, that annexin XIIIb is involved in apical transport of epithelial cells in general, independent of the sorting platform, and, second, that the role of this annexin in trafficking is dedicated to a compartment that is traversed before segregation into lipid-raft dependent and independent apical carriers occurs. Whether annexin XIIIb interacts directly with one of the marker proteins is still unclear and remains to be elucidated.

4.3. Conclusion

Addressing the roles of KIF5C and annexin XIIIb in *post*-Golgi transport, this work shed a new light on the model of apical protein trafficking (Fig. 4.4). Thus, according to the results, apical cargo like SI or p75 exits the TGN and gets associated with KIF5C. It was demonstrated that directly after TGN exit KI5C is associated with the model proteins of both trafficking routes – raft-dependent and raft-independent. As it has been shown already, the proteins of the two different pathways leave the TGN in the same vesicular carriers (Jacob and Naim, 2001).Therefore, it is likely, that KIF5C transports these vesicles, carrying both raft-associated, as well as non-raft-associated cargo. At this point of time KIF5C is not the only motor protein, which is associated with the vesicles, as KIF5C depletion does not result in a complete block of apical transport. KIF5B, another member of kinesin-1 family, was also shown to play a role in *post*-Golgi trafficking of the raft-independent pathway (Jaulin et al., 2007) and additionally KIF5B depletion resulted in a decreased apical surface delivery of both p75 and SI. Nevertheless, the exact step of trafficking where KIF5B functions is still unclear. Possibly, it forms heterodimers with KIF5C (Kanai et al., 2000; Cai et al., 2001) or it acts independently.

After TGN exit apical vesicular carriers traverse several endosomal compartments. The first one is a Rab4-positive endosome, then the cargo is transported to a Rab8-, thereafter – to a Rab11-containing compartments (Cramm-Behrens et al., 2008). According to the biochemical and microscopical studies, KIF5C transports apical proteins througha Rab4- to a Rab8-positive endosomal compartment, which is reached approximately 10 minutes after TGN exit. At this time point of time the final sorting of apical cargo into two distinct vesicle population occurs (Jacob and Naim, 2001). At the same time, the Rab8-positive compartment is enriched in annexin XIIIb, which also plays a role in the trafficking of apical proteins of both routes. It is known, that annexin XIIIb interacts with lipid rafts. Moreover, it can oligomerize, forming di-, tri- and hexamers (Lafont et al., 1998). Thus, knowing that membrane dynamics and organization is one of the main functions of the annexin protein family, it is likely that annexin XIIIb acts as an organizer of the Rab8-positive compartment. Moreover, it can be speculated that this last sorting step, when the two vesicle population are formed, takes place exactly in the Rab8-positive compartment and requires annexin XIIIb. The possible role of protein clustering in apical sorting has been proposed already for galectins (Delacour et al., 2009). Similarly, annexin XIIIb can provide lipid raft domain segregation in a distinct part of the Rab8-compartment. At the same time, it looks like this hypothetic step is crucial for both apical trafficking pathways. Thus, probably, the role of annexin XIIIb is rather in maintaining the membrane organization of a functional Rab8-compartment, than in sorting of apical cargo.

Thereafter, when these two distinct vesicle populations – raft-dependent and raft-independent – are formed, KIF5C (probably, together with KIF5B) transports only non-raft-associated cargo, whereas raft-associated vesicles are moved, presumably, by KIFC3 and dynein (Lafont et al., 1994; Noda et al., 2001). Remarkably, KIF5 is a plus end-directed motor, whereas KIFC3 and dynein possess minus end-directed activity. It can, allow fission of vesicular carriers from a common endosomal compartment (Nath et al., 2007). Additionally, opposite polarity of motor proteins of two distinct vesicle populations may result in distinct cytoskeleton tracks used by these pathways. It was demonstrated, that polarized MDCK cells have two types of microtubules in the apical region: stable ones, with their minus ends facing apical membrane, and dynamic ones, growing from the centrosome toward the apical membrane (Musch, 2004; Jaulin et al., 2007). Thus, it can be speculated, that after a final sorting step raft-associaed vesicles are transported by KIFC3 and dynein along stable microtubules, to their minus ends, whereas KIF5C/KIF5B move non-raft-associated vesicle populations along dynamic microtubules, to their plus ends. Therefore, both studied proteins – KIF5C and annexin XIIIb – play a role in the organization of raft-dependent and raft-independent apical trafficking pathways.

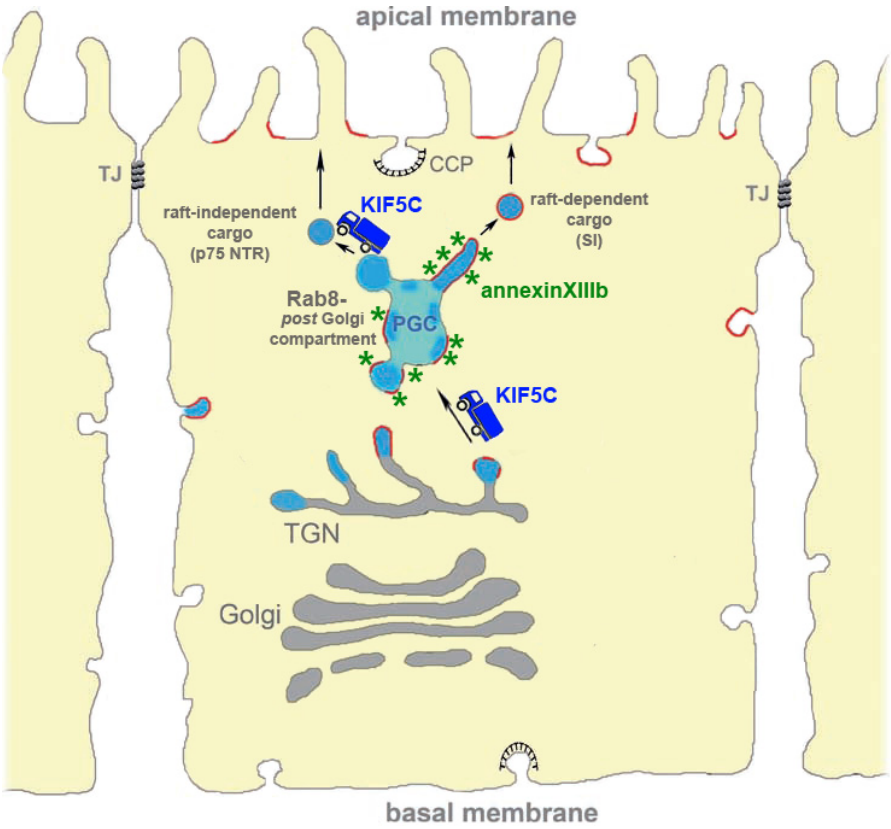

Figure 4.4. Model of the possible role of KIF5C and annexin XIIIb in *post*-TGN apical transport

KIF5C transports raft-dependent and raft-independent cargo from TGN to the Rab8-positive endosomal compartment. Annexin XIIIb accumulates in this compartment and plays a role in membrane reorganization of this organelle. After final sorting of apical cargo two distinct vesicle populations are formed. KIF5C transports raft-independent proteins further to the apical membrane. (Modified from (Delacour and Jacob, 2006))

5. Summary

Epithelial cells are characterized by a polarized organization of their plasma membrane which is divided into apical and basolateral domains. This architecture is maintained by highly specific cargo sorting machinery that efficiently delivers newly synthesized polypeptides to their correct target membrane. After TGN exit apical cargo is segregated by at least two distinct sorting mechanisms into lipid-raft-dependent or lipid-raft-independent apical pathways in MDCK cells. The aim of this study was the identification of proteins which are essential for the transport of apically sorted proteins.

In the first part of the current study, a member of kinesin-1 group, KIF5C, was identified as a kinesin motor for apical trafficking of sucrase-isomaltase, the marker for the raft-associated pathway, and of non-raft-associated p75. KIF5C was found by mass spectrometry in vesicle enriched fractions and on immunoisolated *post*-Golgi vesicles carrying apical cargo. KIF5C associates with vesicles of both raft-dependent and raft-independent pathways directly after TGN exit. The specific knockdown of KIF5C interfered the apical trafficking of both raft-associated and non-raft associated marker proteins significantly (Astanina and Jacob, 2010).

In the second part, annexin XIIIb was identified in raft-independent apical trafficking by mass spectrometry, immunoblotting and confocal microscopy. Annexin XIIIb accumulated in endosomal compartments that are traversed by raft-dependent and raft-independent apical cargo after TGN release. Finally, a specific reduction of annexin XIIIb expression by RNA interference resulted in a significant decrease in the apical delivery of the raft- as well as non-raft apical markers (Astanina et al., 2010).

Taken together, both proteins – KIF5C and annexin XIIIb – act as endosomal organizers of apical protein trafficking in polarized epithelial cells. Based on the confocal microscopy studies and TGN release experiments we came to the conclusion that both proteins function on the first transport steps after TGN exit and accomplish trafficking of raft-associated, as well as non-raft-associated apical cargo.

6. Zusammenfassung

Epithelzellen charakterisieren sich durch die polare Organisation ihrer Zellmembran, welche sich in eine apikale und basolaterale Domäne aufteilt. Diese Struktur wird durch einen hoch spezialisierten Transport- und Sortiermechanismus aufrecht erhalten, welcher neu synthetisierte Plasmamembranproteine effizient zu ihrer korrekten Zielmembran befördert.

In MDCK Zellen erfolgt der apikale Proteintransport nach Verlassen des TGN *Exits* über mindestens zwei verschiedene Sortiermechanismen, zum einen über einen *lipid raft*-abhängigen und zum anderen über einem *lipid raft*-unabhängigen Transportweg. Gegenstand dieser Arbeit war die Identifizierung von Proteinen, welche für den Transport apikaler Proteine essentiell sind.

Im ersten Teil der vorliegenden Arbeit konnte ein Mitglied der Kinesin-1 Gruppe/Familie, KIF5C, als Kinesin Motor für den apikalen Transport der raft-assoziierten Saccharase-Isomaltase, als auch der nicht-*raft*-assoziierten p75 identifiziert werden. KIF5C konnte mit Hilfe von Massenspektrometrie in immunisolierten *post*-Golgi Vesikeln, welche spezifisch apikale Proteine transportieren, nachgewiesen werden. Hierbei wurde es sowohl im *raft*-abhängigen Vesikeln von SI als auch im *raft*-unabhängigen Vesikeln von p75 und LPH direkt nach Verlassen des TGN-*Exits* identifiziert. Die spezifische Unterdrückung der KIF5C-Expression zeigte, dass der apikale Transport von sowohl *raft*-assoziierten als auch nicht-*raft*-assoziierten Markerproteinen signifikant reduziert wurde (Astanina and Jacob, 2010).

Im zweiten Teil der Arbeit konnte ein weiteres Protein, Annexin XIIIb, mit Hilfe der Massenspektrometrie, *Western Blot* Analysen und konfokaler Mikroskopie im *raft*-unabhängigen apikalen Transport identifiziert werden. Hier konnte gezeigt werden, dass Annexin XIIIb in endosomalen Kompartimenten lokalisiert ist, welche sowohl von *raft*-unabhängigen als auch *raft*-abhängigen apikalen Proteinen nach Verlassen des TGN durchlaufen werden. Darüber hinaus führte die siRNA-vermittelte Reduktion der Annexin XIIIb-Expression zu einer Reduktion des apikalen Proteinanteils / des apikalen Proteintransportes von sowohl der *raft*-assoziierten SI als auch der nicht.*raft*-assoziierten Markerproteine p75 und LPH (Astanina et al., 2010).

Zusammenfassend zeigt sich, dass beide in dieser Arbeit identifizierten Proteine, KIF5C and Annexin XIIIb, eine Rolle als endosomale Organisatoren beim apikalen Proteintransport in polaren Epithelzellen spielen. Die konfokalmikroskopischen Analysen sowie die TGN-*release* Experimente lassen den Rückschluss zu, dass beide Proteine direkt nach Verlassen des TGN eine Rolle im apikalen Transport *raft* und nicht-*raft*-assoziierte Proteine spielen.

7. References

1. 'Angelo G, Polishchuk E, Tullio GD, Santoro M, Campli AD, Godi A, West G, Bielawski J, Chuang CC, van der Spoel AC, Platt FM, Hannun YA, Polishchuk R, Mattjus P, De Matteis MA (2007) Glycosphingolipid synthesis requires FAPP2 transfer of glucosylceramide. Nature 449: 62-67.

2. Aizawa H, Sekine Y, Takemura R, Zhang Z, Nangaku M, Hirokawa N (1992) Kinesin family in murine central nervous system. J Cell Biol 119: 1287-1296.

3. Akhmanova A, Hammer III JA (2010) Linking molecular motors to membrane cargo. Current Opinion in Cell Biology In Press, Corrected Proof.

4. Alfalah M, Jacob R, Preuss U, Zimmer KP, Naim H, Naim HY (1999) O-linked glycans mediate apical sorting of human intestinal sucrase- isomaltase through association with lipid rafts. Curr Biol 9: 593-596.

5. Ally S, Larson AG, Barlan K, Rice SE, Gelfand VI (2009) Opposite-polarity motors activate one another to trigger cargo transport in live cells. J Cell Biol 187: 1071-1082.

6. Ang AL, Taguchi T, Francis S, Folsch H, Murrells LJ, Pypaert M, Warren G, Mellman I (2004) Recycling endosomes can serve as intermediates during transport from the Golgi to the plasma membrane of MDCK cells. J Cell Biol 167: 531-543.

7. Asbury CL, Fehr AN, Block SM (2003) Kinesin Moves by an Asymmetric Hand-Over-Hand Mechanism. Science 302: 2130-2134.

8. Astanina K, Delebinski CI, Delacour D, Jacob R (2010) Annexin XIIIb guides raft-dependent and -independent apical traffic in MDCK cells. EJCB.

9. Astanina K, Jacob R (2010) KIF5C, a kinesin motor involved in apical trafficking of MDCK cells. Cellular and Molecular Life Sciences 67: 1331-1342.

10. Babiychuk EB, Draeger A (2000) Annexins in Cell Membrane Dynamics. Ca(2+)-regulated association of lipid microdomains. J Cell Biol 2000 Sep 4;150(5):1113-1124 150: 1113-1124.

11. Bacallao R, Antony C, Dotti C, Karsenti E, Stelzer EH, Simons K (1989) The subcellular organization of Madin-Darby canine kidney cells during the formation of a polarized epithelium. J Cell Biol 109: 2817-2832.

12. Baeuerle PA, Huttner WB (1987) Tyrosine sulfation is a trans-Golgi-specific protein modification. J Cell Biol 105: 2655-2664.

13. Bananis E, Murray JW, Stockert RJ, Satir P, Wolkoff AW (2000) Microtubule and Motor-Dependent Endocytic Vesicle Sorting in Vitro. J Cell Biol 151: 179-186.

14. Barondes SH, Cooper DN, Gitt MA, Leffler H (1994) Galectins. Structure and function of a large family of animal lectins. J Biol Chem 269: 20807-20810.

15. Beau I, Groyer-Picard MT, Desroches A, Condamine E, Leprince J, Tome JP, Dessen P, Vaudry H, Misrahi M (2004) The basolateral sorting signals of the thyrotropin and luteinizing hormone receptors: an unusual family of signals sharing an unusual distal intracellular localization, but unrelated in their structures. Mol Endocrinol 18: 733-746.

16. Benting JH, Rietveld AG, Simons K (1999) N-Glycans mediate the apical sorting of a GPI-anchored, raft- associated protein in Madin-Darby canine kidney cells. J Cell Biol 146: 313-320.

17. Bergmann JE, Kupfer A, Singer SJ (1983) Membrane insertion at the leading edge of motile fibroblasts. Proc Natl Acad Sci U S A 80: 1367-1371.

18. Blocker A, Severin FF, Habermann A, Hyman AA, Griffiths G, Burkhardt JK (1996) Microtubule-associated Protein-dependent Binding of Phagosomes to Microtubules. J Biol Chem 271: 3803-3811.

19. Boehm KJ, Stracke R, Baum M, Zieren M, Unger E (2000a) Effect of temperature on kinesin-driven microtubule gliding and kinesin ATPase activity. FEBS Letters 466: 59-62.

20. Boehm KJ, Stracke R, Unger E (2000b) Speeding up kinesin-driven microtubule gliding in vitro by variation of cofactor composition and physicochemical parameters. Cell Biol Int 24: 335-341.

21. Bonifacino JS, Dell'Angelica EC (1999) Molecular bases for the recognition of tyrosine-based sorting signals. J Cell Biol 145: 923-926.

22. Bradke F, Dotti CG (1997) Neuronal Polarity: Vectorial Cytoplasmic Flow Precedes Axon Formation. Neuron 19: 1175-1186.

23. Burkhardt JK, Echeverri CJ, Nilsson T, Vallee RB (1997) Overexpression of the Dynamitin (p50) Subunit of the Dynactin Complex Disrupts Dynein-dependent Maintenance of Membrane Organelle Distribution. J Cell Biol 139: 469-484.

24. Butowt R, von Bartheld CS (2003) Connecting the dots: trafficking of neurotrophins, lectins and diverse pathogens by binding to the neurotrophin receptor p75NTR. Eur J Neurosci 17: 673-680.

25. Byrd DT, Kawasaki M, Walcoff M, Hisamoto N, Matsumoto K, Jin Y (2001) UNC-16, a JNK-Signaling Scaffold Protein, Regulates Vesicle Transport in C. elegans. Neuron 32: 787-800.

26. Cai Q, Gerwin C, Sheng ZH (2005) Syntabulin-mediated anterograde transport of mitochondria along neuronal processes. J Cell Biol 170: 959-969.

27. Cai Y, Singh BB, Aslanukov A, Zhao H, Ferreira PA (2001) The docking of kinesins, KIF5B and KIF5C, to Ran-binding protein 2 (RanBP2) is mediated via a novel RanBP2 domain. J Biol Chem 276: 41594-41602.

28. Caplan MJ (1997) Membrane polarity in epithelial cells: protein sorting and establishment of polarized domains. Am J Physiol 272: F425-9.

29. Chabrillat ML, Wilhelm C, Wasmeier C, Sviderskaya EV, Louvard D, Coudrier E (2005) Rab8 Regulates the Actin-based Movement of Melanosomes. Mol Biol Cell 16: 1640-1650.

30. Chausovsky A, Bershadsky AD, Borisy GG (2000) Cadherin-mediated regulation of microtubule dynamics. Nat Cell Biol 2: 797-804.

31. Cho K, Cai Y, Yi H, Yeh A, Aslanukov A, Ferrero A (2007) Association of the kinesin-binding domain of RanBP2 to KIF5B and KIF5C determines mitochondria localization and function. Traffic 8: 1722-1735.

32. Cho KI, Yi H, Desai R, Hand AR, Haas AL, Ferreira PA (2009) RANBP2 is an allosteric activator of the conventional kinesin-1 motor protein, KIF5B, in a minimal cell-free system. EMBO Rep 10: 480-486.

33. Chuang JZ, Sung CH (1998) The cytoplasmic tail of rhodopsin acts as a novel apical sorting signal in polarized MDCK cells. J Cell Biol 142: 1245-1256.

34. Cohen D, Brennwald PJ, Rodriguez-Boulan E, Musch A (2004) Mammalian PAR-1 determines epithelial lumen polarity by organizing the microtubule cytoskeleton. J Cell Biol 164: 717-727.

35. Coy DL, Wagenbach M, Howard J (1999) Kinesin Takes One 8-nm Step for Each ATP That It Hydrolyzes. J Biol Chem 274: 3667-3671.

36. Cramm-Behrens CI, Dienst M, Jacob R (2008) Apical Cargo Traverses Endosomal Compartments on the Passage to the Cell Surface. Traffic 9: 2206-2220.

37. Creutz CE, Pazoles CJ, Pollard HB (1978) Identification and purification of an adrenal medullary protein (synexin) that causes calcium-dependent aggregation of isolated chromaffin granules. J Biol Chem 253: 2858-2866.

38. Dagenbach EM, Endow SA (2004) A new kinesin tree. J Cell Sci 117: 3-7.

39. Danielsen EM (1995) Involvement of detergent-insoluble complexes in the intracellular transport of intestinal brush border enzymes. Biochemistry 34: 1596-1605.

40. Danielsen EM, Skovbjerg H, Noren O, Sjostrom H (1984) Biosynthesis of intestinal microvillar proteins. Intracellular processing of lactase-phlorizin hydrolase. Biochem Biophys Res Commun 122: 82-90.

41. Danielsen EM, van Deurs B, Hansen GH (2003) "Nonclassical" secretion of annexin A2 to the lumenal side of the enterocyte brush border membrane. Biochemistry 42: 14670-14676.

42. Dathe V, Pröls F, Brand-Saberi B (2004) Expression of kinesin kif5c during chick development. Anat Embryol (Berl) 207: 475-480.

43. Delacour D, Cramm-Behrens CI, Drobecq H, Le Bivic A, Naim HY, Jacob R (2006) Requirement for galectin-3 in apical protein sorting. Curr Biol 16: 408-414.

44. Delacour D, Gouyer V, Zanetta JP, Drobecq H, Leteurtre E, Grard G, Moreau-Hannedouche O, Maes E, Pons A, Andre S, Le Bivic A, Gabius HJ, Manninen A, Simons K, Huet G (2005) Galectin-4 and sulfatides in apical membrane trafficking in enterocyte-like cells. J Cell Biol 169: 491-501.

45. Delacour D, Jacob R (2006) Apical protein transport. Cell Mol Life Sci 63: 2491-2505.

46. Delacour D, Koch A, Jacob R (2009) The Role of Galectins in Protein Trafficking. Traffic 10: 1405-1413.

47. Dictenberg JB, Swanger SA, Antar LN, Singer RH, Bassell GJ (2008) A Direct Role for FMRP in Activity-Dependent Dendritic mRNA Transport Links Filopodial-Spine Morphogenesis to Fragile X Syndrome. Developmental Cell 14: 926-939.

48. Diefenbach RJ, Diefenbach E, Douglas MW, Cunningham BA (2002) The heavy chain of conventional kinesin interacts with the SNARE proteins SNAP25 and SNAP23. Biochemistry 41: 14906-14915.

49. Diefenbach RJ, Mackay JP, Armati PJ, Cunningham AL (1998) The C-Terminal Region of the Stalk Domain of Ubiquitous Human Kinesin Heavy Chain Contains the Binding Site for Kinesin Light ChainΓÇá. Biochemistry 37: 16663-16670.

50. Dotti CG, Simons K (1990) Polarized sorting of viral glycoproteins to the axon and dendrites of hippocampal neurons in culture. Cell 62: 63-72.

51. Drubin DG (1991) Development of cell polarity in budding yeast. Cell 65: 1093-1096.

52. Dunn S, Morrison EE, Liverpool TB, Molina-París C, Cross RA, Alonso MC, Peckham M (2008) Differential trafficking of Kif5c on tyrosinated and detyrosinated microtubules in live cells. J Cell Sci 121: 1085-1095.

53. Dunphy WG, Rothman JE (1985) Compartmental organization of the golgi stack. Cell 42: 13-21.

54. Emans N, Gorvel JP, Walter C, Gerke V, Kellner R, Griffiths G, Gruenberg J (1993) Annexin II is a major component of fusogenic endosomal vesicles. J Cell Biol 120: 1357-1369.

55. Fath KR, Burgess DR (1993) Golgi-derived vesicles from developing epithelial cells bind actin filaments and possess myosin-I as a cytoplasmically oriented peripheral membrane protein. J Cell Biol 120: 117-127.

56. Fiedler K, Kobayashi T, Kurzchalia TV, Simons K (1993) Glycosphingolipid-enriched, detergent-insoluble complexes in protein sorting in epithelial cells. Biochemistry 32: 6365-6373.

57. Fiedler K, Lafont F, Parton RG, Simons K (1995) Annexin XIIIb: a novel epithelial specific annexin is implicated in vesicular traffic to the apical plasma membrane. J Cell Biol 128: 1043-1053.

58. Field C, Schekman R (1980) Localized secretion of acid phosphatase reflects the pattern of cell surface growth in saccharomyces cerevisiae. J Cell Biol 86: 123-128.

59. Fleming TP, Johnson MH (2003) From EGG to Epithelium. Annual Review of Cell Biology 4: 459-485.

60. Folsch H, Ohno H, Bonifacino JS, Mellman I (1999) A novel clathrin adaptor complex mediates basolateral targeting in polarized epithelial cells. Cell 99: 189-198.

61. Fukushima N, Furuta D, Hidaka Y, Moriyama R, Tsujiuchi T (2009) Post-translational modifications of tubulin in the nervous system. J Neurochem 109(3): 683-693.

62. Futter CE, Felder S, Schlessinger J, Ullrich A, Hopkins CR (1993) Annexin I is phosphorylated in the multivesicular body during the processing of the epidermal growth factor receptor. J Cell Biol 120: 77-83.

63. Gaush CR, Hard WL, Smith TF (1966) Characterization of An Established Line of Canine Kidney Cells (Mdck). Proceedings of the Society for Experimental Biology and Medicine 122: 931-&.

64. Gee MA, Heuser JE, Vallee RB (1997) An extended microtubule-binding structure within the dynein motor domain. Nature 390: 636-639.

65. Gerke V, Moss SE (2002) Annexins: from structure to function. Physiol Rev 82: 331-371.

66. Gerke V, Creutz CE, Moss SE (2005) Annexins: linking Ca2+ signalling to membrane dynamics. Nat Rev Mol Cell Biol 6: 449-461.

67. Gibbons IR, Gibbons BH, Mocz G, Asai DJ (1991) Multiple nucleotide-binding sites in the sequence of dynein beta heavy chain. Nature 352: 640-643.

68. Gindhart JG, Chen J, Faulkner M, Gandhi R, Doerner K, Wisniewski T, Nandlestadt A (2003) The Kinesin-associated Protein UNC-76 Is Required for Axonal Transport in the Drosophila Nervous System. Mol Biol Cell 14: 3356-3365.

69. Girard C, Tinel N, Terrenoire C, Romey G, Lazdunski M, Borsotto M (2002) p11, an annexin II subunit, an auxiliary protein associated with the background K+ channel, TASK-1. EMBO J 21: 4439-4448.

70. Glater EE, Megeath LJ, Stowers RS, Schwarz TL (2006) Axonal transport of mitochondria requires milton to recruit kinesin heavy chain and is light chain independent. J Cell Biol 173: 545-557.

71. Gleeson PA, Anderson TJ, Stow JL, Griffiths G, Toh BH, Matheson F (1996) p230 is associated with vesicles budding from the trans-Golgi network. J Cell Sci 109: 2811-2821.

72. Gluzman Y (1981) SV40-transformed simian cells support the replication of early SV40 mutants. Cell 23: 175-182.

73. Gober JW, Champer R, Reuter S, Shapiro L (1991) Expression of positional information during cell differentiation in caulobacter. Cell 64: 381-391.

74. Gottlieb TA, Ivanov IE, Adesnik M, Sabatini DD (1993) Actin microfilaments play a critical role in endocytosis at the apical but not the basolateral surface of polarized epithelial cells. J Cell Biol 120: 695-710.

75. Grand RJ, Montgomery RK, Chitkara DK, Hirschhorn JN (2003) Changing genes; losing lactase. Gut 52: 617-619.

76. Griffiths G, Simons K (1986) The trans Golgi network: sorting at the exit site of the Golgi complex. Science 234: 438-443.

77. Gross SP, Welte MA, Block SM, Wieschaus EF (2002) Coordination of opposite-polarity microtubule motors. J Cell Biol 156: 715-724.

78. Gruenberg J, Stenmark H (2004) The biogenesis of multivesicular endosomes. Nat Rev Mol Cell Biol 5: 317-323.

79. Gupta V, Palmer KJ, Spence P, Hudson A, Stephens DJ (2008) Kinesin-1 (uKHC/KIF5B) is Required for Bidirectional Motility of ER Exit Sites and Efficient ER-to-Golgi Transport. Traffic 9: 1850-1866.

80. Gut A, Kappeler F, Hyka N, Balda MS, Hauri HP, Matter K (1998) Carbohydrate-mediated Golgi to cell surface transport and apical targeting of membrane proteins. EMBO J 17: 1919-1929.

81. Gyoeva FK, Sarkisov DV, Khodjakov AL, Minin AA (2004) The Tetrameric Molecule of Conventional Kinesin Contains Identical Light ChainsΓÇá. Biochemistry 43: 13525-13531.

82. Hackney D (1995) Highly processive microtubule-stimulated ATP hydrolysis by dimeric kinesin head domains. Nature 377: 448-450.

83. Hackney DD, Levitt JD, Suhan J (1992) Kinesin undergoes a 9 S to 6 S conformational transition. J Biol Chem 267: 8696-8701.

84. Hannan LA, Lisanti MP, Rodriguez-Boulan E, Edidin M (1993) Correctly sorted molecules of a GPI-anchored protein are clustered and immobile when they arrive at the apical surface of MDCK cells. J Cell Biol 120: 353-358.

85. Hansen MDH, Ehrlich JS, Nelson WJ (2002) Molecular Mechanism for Orienting Membrane and Actin Dynamics to Nascent Cell-Cell Contacts in Epithelial Cells. J Biol Chem 277: 45371-45376.

86. Hauri HP, Quaroni A, Isselbacher KJ (1979) Biogenesis of intestinal plasma membrane: posttranslational route and cleavage of sucrase-isomaltase. Proc Natl Acad Sci U S A 76: 5183-5186.

87. Hauri HP, Sterchi EE, Bienz D, Fransen JA, Marxer A (1985) Expression and intracellular transport of microvillus membrane hydrolases in human intestinal epithelial cells. J Cell Biol 101: 838-851.

88. Hauser H, Semenza G (1983) Sucrase-isomaltase: a stalked intrinsic protein of the brush border membrane. CRC Crit Rev Biochem 14: 319-345.

89. Hayes MJ, Merrifield CJ, Shao D, Ayala-Sanmartin J, Schorey CD, Levine TP, Proust J, Curran J, Bailly M, Moss SE (2004) Annexin 2 Binding to Phosphatidylinositol 4,5-

Bisphosphate on Endocytic Vesicles Is Regulated by the Stress Response Pathway. J Biol Chem 279: 14157-14164.

90. Heine M, Cramm-Behrens CI, Ansari A, Chu HP, Ryazanov AG, Naim HY, Jacob R (2005) {alpha}-Kinase 1, a New Component in Apical Protein Transport. J Biol Chem 280: 25637-25643.

91. Helenius J, Brouhard G, Kalaidzidis Y, Diez S, Howard J (2006) The depolymerizing kinesin MCAK uses lattice diffusion to rapidly target microtubule ends. Nature 441: 115-119.

92. Hirokawa N, Noda Y, Tanaka Y, Niwa S (2009) Kinesin superfamily motor proteins and intracellular transport. Nat Rev Mol Cell Biol 10: 682-696.

93. Hirokawa N, Pfister KK, Yorifuji H, Wagner MC, Brady ST, Bloom GS (1989) Submolecular domains of bovine brain kinesin identified by electron microscopy and monoclonal antibody decoration. Cell 56: 867-878.

94. Horiuchi D, Collins CA, Bhat P, Barkus RV, DiAntonio A, Saxton WM (2007) Control of a Kinesin-Cargo Linkage Mechanism by JNK Pathway Kinases. Current Biology 17: 1313-1317.

95. Hunziker W, Spiess M, Semenza G, Lodish HF (1986) The sucrase-isomaltase complex: primary structure, membrane- orientation, and evolution of a stalked, intrinsic brush border protein. Cell 46: 227-234.

96. Imamura T, Huang J, Usui I, Satoh H, Bever J, Olefsky JM (2003) Insulin-Induced GLUT4 Translocation Involves Protein Kinase C-{lambda}-Mediated Functional Coupling between Rab4 and the Motor Protein Kinesin. Mol Cell Biol 23: 4892-4900.

97. Ivanov AI, Mccall IC, Babbin B, Samarin SN, Nusrat A, Parkos CA (2006) Microtubules regulate disassembly of epithelial apical junctions. BMC Cell Biology 7.

98. Jacob R, Alfalah M, Grunberg J, Obendorf M, Naim HY (2000a) Structural determinants required for apical sorting of an intestinal brush-border membrane protein. J Biol Chem 275: 6566-6572.

99. Jacob R, Brewer C, Fransen JA, Naim HY (1994) Transport, function, and sorting of lactase-phlorizin hydrolase in Madin-Darby canine kidney cells. J Biol Chem 269: 2712-2721.

100. Jacob R, Heine M, Alfalah M, Naim HY (2003) Distinct cytoskeletal tracks direct individual vesicle populations to the apical membrane of epithelial cells. Curr Biol 13: 607-612.

101. Jacob R, Heine M, Eikemeyer J, Frerker N, Zimmer KP, Rescher U, Gerke V, Naim HY (2004) Annexin II is required for apical transport in polarized epithelial cells. J Biol Chem 279: 3680-3684.

102. Jacob R, Naim HY (2001) Apical membrane proteins are transported in distinct vesicular carriers. Curr Biol 11: 1444-1450.

103. Jacob R, Zimmer KP, Naim H, Naim HY (1997) The apical sorting of lactase-phlorizin hydrolase implicates sorting sequences found in the mature domain. Eur J Cell Biol 72: 54-60.

104. Jacob R, Zimmer KP, Schmitz J, Naim HY (2000b) Congenital sucrase-isomaltase deficiency arising from cleavage and secretion of a mutant form of the enzyme. J Clin Invest 106: 281-287.

105. Jacobson C, Schnapp B, Banker GA (2006) A change in the selective translocation of the Kinesin-1 motor domain marks the initial specification of the axon. Neuron 49(6): 797-804.

106. Jaulin, Fanny, Xue, Xiaoxiao, Rodriguez-Boulan, Enrique, and Kreitzer, Geri. Polarization-Dependent Selective Transport to the Apical Membrane by KIF5B in MDCK Cells. 13[4], 511-522. 9-10-2007.

Ref Type: Abstract

107. Jensen FC, Koprowski H, Girardi AJ, Gilden RV (1964) Infection of Human + Simian Tissue Cultures with Rous Sarcoma Virus. Proceedings of the National Academy of Sciences of the United States of America 52: 53-&.

108. Johnson D, Lanahan A, Buck CR, Sehgal A, Morgan C, Mercer E, Bothwell M, Chao M (1986) Expression and structure of the human NGF receptor. Cell 47: 545-554.

109. Jost M, Zeuschner D, Seemann J, Weber K, Gerke V (1997) Identification and characterization of a novel type of annexin-membrane interaction: Ca2+ is not required for the association of annexin II with early endosomes. J Cell Sci 110 (Pt 2): 221-228.

110. Kaetzel MA, Chan HC, Dubinsky WP, Dedman JR, Nelson DJ (1994) A role for annexin IV in epithelial cell function. Inhibition of calcium-activated chloride conductance. J Biol Chem 269: 5297-5302.

111. Kamal A, Ying Y, Anderson RGW (1998) Annexin VI-mediated Loss of Spectrin during Coated Pit Budding Is Coupled to Delivery of LDL to Lysosomes. J Cell Biol 142: 937-947.

112. Kamal A, Stokin GB, Yang Z, Xia CH, Goldstein LSB (2000) Axonal Transport of Amyloid Precursor Protein Is Mediated by Direct Binding to the Kinesin Light Chain Subunit of Kinesin-I. Neuron 28: 449-459.

113. Kanai Y, Okada Y, Tanaka Y, Harada A, Terada S, Hirokawa N (2000) KIF5C, a novel neuronal kinesin enriched in motor neurons. J Neurosci 20: 6374-6384.

114. Kanai Y, Dohmae N, Hirokawa N (2004) Kinesin Transports RNA: Isolation and Characterization of an RNA-Transporting Granule. Neuron 43: 513-525.

115. King SM (2000) AAA domains and organization of the dynein motor unit. J Cell Sci 113: 2521-2526.

116. King SJ, Schroer TA (2000) Dynactin increases the processivity of the cytoplasmic dynein motor. Nat Cell Biol 2: 20-24.

117. Konishi Y, Setou M (2009) Tubulin tyrosination navigates the kinesin-1 motor domain to axons. Nat Neurosci 12(5): 559-567.

118. Kreitzer G, Marmorstein A, Okamoto P, Vallee R, Rodriguez-Boulan E (2000) Kinesin and dynamin are required for post-Golgi transport of a plasma-membrane protein. Nat Cell Biol 2000 Feb;2(2):125-7 2: 125-127.

119. Kron SJ, Spudich JA (1986) Fluorescent actin filaments move on myosin fixed to a glass surface. Proceedings of the National Academy of Sciences of the United States of America 83: 6272-6276.

120. Lafont F, Burkhardt JK, Simons K (1994) Involvement of microtubule motors in basolateral and apical transport in kidney cells. Nature 372: 801-803.

121. Lafont F, Lecat S, Verkade P, Simons K (1998) Annexin XIIIb associates with lipid microdomains to function in apical delivery. J Cell Biol 142: 1413-1427.

122. Lakämper S, Meyhöfer E (2006) Back on track ΓÇô On the role of the microtubule for kinesin motility and cellular function. Journal of Muscle Research and Cell Motility 27: 161-171.

123. Lawrence CJ, Dawe RK, Christie KR, Cleveland DW, Dawson SC, Endow SA, Goldstein LSB, Goodson HV, Hirokawa N, Howard J, Malmberg RL, McIntosh JR, Miki H, Mitchison TJ, Okada Y, Reddy ASN, Saxton WM, Schliwa M, Scholey JM, Vale RD, Walczak CE, Wordeman L (2004) A standardized kinesin nomenclature. J Cell Biol 167: 19-22.

124. Le Bivic A, Garcia M, Rodriguez-Boulan E (1993) Ricin-resistant Madin-Darby canine kidney cells missort a major endogenous apical sialoglycoprotein. J Biol Chem 268: 6909-6916.

125. Lecat S, Verkade P, Thiele C, Fiedler K, Simons K, Lafont F (2000) Different properties of two isoforms of annexin XIII in MDCK cells. J Cell Sci 113: 2607-2618.

126. Leitinger B, Hille-Rehfeld A, Spiess M (1995) Biosynthetic transport of the asialoglycoprotein receptor H1 to the cell surface occurs via endosomes. Proc Natl Acad Sci U S A 92: 10109-10113.

127. Lin S, Naim HY, Rodriguez AC, Roth MG (1998) Mutations in the middle of the transmembrane domain reverse the polarity of transport of the influenza virus hemagglutinin in MDCK epithelial cells. J Cell Biol 142: 51-57.

128. Lin S, Naim HY, Roth MG (1997) Tyrosine-dependent basolateral sorting signals are distinct from tyrosine-dependent internalization signals. J Biol Chem 272: 26300-26305.

129. Lippincott-Schwartz J, Cole NB, Marotta A, Conrad PA, Bloom GS (1995) Kinesin is the motor for microtubule-mediated Golgi-to-ER membrane traffic. J Cell Biol 128: 293-306.

130. Lombardi T, Montesano R, Orci L (1985) Polarized plasma membrane domains in cultured endothelial cells. Experimental Cell Research 161: 242-246.

131. Lu HL, Ali MY, Bookwalter CS, Warshaw DM, Trybus KM (2009) Diffusive Movement of Processive Kinesin-1 on Microtubules. Traffic 10: 1429-1438.

132. Luftig RB, McMillan PN, Weatherbee JA, Weihing RR (1977) Increased visualization of microtubules by an improved fixation procedure. J Histochem Cytochem 25: 175-187.

133. Mallik R, Carter BC, Lex SA, King SJ, Gross SP (2004) Cytoplasmic dynein functions as a gear in response to load. Nature 427: 649-652.

134. Mannowetz N, Kartarius S, Wennemuth G, Montenarh M (2010) Protein kinase CK2 and new binding partners during spermatogenesis. Cellular and Molecular Life Sciences.

135. Maples CJ, Ruiz WG, Apodaca G (1997) Both microtubules and actin filaments are required for efficient postendocytotic traffic of the polymeric immunoglobulin receptor in polarized Madin-Darby canine kidney cells. J Biol Chem 272: 6741-6751.

136. Matter K, Mellman I (1994) Mechanisms of cell polarity: sorting and transport in epithelial cells. Curr Opin Cell Biol 6: 545-554.

137. Mayran N, Parton RG, Gruenberg J (2003) Annexin II regulates multivesicular endosome biogenesis in the degradation pathway of animal cells. EMBO J 22: 3242-3253.

138. Mehta AD, Rock RS, Rief M, Spudich JA, Mooseker MS, Cheney RE (1999) Myosin-V is a processive actin-based motor. Nature 400: 590-593.

139. Mellman I, Warren G (2000) The Road Taken: Past and Future Foundations of Membrane Traffic. Cell 100: 99-112.

140. Merrifield CJ, Rescher U, Almers W, Proust J, Gerke V, Sechi AS, Moss SE (2001) Annexin 2 has an essential role in actin-based macropinocytic rocketing. Curr Biol 11: 1136-1141.

141. Miki H, Setou M, Kaneshiro K, Hirokawa N (2001) All kinesin superfamily protein, KIF, genes in mouse and human. Proc Natl Acad Sci USA 98: 7004-7011.

142. Montes dO, Lezama RA, Mondragon R, Castillo AM, Meza I (1997) Myosin I interactions with actin filaments and trans-Golgi-derived vesicles in MDCK cell monolayers. Arch Med Res 28: 321-328.

143. Morfini G, Pigino G, Szebenyi G, You Y, Pollema S, Brady ST (2006) JNK mediates pathogenic effects of polyglutamine-expanded androgen receptor on fast axonal transport. Nat Neurosci 9: 907-916.

144. Morfini G, Szebenyi G, Elluru R, Ratner N, Brady ST (2002) Glycogen synthase kinase 3 phosphorylates kinesin light chains and negatively regulates kinesin-based motility. EMBO J 21: 281-293.

145. Morgan RO, Fernandez MP (1997) Distinct Annexin Subfamilies in Plants and Protists Diverged Prior to Animal Annexins and from a Common Ancestor. J Mol Evol 44: 178-188.

146. Moss SE, Morgan RO (2004) The annexins. Genome Biol 5: 219.

147. Mu FT, Callaghan JM, Steele-Mortimer O, Stenmark H, Parton RG, Campbell PL, McCluskey J, Yeo JP, Tock EPC, Toh BH (1995) EEA1, an Early Endosome-Associated Protein. J Biol Chem 270: 13503-13511.

148. Murray JW, Bananis E, Wolkoff AW (2000) Reconstitution of ATP-dependent Movement of Endocytic Vesicles Along Microtubules In Vitro: An Oscillatory Bidirectional Process. Mol Biol Cell 11: 419-433.

149. Musch A (2004) Microtubule organization and function in epithelial cells. Traffic 5: 1-9.

150. Naim HY (1992) Processing of human pro-lactase-phlorizin hydrolase at reduced temperatures: cleavage is preceded by complex glycosylation. Biochem J 285: 13-16.

151. Naim HY, Lacey SW, Sambrook JF, Gething MJ (1991) Expression of a full-length cDNA coding for human intestinal lactase- phlorizin hydrolase reveals an uncleaved, enzymatically active, and transport-competent protein. J Biol Chem 266: 12313-12320.

152. Naim HY, Lentze MJ (1992) Impact of O-glycosylation on the function of human intestinal lactase- phlorizin hydrolase. Characterization of glycoforms varying in enzyme activity and localization of O-glycoside addition. J Biol Chem 267: 25494-25504.

153. Naim HY, Sterchi EE, Lentze MJ (1987) Biosynthesis and maturation of lactase-phlorizin hydrolase in the human small intestinal epithelial cells. Biochem J 241: 427-434.

154. Naim HY, Sterchi EE, Lentze MJ (1988) Biosynthesis of the human sucrase-isomaltase complex. Differential O- glycosylation of the sucrase subunit correlates with its position within the enzyme complex. J Biol Chem 263: 7242-7253.

155. Nakata T, Hirokawa N (1995) Point mutation of adenosine triphosphate-binding motif generated rigor kinesin that selectively blocks anterograde lysosome membrane transport. J Cell Biol 131: 1039-1053.

156. Nangaku M, Sato-Yoshitake R, Okada Y, Noda Y, Takemura R, Yamazaki H, Hirokawa N (1994) KIF1B, a novel microtubule plus end-directed monomeric motor protein for transport of mitochondria. Cell 79: 1209-1220.

157. Nath S, Bananis E, Sarkar S, Stockert RJ, Sperry AO, Murray JW, Wolkoff AW (2007) Kif5B and Kifc1 Interact and Are Required for Motility and Fission of Early Endocytic Vesicles in Mouse Liver. Mol Biol Cell 18: 1839-1849.

158. Nilius B, Gerke V, Prenen J, Sz++cs G, Heinke S, Weber K, Droogmans G (1996) Annexin II Modulates Volume-activated Chloride Currents in Vascular Endothelial Cells. J Biol Chem 271: 30631-30636.

159. Nishiyama M, Higuchi H, Yanagida T (2002) Chemomechanical coupling of the forward and backward steps of single kinesin molecules. Nat Cell Biol 4: 790-797.

160. Noda Y, Okada Y, Saito N, Setou M, Xu Y, Zhang Z, Hirokawa N (2001) KIFC3, a microtubule minus end-directed motor for the apical transport of annexin XIIIb-associated Triton-insoluble membranes. J Cell Biol 155: 77-88.

161. Ogawa K, Kamiya R, Wilkerson CG, Witman GB (1995) Interspecies conservation of outer arm dynein intermediate chain sequences defines two intermediate chain subclasses. Mol Biol Cell 6: 685-696.

162. Ohno H, Stewart J, Fournier MC, Bosshart H, Rhee I, Miyatake S, Saito T, Gallusser A, Kirchhausen T, Bonifacino JS (1995) Interaction of tyrosine-based sorting signals with clathrin-associated proteins. Science 269: 1872-1875.

163. Oliferenko S, Paiha K, Harder T, Gerke V, Schwarzler C, Schwarz H, Beug H, Gunthert U, Huber LA (1999) Analysis of CD44-containing lipid rafts: Recruitment of annexin II and stabilization by the actin cytoskeleton. J Cell Biol 146: 843-854.

164. Paladino S, Pocard T, Catino MA, Zurzolo C (2006) GPI-anchored proteins are directly targeted to the apical surface in fully polarized MDCK cells. J Cell Biol 172: 1023-1034.

165. Panzer P, Preuss U, Joberty G, Naim HY (1998) Protein domains implicated in intracellular transport and sorting of lactase-phlorizin hydrolase. J Biol Chem 273: 13861-13869.

166. Parczyk K, Haase W, Kondor-Koch C (1989) Microtubules are involved in the secretion of proteins at the apical cell surface of the polarized epithelial cell, Madin-Darby canine kidney. J Biol Chem 264: 16837-16846.

167. Peng I, Dennis JE, Rodriguez-Boulan E, Fischman DA (1990) Polarized release of enveloped viruses in the embryonic chick heart: Demonstration of epithelial polarity in the presumptive myocardium. Developmental Biology 141: 164-172.

168. Plitz T, Pfeffer K (2001) Intact Lysosome Transport and Phagosome Function Despite Kinectin Deficiency. Mol Cell Biol 21: 6044-6055.

169. Porter ME (1996) Axonemal dyneins: assembly, organization, and regulation. Current Opinion in Cell Biology 8: 10-17.

170. Potter BA, Ihrke G, Bruns JR, Weixel KM, Weisz OA (2004) Specific N-glycans direct apical delivery of transmembrane, but not soluble or glycosylphosphatidylinositol-anchored forms of endolyn in Madin-Darby canine kidney cells. Mol Biol Cell 15: 1407-1416.

171. Rapoport I, Chen YC, Cupers P, Shoelson SE, Kirchhausen T (1998) Dileucine-based sorting signals bind to the beta chain of AP-1 at a site distinct and regulated differently from the tyrosine-based motif-binding site. EMBO J 17: 2148-2155.

172. Rescher U, Gerke V (2004) Annexins - unique membrane binding proteins with diverse functions. J Cell Sci 117: 2631-2639.

173. Rescher U, Ruhe D, Ludwig C, Zobiack N, Gerke V (2004) Annexin 2 is a phosphatidylinositol (4,5)-bisphosphate binding protein recruited to actin assembly sites at cellular membranes. J Cell Sci 117: 3473-3480.

174. Rief M, Rock RS, Mehta AD, Mooseker MS, Cheney RE, Spudich JA (2000) Myosin-V stepping kinetics: A molecular model for processivity. Proceedings of the National Academy of Sciences of the United States of America 97: 9482-9486.

175. Rindler MJ, Ivanov IE, Sabatini DD (1987) Microtubule-acting drugs lead to the nonpolarized delivery of the influenza hemagglutinin to the cell surface of polarized Madin-Darby canine kidney cells. J Cell Biol 104: 231-241.

176. Rocha N, Kuijl C, van der Kant R, Janssen L, Houben D, Janssen H, Zwart W, Neefjes J (2009) Cholesterol sensor ORP1L contacts the ER protein VAP to control Rab7ΓÇôRILPΓÇôp150Glued and late endosome positioning. J Cell Biol 185: 1209-1225.

177. Rodriguez-Boulan E, Gonzalez A (1999) Glycans in post-Golgi apical targeting: sorting signals or structural props? Trends Cell Biol 9: 291-294.

178. Rodriguez-Boulan E, Kreitzer G, Musch A (2005) Organization of vesicular trafficking in epithelia. Nat Rev Mol Cell Biol 6: 233-247.

179. Rodriguez-Boulan E, Nelson WJ (1989) Morphogenesis of the polarized epithelial cell phenotype. Science 245: 718-725.

180. Rodriguez-Boulan E, Powell SK (1992) Polarity of epithelial and neuronal cells. Annu Rev Cell Biol 8: 395-427.

181. Rodriguez-Tebar A, Dechant G, Götz R, Barde YA (1992) Binding of neurotrophin-3 to its neuronal receptors and interactions with nerve growth factor and brain-derived neurotrophic factor. EMBO J 11: 917-922.

182. Roux PP, Barker PA (2002) Neurotrophin signaling through the p75 neurotrophin receptor. Progress in Neurobiology 67: 203-233.

183. Salas PJ, Misek DE, Vega-Salas DE, Gundersen D, Cereijido M, Rodriguez-Boulan E (1986) Microtubules and actin filaments are not critically involved in the biogenesis of epithelial cell surface polarity. J Cell Biol 102: 1853-1867.

184. Samso M, Koonce MP (2004) 25 Angstrom Resolution Structure of a Cytoplasmic Dynein Motor Reveals a Seven-member Planar Ring. Journal of Molecular Biology 340: 1059-1072.

185. Santama N, Er CPN, Ong LL, Yu H (2004) Distribution and functions of kinectin isoforms. J Cell Sci 117: 4537-4549.

186. Sarafian T, Pradel LA, Henry JP, Aunis D, Bader MF (1991) The participation of annexin II (calpactin I) in calcium-evoked exocytosis requires protein kinase C. J Cell Biol 114: 1135-1147.

187. Sato-Yoshitake R, Yorifuji H, Inagaki M, Hirokawa N (1992) The phosphorylation of kinesin regulates its binding to synaptic vesicles. J Biol Chem 267: 23930-23936.

188. Schäfer B, Götz C, Dudek J, Hessenauer A, Matti U, Montenarh M (2009) KIF5C: a new binding partner for protein kinase CK2 with a preference for the CK2alpha' subunit. Cell Mol Life Sci 66: 339-349.

189. Scheiffele P, Peranen J, Simons K (1995) N-glycans as apical sorting signals in epithelial cells. Nature 378: 96-98.

190. Schnapp BJ (2003) Trafficking of signaling modules by kinesin motors. J Cell Sci 116: 2125-2135.

191. Schuck S, Simons K (2004) Polarized sorting in epithelial cells: raft clustering and the biogenesis of the apical membrane. J Cell Sci 117: 5955-5964.

192. Seiler S, Kirchner J, Horn C, Kallipolitou A, Woehlke G, Schliwa M (2000) Cargo binding and regulatory sites in the tail of fungal conventional kinesin. Nat Cell Biol 2: 333-338.

193. Setou M, Seog DH, Tanaka Y, Kanai Y, Takei Y, Kawagishi M, Hirokawa N (2002) Glutamate-receptor-interacting protein GRIP1 directly steers kinesin to dendrites. Nature 173: 545-557.

194. Shin K, Fogg VC, Margolis B (2006) Tight junctions and cell polarity. Annu Rev Cell Dev Biol 22: 207-235.

195. Simons K, Ikonen E (1997) Functional rafts in cell membranes. Nature 387: 569-572.

196. Skoufias DA, Cole DG, Wedaman KP, Scholey JM (1994) The carboxyl-terminal domain of kinesin heavy chain is important for membrane binding. J Biol Chem 269: 1477-1485.

197. Smith MJ, Pozo K, Brickley K, Stephenson FA (2006) Mapping the GRIF-1 binding domain of the kinesin, KIF5C, substantiates a role for GRIF-1 as an adaptor protein in the anterograde trafficking of cargoes. J Biol Chem 281: 27216-27228.

198. Spodsberg N, Alfalah M, Naim HY (2001) Characteristics and structural requirements of apical sorting of the rat growth hormone through the O-glycosylated stalk region of intestinal sucrase-isomaltase. J Biol Chem 276: 46597-46604.

199. Stagi M, Gorlovoy P, Larionov S, Takahashi K, Neumann H (2006) Unloading kinesin transported cargoes from the tubulin track via the inflammatory c-Jun N-terminal kinase pathway. FASEB J 20: 2573-2575.

200. Su Q, Cai Q, Gerwin C, Smith CL, Sheng ZH (2004) Syntabulin is a microtubule-associated protein implicated in syntaxin transport in neurons. Nat Cell Biol 6: 941-953.

201. Svoboda K, Block SM (1994) Force and velocity measured for single kinesin molecules. Cell 77: 773-784.

202. Szodorai A, Kuan YH, Hunzelmann S, Engel U, Sakane A, Sasaki T, Takai Y, Kirsch J, Muller U, Beyreuther K, Brady S, Morfini G, Kins S (2009) APP Anterograde Transport Requires Rab3A GTPase Activity for Assembly of the Transport Vesicle. J Neurosci 29: 14534-14544.

203. Tanaka Y, Zhang Z, Hirokawa N (1995) Identification and molecular evolution of new dynein-like protein sequences in rat brain. J Cell Sci 108: 1883-1893.

204. Tanaka Y, Kanai Y, Okada Y, Nonaka S, Takeda S, Harada A, Hirokawa N (1998) Targeted Disruption of Mouse Conventional Kinesin Heavy Chain kif5B, Results in Abnormal Perinuclear Clustering of Mitochondria. Cell 93: 1147-1158.

205. Terada S (2003) Where does slow axonal transport go? Neuroscience Research 47: 367-372.

206. Tilney LG, Hatano S, Ishikawa H, Mooseker MS (1973) The polymerization of actin: its role in the generation of the acrosomal process of certain echinoderm sperm. J Cell Biol 59: 109-126.

207. Titus MA, Gilbert SP (1999) The diversity of molecular motors: an overview. Cell Mol Life Sci 56: 181-183.

208. Toda H, Mochizuki H, Flores R, Josowitz R, Krasieva TB, LaMorte VJ, Suzuki E, Gindhart JG, Furukubo-Tokunaga K, Tomoda T (2008) UNC-51/ATG1 kinase regulates axonal transport by mediating motor–cargo assembly. Genes & Development 22: 3292-3307.

209. Tomas A, Futter C, Moss SE (2004) Annexin 11 is required for midbody formation and completion of the terminal phase of cytokinesis. J Cell Biol 165: 813-822.

210. Torkko JM, Manninen A, Schuck S, Simons K (2008) Depletion of apical transport proteins perturbs epithelial cyst formation and ciliogenesis. J Cell Sci 121: 1193-1203.

211. Tsai MY, Morfini G, Szebenyi G, Brady ST (2000) Release of Kinesin from Vesicles by hsc70 and Regulation of Fast Axonal Transport. Mol Biol Cell 11: 2161-2173.

212. Turpin E, Russo-Marie F, Dubois T, de Paillerets C, Alfsen A, Bomsel M (1998) In adrenocortical tissue, annexins II and VI are attached to clathrin coated vesicles in a calcium-independent manner. Biochimica et Biophysica Acta (BBA) - Molecular Cell Research 1402: 115-130.

213. Tveit H, Akslen LKA, Fagereng GL, Tranulis MA, Prydz K (2009) A Secretory Golgi Bypass Route to the Apical Surface Domain of Epithelial MDCK Cells. Traffic 10: 1685-1695.

214. Urban J, Parczyk K, Leutz A, Kayne M, Kondor-Koch C (1987) Constitutive apical secretion of an 80-kD sulfated glycoprotein complex in the polarized epithelial Madin-Darby canine kidney cell line. J Cell Biol 105: 2735-2743.

215. Vale RD (2003) The Molecular Motor Toolbox for Intracellular Transport. Cell 112: 467-480.

216. Vale RD, Milligan RA (2000) The Way Things Move: Looking Under the Hood of Molecular Motor Proteins. Science 288: 88-95.

217. Vale RD, Reese TS, Sheetz MP (1985) Identification of a novel force-generating protein, kinesin, involved in microtubule-based motility. Cell 42: 39-50.

218. van de Graaf SF, Hoenderop JG, Gkika D, Lamers D, Prenen J, Rescher U, Gerke V, Staub O, Nilius B, Bindels RJ (2003) Functional expression of the epithelial Ca(2+) channels (TRPV5 and TRPV6) requires association of the S100A10-annexin 2 complex. EMBO J 22: 1478-1487.

219. van Meer G, Simons K (1988) Lipid polarity and sorting in epithelial cells. J Cell Biochem 36: 51-58.

220. van Zeijl MJ, Matlin KS (1990) Microtubule perturbation inhibits intracellular transport of an apical membrane glycoprotein in a substrate-dependent manner in polarized Madin-Darby canine kidney epithelial cells. Cell Regul 1: 921-936.

221. Verhey KJ, Meyer D, Deehan R, Blenis J, Schnapp BJ, Rapoport TA, Margolis B (2001) Cargo of kinesin identified as JIP scaffolding proteins and associated signaling molecules. J Cell Biol 152(5): 959-970.

222. Visscher K, Schnitzer MJ, Block SM (1999) Single kinesin molecules studied with a molecular force clamp. Nature 400: 184-189.

223. Wang X, Schwarz TL (2009) The Mechanism of Ca2+-Dependent Regulation of Kinesin-Mediated Mitochondrial Motility. Cell 136: 163-174.

224. Wang Z, Khan S, Sheetz MP (1995) Single cytoplasmic dynein molecule movements: characterization and comparison with kinesin. Biophysical Journal 69: 2011-2023.

225. Weisz OA, Rodriguez-Boulan E (2009) Apical trafficking in epithelial cells: signals, clusters and motors. J Cell Sci 122: 4253-4266.

226. Wice BM, Gordon JI (1992) A strategy for isolation of cDNAs encoding proteins affecting human intestinal epithelial cell growth and differentiation: characterization of a novel gut-specific N-myristoylated annexin. J Cell Biol 116: 405-422.

227. Wong YL, Rice SE (2010) KinesinΓÇÖs light chains inhibit the head- and microtubule-binding activity of its tail. Proceedings of the National Academy of Sciences 107: 11781-11786.

228. Wozniak M, Melzer M, Dorner C, Haring HU, Lammers R (2005) The novel protein KBP regulates mitochondria localization by interaction with a kinesin-like protein. BMC Cell Biology 6: 35.

229. Wozniak MJ, Allan VJ (2006) Cargo selection by specific kinesin light chain 1 isoforms. EMBO J 25: 5457-5468.

230. Xue X, Jaulin F, Espenel C, Kreitzer G (2010) PH-domain-dependent selective transport of p75 by kinesin-3 family motors in non-polarized MDCK cells. J Cell Sci 123: 1732-1741.

231. Ye B, Jan YN (2006) Visualizing the Breaking of Symmetry. Dev Cell 10: 411-412.

232. Yeaman C, Le Gall AH, Baldwin AN, Monlauzeur L, Le Bivic A, Rodriguez-Boulan E (1997) The O-glycosylated stalk domain is required for apical sorting of neurotrophin receptors in polarized MDCK cells. J Cell Biol 139: 929-940.

233. Yi M, Weaver D, Hajnoczky G (2004) Control of mitochondrial motility and distribution by the calcium signal. J Cell Biol 167: 661-672.

234. Yildiz A, Tomishige M, Vale RD, Selvin PR (2004) Kinesin Walks Hand-Over-Hand. Science 303: 676-678.

235. Zampieri N, Chao MV (2004) STRUCTURAL BIOLOGY: Enhanced: The p75 NGF Receptor Exposed. Science 304: 833-834.

236. Zobiack N, Rescher U, Laarmann S, Michgehl S, Schmidt MA, Gerke V (2002) Cell-surface attachment of pedestal-forming enteropathogenic E. coli induces a clustering of raft components and a recruitment of annexin 2. J Cell Sci 115: 91-98.

237. Zurzolo C, van't Hof W, van Meer G, Rodriguez-Boulan E (1994) VIP21/caveolin, glycosphingolipid clusters and the sorting of glycosylphosphatidylinositol-anchored proteins in epithelial cells. EMBO J 13: 42-53.

8. Appendix

8.1. List of figures

8.2. List of tables

8.3. List of abbreviations

AAA	ATPase associated with diverse cellular activities
ADH	antidiuretic hormone
ADP	adenosine diphosphate
AF	AlexaFluor
ALPK1	alpha-kinase I
AMPA	α-amino-3-hydroxy-5-methylisoxazole-4-propionate
AnxXIIIb	annexin XIIIb
AP	adaptor protein
aPKC	atypical protein kinase C
APP	β-Amyloid precursor protein
Arg	arginine
ATP	adenosine triphosphate
Br	basolateral recycling route
BSA	bovine serum albumine
C	creatine
Caco-2	colon carcinoma cell line
CAR	coxsackie-adenovirus receptor
CBD	cargo-binding domains
CDK4	cell division kinase 4
cDNA	complementary DANN
CEA	carcinoembryonic antigen
CFP	cyan fluorescent protein
CFTR	cystic fibrosis transmembrane conductance regulator
Ci	curie
COS	CV-1 (simian) in Origin, and carrying the SV40 genetic material
CPK	creatine phosphokinase
CRB3	Crumbs 3
CRE	common recycling endosome
CRMP	collapsin response mediator protein family
Da	Dalton
DEAE	diethylaminoethyl cellulose
DMEM	Dulbecco/Vogt modified Eagle's minimal essential medium
DNA	deoxyribonucleic acid
DsRed	red fluorescent protein from *Discosoma sp.*
E	endocytic route
E-Cad	E-cadherin
EEA1	early endosome antigen 1
ER	endoplasmic reticulum
FAPP	phosphatidylinositol 4-phosphate adaptor protein
FCS	fetal calf serum
FMRP	fragile X mental retardation protein
GAPDH	glyceraldehyde 3-phosphate dehydrogenase
GAT	γ-aminobutyric acid transporter
GFP	green fluorescent protein
GM130	Golgi matrix protein 130
gp	glycoprotein
GPI	glycosyl phosphatidyl inositol

GRIP1	glutamate receptor-interacting protein 1
GSK3β	glycogen synthase kinase 3β
GTB	general Tubulin Buffer
GTP	guanosine triphosphate
HA	Influenza virus hemagglutinin
HRP	horseradish peroxidase
IC	intermediate chain
Ile	isoleucine
IP	immunoprecipitation
JAMs	junctional adhesion molecules
JIP	JNK-interacting protein
JNK	JUN N-terminal kinase
KHC	kinesin heavy chain
KIF	kinesin family member
KLC	kinesin light chain
Leu	leucine
LPH	lactase-phlorizin hydrolase
LPH_c	complex glycosylated form of LPH
LPH_h	mannose-rich glycosylated form of LPH
LPH_m	mature form of LPH
MAGI	membrane-associated guanylate kinase with inverted domain structure
MAL	myelin and lymphocyte protein
MALDI-TOF	matrix-assisted laser desorption/ionization time-of-flight mass spectrometry
MCF	Michigan Cancer Foundation
MCT	monocarboxylate transporter
MDCK	Madine Darby Canine Kidney cell line
MEM	minimal essential medium
mRNA	messenger RNA
mRNP	messenger ribonucleoprotein
MT	microtubule(s)
MTOC	microtubule-organizing center
MUPP1	multi-PDZ domain protein 1
NGF	nerve growth factor
NGF	nerve growth factor
NTR	neurotrophin receptor
ORP1L	oxysterol-binding protein-related protein
OSS	oxygen scavenging system/
$p75_c$	complex glycosylated form of p75
$p75_h$	mannose-rich glycosylated form of p75
PAGE	polyacrylamide gel electrophoresis
PALS1	protein associated with Lin seven 1
Par	partitioning defective
PAS	protein-A sepharose
PATJ	PALS1-associated tight junction protein
PC	phosphocreatine
PCT	proximal convoluted tubule
PDI	protein disulfide isomerase
PDZ domain	postsynaptic density protein-95/discs large/zonula occludens domain

pIgR	polymeric immunoglobulin receptor
pIgR	polymeric immunoglobulin receptor
PIPES	piperazine-N,N′-bis(2-ethanesulfonic acid)
PKC	protein kinase C
pN	piconewton
PtdIns(4,5)P_2	phosphatidylinositol 4,5-bisphosphate
PTH	parathyroid hormone
Rab	Ras-related proteins in brain
RalA	Ras-like GTPase
Ran	Ras-related nuclear protein
RanBP2	Ran-binding protein 2
Ras	rat sarcoma
rGH	rat growth hormone
RNA	ribonucleic acid
RS	ATP-Regenerating System
SDS	sodium dodecyl sulfate
Ser	serine
SHP2	SH2-domain containing phosphatise-2
SI	sucrase-isomaltase
SI_c	complex glycosylated form of SI
SI_h	mannose-rich glycosylated form of SI
siRNA	short interfering RNA
SNAP25	synaptosomal-associated protein 25
TASK1	potassium channel subfamily K member 3
TGN	*Trans*-Golgi network
Thr	threonine
Tiam1	T-lymphoma invasion and metastasis
TIRF	total internal reflection microscopy
TJ	tight junction
TM	transmembrane
TPR	tetratricopeptide repeat
Trk	tyrosine kinase
TRPV5	transient receptor potential cation channel subfamily V member 5
Tyr	tyrosine
TyrTub	tyrosinated tubulin
UNC	uncoordinated phenotype
VSVG	vesicular stomatitis virus glycoprotein
WB	Western blot
YFP	yellow fluorescent protein
ZA	zonula adherens
ZO	zonula occludens
ZONAB	ZO-1-associated nucleic acid–binding protein

8.4. Eidesstattliche Erklärung

Ich versichere, dass ich meine Dissertation mit dem Titel „Endosomal organizers of *post*-Golgi apical trafficking in polarized epithelial cells“ selbstständig ohne unerlaubte Hilfe verfasst habe und mich dabei keiner anderen als der von mir ausdrücklich bezeichneten Quellen und Hilfen bedient habe.

Die Dissertation wurde in der jetzigen oder ähnlichen Form noch bei keiner Hochschule eingereicht und hat noch keinen sonstigen Prüfungszwecken gedient.

_____ _____

Datum Ksenia Astanina

8.5. Publications

Parts of the work presented in this thesis are based on the following publications. I want to thank all co-authors and all people acknowledged therein for the successful collaboration.

Astanina, K. and Jacob, R.. 2010. KIF5C, a kinesin motor involved in apical trafficking of MDCK cells. Cellular and Molecular Life Sciences 67:1331-1342.

Astanina, K*., Delebinski, C. I.*, Delacour, D., Jacob, R.. 2010. Annexin XIIIb guides raft-dependent and –independent apical traffic in MDCK cells. European Journal of Cell Biology, in press. (* Both authors have contributed equally to this work)

8.6. Curriculum vitae

Die Seite 119 (Lebenslauf) enthält persönliche Daten und ist deshalb nicht Bestandteil der Online-Veröffentlichung.

The page 119 (Curriculum vitae) contains private information and has been removed from online version.

8.7. Acknowledgements

First of all, I would like to thank Prof. Dr. Ralf Jacob for inviting me for a PhD in his lab, for supervising me during these years, for letting me learning to be a scientist (sometimes on my own faults), for motivating me and believing in me, for giving me enough research freedom, for the friendly working atmosphere.

I also thank Prof. Dr. Uwe Maier for being my official *Doktorvater* and for organizing the GK "Intra- and Intercellular transport and communication".

I am very greatful to Dr. Catharina Delebinski and Dr. Sabrina Zink for the proofreading of this thesis, for correcting my russian-german English and for adding hundreds of articles into this thesis.

Special thanks to Martina Dienst for her help in many experiments.

Of course, many thanks are going to all members (former and present) of AG Jacob and the whole *Institut für Zytobiologie* for making every day in the lab, independently of the weather and results, cheerful and full of joy and smiles. Thank you for tolerating my English during the first years and for understanding my German during the last years. Also the cakes were always very tasty.

I would like to thank Catharina Delebinski, Katharina Schneider and Sabrina Zink for the nice time inside and outside the lab, for making me laugh and for being my friends. And, of course, Tamara Straube – for our joint music hobby.

Not to be forgotten are also all my *Praktikanten* for many funny moments and for making me feel that I have learned a lot during my university and PhD years.

Many thanks to my friends from all over the world for their support and a lot of good mood.

Finally, the very sincere gratitude goes to my family, because without them I would never be here right now and would never write the acknowledgments in my PhD thesis. Thank you so much for your unconditional love, for your support, for your patience, for believing in me even more, than I believe myself. Thank you for being always so close to me, in spite of any distances. With all my heart I thank my parents and my husband for making me so happy.